

ผลของขนาดอนุภาคฟลูมซิลิกาและสารเติมแต่งพอลิเมอร์
ต่อเจลอิเล็กโทรไลต์ในแบตเตอรี่ตะกั่ว-กรดแบบมีวาล์วควบคุม

นางสาวปรียาภรณ์ สง่ารัตนพิमान

วิทยานิพนธ์นี้เป็นส่วนหนึ่งของการศึกษาตามหลักสูตรปริญญาวิทยาศาสตรมหาบัณฑิต
สาขาวิชาปิโตรเคมีและวิทยาศาสตร์พอลิเมอร์
คณะวิทยาศาสตร์ จุฬาลงกรณ์มหาวิทยาลัย
ปีการศึกษา 2553
ลิขสิทธิ์ของจุฬาลงกรณ์มหาวิทยาลัย

บทคัดย่อและแฟ้มข้อมูลฉบับเต็มของวิทยานิพนธ์ตั้งแต่ปีการศึกษา 2554 ที่ให้บริการในคลังปัญญาจุฬาฯ (CUIR)
เป็นแฟ้มข้อมูลของนิสิตเจ้าของวิทยานิพนธ์ที่ส่งผ่านทางบัณฑิตวิทยาลัย

The abstract and full text of theses from the academic year 2011 in Chulalongkorn University Intellectual Repository (CUIR)
are the thesis authors' files submitted through the Graduate School.

EFFECT OF FUMED SILICA PARTICLE SIZES AND POLYMER ADDITIVES ON
GELLED ELECTROLYTE IN VALVE-REGULATED LEAD-ACID BATTERY

Miss Preeyaporn Sangarattanapiman

A Thesis Submitted in Partial Fulfillment of the Requirements
for the Degree of Master of Science Program in Petrochemistry and Polymer Science
Faculty of Science
Chulalongkorn University
Academic Year 2010
Copyright of Chulalongkorn University

Thesis Title EFFECT OF FUMED SILICA PARTICLE SIZES AND
POLYMER ADDITIVES ON GELLED ELECTROLYTE IN
VALVE-REGULATED LEAD-ACID BATTERY
By Miss Preeyaporn Sangarattanapiman
Field of Study Petrochemistry and Polymer Science
Advisor Associate Professor Orawon Chailapakul, Ph.D.

Accepted by the Faculty of Science, Chulalongkorn University in
Partial Fulfillment of the Requirements for the Master's Degree

.....Dean of the Faculty of Science
(Professor Supot Hannongbua, Dr.rer.nat.)

THESIS COMMITTEE

.....Chairman
(Assistant Professor Aroonsiri Shitangkoon, Ph.D.)

.....Thesis advisor
(Associate Professor Orawon Chailapakul, Ph.D.)

.....Examiner
(Associate Professor Nuanphun Chantarasiri, Ph.D.)

.....External Examiner
(Weena Siangproh, Ph.D.)

ปริยาภรณ์ สง่ารัตนพิमान : ผลของขนาดอนุภาคฟุ้งซิลิกาและสารเติมแต่งพอลิเมอร์ต่อ
 เจลอิเล็กโทรไลต์ในแบตเตอรี่ชนิดตะกั่ว-กรดแบบมีวาล์วควบคุม . (EFFECT OF FUMED
 SILICA PARTICLE SIZES AND POLYMER ADDITIVES ON GELLED
 ELECTROLYTE IN VALVE-REGULATED LEAD-ACID BATTERY) อ.ที่ปรึกษา
 วิทยานิพนธ์หลัก : รศ.ดร. อรวรรณ ชัยลภากุล, 109 หน้า.

งานวิจัยนี้ศึกษาผลของขนาดอนุภาคฟุ้งซิลิกาและสารเติมแต่งต่างๆ ในเจลอิเล็กโทรไลต์ที่มีผลต่อแบตเตอรี่ตะกั่ว-กรดแบบมีวาล์วควบคุม ด้วยการวัดค่าความจุไฟฟ้าของแบตเตอรี่ขณะคายประจุ วัดค่าการนำไฟฟ้า และทดสอบการสูญเสียไฮโดรเจน- ออกซิเจนของเจลอิเล็กโทรไลต์ต่างๆ โดยเจลอิเล็กโทรไลต์ประกอบด้วยฟุ้งซิลิการ้อยละ 2-5 โดยมวลต่อปริมาตร ความถ่วงจำเพาะของกรดซัลฟิวริก 1.280 ความเข้มข้นสารเติมแต่งร้อยละ 0.005, 0.01 และ 0.02 โดยมวลต่อปริมาตร พบว่า ปริมาณฟุ้งซิลิกาที่เพิ่มขึ้นจะทำให้เกิดเป็นเจลได้ดีขึ้น เช่นเดียวกับสารเติมแต่งบางชนิดที่มีผลทำให้เกิดเจลได้ดีขึ้น นอกจากนี้ขนาดอนุภาคของฟุ้งซิลิกา ปริมาณของฟุ้งซิลิกา ชนิดของสารเติมแต่ง ความเข้มข้นของสารเติมแต่ง ที่เหมาะสมมีผลทำให้ค่าความจุไฟฟ้าของแบตเตอรี่รวมถึงค่าการนำไฟฟ้าสูงขึ้น ขณะที่ฟุ้งซิลิกาขนาด 12 นาโนเมตรลดการสูญเสียไฮโดรเจน-ออกซิเจนได้ดีกว่าฟุ้งซิลิกาขนาด 7 นาโนเมตร โดยสารเติมแต่งและความเข้มข้นของสารเติมแต่งบางชนิดไม่มีผลต่อการสูญเสียไฮโดรเจน- ออกซิเจน ซึ่งผลของการสูญเสียออกซิเจน- ไฮโดรเจนนี้จะมีผลต่ออายุการใช้งานของแบตเตอรี่ สำหรับเจลอิเล็กโทรไลต์ที่ให้ค่าความจุไฟฟ้าของแบตเตอรี่ตะกั่ว-กรดแบบมีวาล์วควบคุมสูงสุดคือ เจลอิเล็กโทรไลต์ที่เติมสารเติมแต่งพอลิเมอร์พอลิพีโรล ความเข้มข้นร้อยละ 0.01 ฟุ้งซิลิกาความเข้มข้นร้อยละ 4 ความถ่วงจำเพาะของกรดซัลฟิวริก 1.280 ให้ค่าความจุไฟฟ้า 2.5 แอมป์ชั่วโมง ซึ่งสูงกว่ามาตรฐานแบตเตอรี่ตะกั่ว-กรดแบบมีวาล์วควบคุมทั่วไป ขณะที่เจลอิเล็กโทรไลต์ที่ให้ค่าการนำไฟฟ้าสูงสุด 836 มิลลิซีเมนส์ต่อเซนติเมตร คือ เจลอิเล็กโทรไลต์ที่เติมสารเติมแต่งสีย้อมความเข้มข้นร้อยละ 0.01 ฟุ้งซิลิกาความเข้มข้นร้อยละ 3 ความถ่วงจำเพาะของกรดซัลฟิวริก 1.280 และเจลอิเล็กโทรไลต์ที่ช่วยลดการสูญเสียไฮโดรเจนและออกซิเจนสูงสุดคือเจลอิเล็กโทรไลต์ที่เติมสารเติมแต่งไอออนิกเหลว ขณะที่การวิเคราะห์ผลด้วย XRD พบว่าการเติมสารเติมแต่งต่างๆ ในเจลอิเล็กโทรไลต์นี้ไม่ส่งผลต่อการเกิดปฏิกิริยาบนพื้นที่ผิวของแผ่นธาตุลบในแบตเตอรี่ตะกั่ว-กรดแบบมีวาล์วควบคุม

สาขาวิชา.....ปิโตรเคมีและวิทยาศาสตร์พอลิเมอร์.....ลายมือชื่อนิสิต.....
 ปีการศึกษา.....2553.....ลายมือชื่อ อ.ที่ปรึกษาวิทยานิพนธ์หลัก.....

5172571323: MAJOR PETROCHEMISTRY AND POLYMER SCIENCE
 KEYWORDS : VALVE-REGULATED LEAD ACID BATTERY / GELLED
 ELECTROLYTE / GEL VRLA BATTERY/ FUMED SILICA

PREEYAPORN SANGARATTANAPIMAN : EFFECT OF FUMED SILICA
 PARTICLE SIZES AND POLYMER ADDITIVES ON GELLED
 ELECTROLYTE IN VALVE REGULATED LEAD-ACID BATTERY.
 ADVISOR : ASSOC. PROF. ORAWON CHAILAPAKUL, Ph.D., 109 pp.

This research studied the effects of fumed silica particle sizes and additives on gelled electrolyte in valve regulated lead-acid battery by measuring the discharge capacity of battery, conductivity values and the hydrogen-oxygen evolution of gelled electrolytes. The gelled electrolytes consist of 2-5% (w/v) of fumed silica, 1.280 specific gravity of sulfuric acid and 0.005, 0.01, 0.02% (w/v) of additives. The results showed that increasing fumed silica content provided the better gelation likewise some additives. In addition, the fumed silica particle sizes, fumed silica content, types of additive and concentration of additive resulted in higher discharge capacity and conductivity. For the hydrogen-oxygen evolution study it was shown that fumed silica particle size 12 nanometers decreased the hydrogen-oxygen evolution better than fumed silica particle size 7 nanometers. Some additives and their concentration were inefficient on the hydrogen-oxygen evolution. The effect of hydrogen-oxygen evolution could influence the cycle life of VRLA battery. For the gelled electrolyte with 0.01 (w/v) of polypyrrole, 4% (w/v) of fumed silica content and 1.280 specific gravity of H₂SO₄ provided the highest discharge capacity of 2.5 Ah. This capacity was higher than the standard VRLA battery. The gelled electrolyte with 0.01% (w/v) of dye, 3% (w/v) of fumed silica content and 1.280 specific gravity of H₂SO₄ offers the highest conductivity values of 836 mS/cm. The decreasing of hydrogen-oxygen evolution was improved by gelled electrolyte with ionic liquid. From XRD analysis, it was found that adding the additives in gelled electrolyte showed no effect on the reaction on negative plate electrode of VRLA battery.

Field of Study : Petrochemistry and Polymer Science Student's Signature

Academic Year : 2010

Advisor's Signature

ACKNOWLEDGEMENTS

Firstly, I would like to express my gratitude to my advisor, Associate Professor Dr. Orawon Chailapakul, for giving the great opportunity and paying attention to me throughout three year of Master's Degree study at Chulalongkorn University. I also would like to thank members of the thesis examination committee, Assistant Professor Dr. Warinthorn Chavasiri, Associate Professor Dr. Nuanphun Chantarasiri and Dr. Weena Siangproh, who give helpful comments and advice in this thesis. My sincere appreciation is also extended to the external committee member, Dr. Weena Siangproh, for her many suggestions.

I really acknowledge the manager of N.V. Battery, Mr. Krisana Watakeyanon, who gives and supports conveniently the knowledge, time, place and batteries throughout this research. I also would like to thank Dr. Nisit Tantavichet, for his kindly helpful knowledge and suggestions for this research. I also thank Ms. Titiporn Tantichanakul who provides the suggestion, help and morale in this research.

I especially want to thank the members of electrochemical groups at Chulalongkorn University, who provide their help throughout this research. Also I would like to gratefully thank the Thailand Research Fund, Center of Excellence for Petroleum, Petrochemicals, Asian Development Bank and Advanced Materials and CU. Graduate School Thesis Grant for financial support. I also thank Chulalongkorn University for partial financial supports and giving the opportunity to study, laboratory facilities, chemical and equipments.

Finally, I am appreciative to my family, Mr. Boonzong Sangarattanapiman, Ms. Phattharaporn Kijbanasiri and Mr. Sunsith Sangarattanapiman for ideas, equipments supplies, helpful and heartfelt unlimited support, financial support, kindness, and encouragement throughout my education, research and my life.

CONTENTS

	PAGE
ABSTRACT (Thai)	iv
ABSTRACT (English)	v
ACKNOWLEDGEMENTS	vi
CONTENTS	vii
LIST OF TABLES	xi
LIST OF FIGURES	xiii
LIST OF ABBREVIATIONS	xvii
CHAPTER I INTRODUCTION	1
1.1 Introduction.....	1
1.2 Objectives of the research.....	3
1.3 Scope of the research.....	3
CHAPTER II THEORY AND LITERATURE SURVEY	4
2.1 History.....	4
2.1.1 Lead-acid battery.....	4
2.1.2 VRLA battery.....	7
2.1.3 Type of VRLA battery.....	7
2.1.4 Construction of VRLA battery.....	8
2.1.5 Applications of VRLA battery.....	11
2.2 Performance characteristics of VRLA battery.....	11
2.2.1 Electrochemical reactions.....	11
2.2.2 Equilibrium voltage.....	14
2.2.3 Electrolyte stratification.....	17
2.2.4 Conductivity of sulfuric acid.....	19
2.2.5 Self-discharge.....	20
2.2.6 Aging and failure mechanisms	20
2.2.6.1 Dryout.....	21
2.2.6.2 Thermal runaway.....	21
2.2.6.3 Negative plate self-discharge.....	21

	PAGE
2.2.6.4 Seal or valve failures.....	22
2.2.6.5 Temperature effects.....	22
2.2.6.6 Loss of absorbed glass mat compression.....	22
2.2.6.7 Ripple current.....	22
2.2.7 Electrolyte specific gravity	23
2.2.8 Charging voltage	23
2.2.8.1 Float voltage	23
2.2.8.2 Temperature compensation of charging voltage	23
2.2.9 Historical service life	24
2.3 Battery parameters and definition	24
2.3.1 Current	24
2.3.2 Voltage	24
2.3.3 Capacity	25
2.3.4 Cycling, Depth of discharge (DOD)	25
2.3.5 Deep discharge.....	26
2.3.6 Internal resistance.....	26
2.3.7 Service life.....	27
2.3.8 Specific gravity.....	27
2.4 Advantages for VRLA battery.....	27
2.5 Gelled electrolyte immobilization with fumed silica	29
2.6 Additives.....	32
2.6.1 Polypyrrole (PPy).....	32
2.6.2 Poly(3,4-ethylenedioxythiophene) : poly(styrenesulfonate)...	34
2.6.3 Ponceau SS (Pss).....	36
2.6.4 Ionic liquid (IL).....	36
2.7 Cyclic voltammetry.....	38
2.8 Electrochemical cells.....	40
2.9 Electrical Conductivity.....	41
2.9.1 Definition of conductivity.....	41
2.9.2 The measurement of conductivity.....	42
2.9.3 Units of Measurement.....	43
2.9.4 Conductive solution.....	43

	PAGE
2.9.4.1 Strong electrolytes.....	44
2.9.4.2 Weak electrolytes.....	44
2.9.5 Definition of terms.....	44
2.9.5.1 Resistance.....	44
2.9.5.2 Conductance.....	44
2.9.5.3 Cell constant.....	45
2.9.5.4 Conductivity.....	45
2.10 Scanning electron microscopy	45
2.11 X-ray diffractometry	47
2.12 Literature reviews of lead-acid batteries.....	49
CHAPTER III EXPERIMENTAL.....	53
3.1 Gelled electrolyte preparations.....	53
3.1.1 Instrument.....	53
3.1.2 Chemicals.....	53
3.1.3 Methodology.....	55
3.2 Battery testing	56
3.2.1 Instruments.....	56
3.2.2 Gelled electrolytes for battery testing.....	57
3.2.3 Methodology.....	60
3.3 Electrical conductivity test.....	60
3.2.1 Instruments.....	60
3.2.2 Gelled electrolytes for conductivity test.....	61
3.2.3 Methodology.....	63
3.4 Electrochemical test.....	63
3.4.1 Instruments	63
3.4.2 Gelled electrolytes and acid solution for electrochemical test.....	64
3.4.3 Methodology.....	64
3.5 Scanning electron microscopic (SEM) analysis	65
3.5.1 Instruments.....	65
3.5.2 Methodology.....	65

	PAGE
3.6 X-ray diffraction (XRD) analysis	66
3.6.1 Instruments	66
3.6.2 Methodology.....	66
CHAPTER IV RESULTS AND DISCUSSION.....	68
4.1 Characterization of gelled electrolytes	68
4.2 Battery testing	70
4.2.1 The discharge capacity of VRLA batteries	70
4.2.1.1 No additive	70
4.2.1.2 Polypyrrole (PPy).....	71
4.2.1.3 PEDOT:PSS.....	73
4.2.1.4 Ponceau SS (Pss)	75
4.2.1.5 Ionic liquid (IL)	78
4.2.2 Initial discharge curves of VRLA batteries.....	80
4.3 Conductivity of gelled electrolytes	82
4.3.1 Different fumed silica contents and particle sizes	82
4.3.2 Different concentration of additives	83
4.4 Hydrogen and oxygen evolution of gelled electrolyte	85
4.5 Morphology of gelled electrolyte	92
4.6 XRD analysis	93
CHAPTER V CONCLUSIONS AND FUTURE PERSPECTIVE.....	95
5.1 Conclusions.....	95
5.2 Future perspective.....	96
REFERENCES.....	97
APPENDICES.....	102
APPENDIX A.....	103
APPENDIX B.....	105
APPENDIX C.....	107
VITA.....	109

LIST OF TABLES

TABLE	PAGE
2.1 Events in Technical Development of Lead-Acid Battery.....	4
2.2 Acid-concentration parameters: acid density (kg/L), H ₂ SO ₄ content and H ₂ SO ₄ concentration in mol/L, and molality. Cell voltage and electrode potentials referred to the standard hydrogen electrode, T=25°C.....	16
3.1 List of chemicals for gelled electrolyte preparations.....	55
3.2 List of instruments for performance of battery testing.....	56
3.3 List of VRLA batteries with different gelled electrolytes for testing the performance of battery.....	57
3.4 List of gelled electrolytes without adding additives for electrical conductivity test.....	62
3.5 List of gelled electrolytes with adding additives for electrical conductivity test.....	62
3.6 List of gelled electrolytes with adding additives for the effect of concentration on conductivity of gelled electrolytes	63
3.7 List of instruments for electrochemical test.....	64
3.8 List of gelled electrolytes from VRLA battery for SEM.....	66
4.1 The characterization of gelled electrolytes with various components.....	68
4.2 The conductivity values of gelled electrolytes containing various concentration of PPy.....	84
4.3 The conductivity values of gelled electrolytes containing various concentration of PEDOT:PSS.....	84
4.4 The conductivity values of gelled electrolytes containing various concentration of Pss.....	84
4.5 The conductivity values of gelled electrolytes containing various concentration of IL.....	85

LIST OF FIGURES

FIGURE	PAGE
2.1	The construction of VRLA battery..... 8
2.2	Discharge and charge reactions of the lead-acid cell (a) Discharge reactions. (b) Charge reactions..... 13
2.3	Typical voltage and specific gravity characteristics of lead-acid cell at constant rate discharge and charge..... 14
2.4	Acid-concentration parameters: acid density (kg/L), H ₂ SO ₄ content and density and acid concentration in weight% H ₂ SO ₄ . The dashed line represents the approximation of equation (2.10)..... 15
2.5	The origin of acid stratification, when the lead-acid battery is discharged and recharged without gassing or other means of mixing the electrolyte.. 18
2.6	Specific electric conductance of aqueous solution of sulfuric acid and its dependence on temperature. The dotted line denotes the maximum..... 19
2.7	Cycle service life in relation to depth of discharge for VRLA battery 26
2.8	Pyrogenic silica (a) Powder of pyrogenic silica and (b) TEM of pyrogenic silic..... 29
2.9	Hydrogen bridge linkages between particles..... 30
2.10	Interaction effect of solvent between fumed silica particle: (a) a strongly hydrogen-bonding liquid (water layer/hydration force is formed on the particles by hydrogen-bonding, resulting in a stable sol); (b) a weakly hydrogen-bonding liquid (the particles interact directly by hydrogen- bonding to form a gel)..... 31
2.11	The formation of the GEL structure is reversible at the beginning, by dispersing SOL and by setting GEL..... 31
2.12	Electronic structures of (a) neutral PPy, (b) polaron in partially doped PPy and (c) bipolaron in fully doped PPy..... 33
2.13	Electronic energy diagrams for (a) neutral PPy, (b) polaron, (c) bipolaron and (d) fully doped PPy..... 34
2.14	Structures of Poly(3,4-ethylenedioxythiophene) : poly(styrenesulfonate).. 35

FIGURE	PAGE
2.15 Structures of Ponceau SS molecule.....	36
2.16 The potential-time excitation signal in a cyclic voltammetric experiment.	39
2.17 Typical cyclic voltammogram for a reversible O + ne ⁻ \rightleftharpoons R redox process	40
2.18 Schematic diagram of a cell for voltammetric measurements: WE-working electrodes; RE-reference electrode; CE-counter electrode. The electrodes are inserted through holes in the cell cover.....	41
2.19 The relationship between conductivity and ion concentration for two common solutions.....	42
2.20 Migration of ions in solution.....	43
2.21 Fundamental of Scanning Electron Microscopy.....	47
2.22 Fundamental of X-ray diffractometer	48
3.1 The setting of instruments for the gelled electrolyte preparation on lab scale.....	53
3.2 The setting of instruments for the gelled electrolyte preparation on industrial scale.....	54
3.3 The gelled electrolyte consisting of fumed silica, H ₂ SO ₄ and (a) fumed silica A200 without adding additives, (b) fumed silica A300 without adding additives, (c) adding PPy, (d) adding PEDOT:PSS, (e) adding IL, (f) adding Pss.....	56
3.4 The setting of experimental for (a) battery charging and (b) battery discharging.....	60
3.5 The conductivity meter and conductivity probe for electrical conductivity test.....	61
3.6 The electrochemical cell for electrochemical technique.....	64
3.7 Planar lead (Pb) electrode as working electrode (WE) with area of 0.5 cm ² and (a) 0.5 cm of WE width, (b) 1 cm of WE length.....	65
3.8 The sample of gelled electrolyte for SEM.....	66
3.9 The negative plate electrode (a) negative plate electrode from VRLA battery (b) a sample cubic negative plate for XRD.....	67
4.1 The discharge capacity of S12-1 to S12-3 batteries at C ₁ during 4 cycles..	70

FIGURE	PAGE
4.2 The discharge capacity of gel batteries without additive at C_1 during 15 cycles: a) batteries with fumed silica particle size 12 nm (A200) at 2-4% (w/v) of fumed silica content, b) batteries with fumed silica particle size 7 nm (A300) at 2-4% (w/v) of fumed silica content.....	72
4.3 The discharge capacity of gel batteries containing PPy as an additive at C_1 during 15 cycles: a) batteries with fumed silica particle size 12 nm (A200) at 2-4% (w/v) of fumed silica content, b) batteries with fumed silica particle size 7 nm (A300) at 2-4% (w/v) of fumed silica content.....	74
4.4 The discharge capacity of gel VRLA batteries with 0.005% (w/v) (SP12-3), 0.01% (w/v) (SP12-5) and 0.02% (w/v) of PPy containing (SP12-6) at C_1 during 15 cycles.....	74
4.5 The discharge capacity of gel batteries containing PEDOT:PSS as an additive at C_1 during 15 cycles: a) batteries with fumed silica particle size 12 nm (A200) at 2-4%(w/v) of fumed silica content, b) batteries with fumed silica particle size 7 nm (A300) at 2-4% (w/v) of fumed silica content.....	75
4.6 The discharge capacity of gel batteries with 0.005, 0.01 and 0.02% (w/v) of PEDOT:PSS containing at C_1 during 15 cycles.....	76
4.7 The discharge capacity of gel batteries containing Pss as an additive at C_1 during 15 cycles: a) batteries with fumed silica particle size 12 nm (A200) at 2-4% (w/v) of fumed silica content, b) batteries with fumed silica particle size 7 nm (A300) at 2-4% (w/v) of fumed silica content...	77
4.8 The discharge capacity of gel batteries with 0.005, 0.01 and 0.02%(w/v) of Pss containing at C_1 during 15 cycles	78
4.9 The discharge capacity of gel batteries containing IL as an additive at C_1 during 15 cycles: a) batteries with fumed silica particle size 12 nm (A200) at 2-4% (w/v) of fumed silica content, b) batteries with fumed silica particle size 7 nm (A300) at 2-4%(w/v) of fumed silica content ...	79
4.10 The discharge capacity of gel batteries with 0.005, 0.01 and 0.02% (w/v) of IL containing at C_1 during 15 cycles.....	79
4.11 The discharge capacity of various gel batteries.....	80
4.12 Initial discharge curves of battery with gelled electrolytes.....	81

FIGURE	PAGE
4.13 Comparison the conductivity of gelled electrolytes between various A300 and A200 fumed silica content; a) without additive, b) PPy, c) PPEDOT:PSS, d) Pss, e) IL.....	82
4.14 Cyclic voltammogram of gelled electrolytes without additive at -5% (w/v) of A300 and A200 fumed silica, scan rate of 20 mV s ⁻¹	86
4.15 Cyclic voltammogram of gelled electrolytes with 0.01% (w/v) PPy at 2-5% (w/v) of A300 and A200 fumed silica, scan rate of 20 mV s ⁻¹	86
4.16 Cyclic voltammogram of gelled electrolytes with PPy at 4% (w/v) of A200 fumed silica, scan rate of 20 mV s ⁻¹	87
4.17 Cyclic voltammogram of gelled electrolytes with 0.01% (w/v) PEDOT:PSS at 2-5% (w/v) of fumed silica content, scan rate of 20 mV s ⁻¹	88
4.18 Cyclic voltammogram of gelled electrolytes with PEDOT:PSS at 4% (w/v) of A200 fumed silica, scan rate of 20 mV s ⁻¹	88
4.19 Cyclic voltammogram of gelled electrolytes with 0.01% (w/v) Pss at 2-5% (w/v) of fumed silica content, scan rate of 20 mV s ⁻¹	89
4.20 Cyclic voltammogram of gelled electrolytes with Pss at 4% (w/v) of A300 fumed silica, scan rate of 20 mV s ⁻¹	90
4.21 Cyclic voltammogram of gelled electrolytes with 0.01% (w/v) IL at 2-5% (w/v) of A300 and A200 fumed silica, scan rate of 20 mV s ⁻¹ ...	90
4.22 Cyclic voltammogram of gelled electrolytes with IL at 3% (w/v) of A300 fumed silica, scan rate of 20 mV s ⁻¹	91
4.23 Cyclic voltammogram of various gelled electrolytes.....	91
4.24 Morphology of gelled electrolytes from VRLA battery.....	92
4.25 XRD pattern of PbSO ₄ and Pb on negative electrode from various VRLA battery; a) S7-2, b) S12-5, c) SP12-3, d) SPD12-5, e) SPS7-2, f) SI7-2.....	94

LIST OF ABBREVIATIONS

a	effective area
a_i	activity of the reacting component i
A	ampere
A	area
A200	fumed silica particle size 12 nanometers
A300	fumed silica particle size 7 nanometers
ABS	acrylonitrile butadiene styrene
AC	alternating current
AGM	absorptive glass-mat
Ah	Ampere hour
BET	Brunauer, Emmett and Teller
cm	centimeter
cm^2	square centimeter
cm^3	cubic centimeter
C	conductivity
CFR	code of Federal regulation
CE	counter electrode
CSGE	colloid silica gelled electrolyte
CV	cyclic voltammetry
d	distance
dm^3	cubic decimeter
DC	direct current
DOT	department of transportation
eV	electron volt

E	potential
E°	Nernst-potential
F	Faraday constant
FSGE	fumed silica gelled electrolyte
g	gram
G	conductance
h	hour
I	current
IATA	international air transport association
IL	ionic liquid
J	Joule
kg	kilogram
K	degree Kelvin
L	length
mol	mole
m^2	square meter
mL	milliliter
min	minute
mS	milli Siemens
mV	milli volt
M	molar
MW	molecular weight
M_w	weight average of molecular weight
M_n	number average of molecular weight
nm	nanometer
PBGE	polysiloxane-based gelled electrolyte
PEDOT:PSS	poly(3,4-Ethylenedioxythiophene)/poly(styrenesulfonate)

PPy	polypyrrole, doped composite with carbon black
Pss	ponceau SS
rpm	revolutions per minute
R	molar gas constant for an ideal gas
R	resistivity
R	resistance
RE	reference electrode
s	second
sp.gr.	specific gravity
S	Siemens
SD	standard deviation
Si	fumed silica
SLA	sealed lead-acid
t	time
T	temperature
TEM	transmission electron microscopy
Tg	glass transition temperature
Tm	melt temperature
U ^o	equilibrium voltage of the cell
UPS	uninterruptible power supply
V	voltage
VRLA	valve-regulated lead-acid
w/v	weight by volume
wt.%	weight-weight percentage
W	Watts
WE	working electrode

Wh	Watts-hour
σ	specific conductivity
Ω	Ohm
$^{\circ}\text{C}$	degree Celsius
$^{\circ}\text{F}$	degree Fahrenheit
α	alpha
β	beta
μm	micrometer

CHAPTER I

INTRODUCTION

1.1 Introduction

Nowadays energy consumption in the world increases every year. The most primary energy is the fossil fuel which is used to convert to electricity. Unfortunately, the burning fossil fuels, the profligate consumption of these fuels affect to the cumulative environment. One strategy for safeguarding the future is to move towards to renewable sources of energy. Anyway, the renewable sources such as wind, solar, wave, biomass, etc. can be hardly stored. Thus, an effective storage system is critical for the efficient use of energy, and for the good stewardship of energy supply. The development means to store electrical energy for an ever-increasing number of applications of great variety. This is a major challenge to scientists, technologists, and engineers to present the creative idea in this research area.

The needs of small electrical appliances can be supplied by (i) primary batteries (disposable batteries), which irreversibly transform the chemical energy to electrical energy. When the initial supply of reactants is exhausted, the energy cannot be readily restored to the battery by electrical means. Common types of disposable batteries are zinc-carbon batteries and alkaline batteries and (ii) secondary batteries (rechargeable batteries) can be recharged by applied electric current, which reverses the chemical reactions during its use. Devices to supply the appropriate current are chargers or rechargers. The oldest rechargeable battery is the lead-acid battery. In 1859, the lead-acid battery was invented by the French physicist Gaston Planté [1]. This battery is notable in that it contains an acid solution in an unsealed container. Therefore, the battery need to be keep upright and the area be well ventilated to ensure safe dispersal of the hydrogen gas produced by these batteries during overcharging. Despite this, it had a low manufacturing cost and it provided the high surge current levels that made it is used commonly. An improved type of liquid electrolyte battery is the sealed valve regulated

lead acid (VRLA) battery. They are popular in the automotive industry as a replacement for the lead-acid wet cell. The VRLA battery uses an immobilized sulfuric acid electrolyte, reducing the chance of leakage and extending shelf life. The VRLA batteries have the electrolyte immobilized, usually by one of two means:

- Gel batteries (or “gel cell”) contain a semi-solid electrolyte to prevent spillage.
- Absorbed Glass Mat (AGM) batteries absorb the electrolyte in special fiberglass matting.

For many years, scientists attempted to develop the valve-regulated lead-acid battery such applied the formation of positive and negative plates to improve the function and properties of separator, modified AGM, including the use of additive in positive plate and liquid electrolyte to enhance formation and battery performance, etc.

Conducting polymers are generally composed of conjugated monomer units with π -electrons delocalized along the polymer back bone. Conducting polymers such as polyaniline, polyparaphenylene and polyacetylene were used to add in positive paste. They improved a power capability of the lead-acid battery because of their high conductivity. Moreover, their chemical can be stable in sulfuric acid solution [1].

To improve the performance of gel valve-regulated lead-acid battery, the conducting polymers and dye was chosen in this work. This way is easy process for the manufacturer and it provides the high performance battery for various applications. Gelled electrolyte was prepared by mixing sulfuric acid with fumed silica and forms a gel. The recombination reaction of oxygen from the positive to the negative plate occurs through a network of micro-cracks in the gelled electrolyte. This reaction makes needless maintenance and no acid leakage for the gel valve-regulated lead-acid battery.

Therefore, the gel batteries provide a very long service-life and have an extremely high reliability, even under deep discharge periods or higher temperatures. In addition, they can be stored for a rather long time at room temperature without any charging due to the very low rate self-discharge and excellent recharge behavior. These are the advantages of gel batteries which is better than AGM batteries.

1.2 Objective of the research

This research is aimed to improve gelled electrolyte for good performance of VRLA batteries using conducting polymers and dye. The conducting polymer including polypyrrole (PPy) and poly(3,4-ethylenedioxythiophene)/poly(styrenesulfonate) (PEDOT:PSS) were chosen to increase the conductivity of the gelled electrolyte. The Ponceau SS (Pss) was used as dye to indicate the expiration of battery. In addition, several of the gelled electrolytes performance were optimized by conductometry and the cycling of the batteries was investigated by measuring the capacities.

1.3 Scope of the research

To achieve the research objective, the following scope was set:

(i) To research and study the information of lead-acid batteries, VRLA batteries and gelled electrolytes.

(ii) To study the effect of fumed silica, sulfuric acid and additives on the performance of VRLA batteries.

(iii) To prepare the gelled electrolyte using fumed silica particle size 7 nm or 12 nm, sulfuric acid (H_2SO_4), a dye or conducting polymers such as PPy, PEDOT:PSS and Pss.

(iv) To investigate the discharge capacity of gel batteries, the conductivity values, the hydrogen-oxygen evolution of the gelled electrolytes, and morphology of gelled electrolytes.

(v) Finally, all the results are discussed.

CHAPTER II

THEORY AND LITERATURE SURVEY

2.1 History

2.1.1 Lead-acid battery [2]

Practical lead-acid batteries began with the inventions of Raymond Gaston Planté in 1860, although batteries containing sulfuric acid or lead components were discussed earlier. Table 2.1 lists the events in the technical development of the lead-acid battery.

Table 2.1 Events in Technical Development of Lead-Acid Battery

Precursor systems		
1836	Daniell	Two-fluid cell; copper/copper sulfate/sulfuric acid/zinc
1840	Grove	Two-fluid cell; carbon/fuming nitric acid/sulfuric acid/zinc
1854	Sindesten	Polarized lead electrodes with external source
Lead-acid battery development		
1860	Planté	First practical lead-acid battery, corroded lead foils to form active material
1881	Faure	Pasted lead foils with lead oxide-sulfuric acid pastes for positive electrode, to increase capacity
1881	Sellon	Lead-antimony alloy grid
1881	Volckmar	Perforated lead plates to provide pockets for support of oxide
1882	Brush	Mechanically bonded lead oxide to lead plates

Table 2.1 Events in Technical Development of Lead-Acid Battery (continued)

Lead-acid battery development		
1882	Gladstone and Tribbs	Double sulfate theory of reaction in lead-acid battery: $\text{PbO}_2 + \text{Pb} + 2\text{H}_2\text{SO}_4 \rightleftharpoons 2\text{PbSO}_4 + 2\text{H}_2\text{O}$
1883	Tudor	Pasted mixture of lead oxides on grid pretreated by Planté method
1886	Lucas	Formed lead plates in solutions of chlorates and perchlorates
1890	Phillipart	Early tubular construction-individual rings
1890	Woodward	Early tubular construction
1910	Smith	Slotted rubber tube, Exide tubular construction
1920 to present		Materials and equipment research, especially expanders, oxides, and fabrication techniques
1935	Haring and Thomas	Lead-calcium alloy grid
1935	Hamer and Harned	Experimental proof of the double sulfate theory of reaction
1956-1960	Bobbe and Voss Ruetschi and Cahan Burbank Feitknecht	Clarification of properties of two crystalline forms of PbO_2 (alpha and beta)
1970s	McClelland and Devit	Commercial spiral-wound sealed lead acid battery Expanded metal grid technology; composite plastic/metal grids; sealed and maintenance-free lead-acid batteries; glass fiber and improved separators; through-the-partition intercell connectors; heat-sealed plastic case-to-cover assemblies; high-energy-density batteries; conical grid cell for long-life float service in telecommunications

Table 2.1 Events in Technical Development of Lead-Acid Battery (continued)

Lead-acid battery development	
1980s	Sealed valve-regulated batteries; quasi-bipolar engine starter batteries; improved low-temp. performance; world's largest battery installed (Chino, Calif.); 40-MWh lead-acid load leveling
1990s	Electric-vehicle interest reemerges; bipolar battery designs for high power

Subsequent to Planté's first developments, numerous experiments were done to accelerate the plate formation process by coating lead foil with oxides on a lead plate pretreated by the Planté method. Attention then turned to other methods for retaining an active material, and two main technological paths were evolved. One is the flat-plate design, in which the active material is developed the structural strength and retention properties by a cementation process (interlocked crystalline lattice) through the grid and the active mass. Another is the tubular electrode design, in which a central conducting wire or rod is surrounded by active material and the assembly is encased in an electrolyte that is porous and insulated.

The technical knowledge for economically manufacturing reliable lead-acid batteries was in place the end of the nineteenth century, leading to subsequently rapid growth of the industry. Improvements in design, manufacturing equipment and methods, recovery methods, active material utilization and production, supporting structures and components, and inactive components such as separators, cases, and seals continue to improve the economic and performance characteristics of lead-acid batteries. Recently more intensive development has started for new applications, especially for energy storage and electric vehicles.

2.1.2 Valve-regulated lead-acid (VRLA) battery

Among the many advances in lead-acid battery technology, the development of design is probably one of the most important. An earlier proposal of VRLA battery was „sealed valve-regulated lead-acid battery“, but the term „sealed“ is redundant because a valve can operate only when the battery is sealed by itself. The term now mostly accepted is in „valve-regulated lead-acid battery“, and this name describes quite well the special feature of this design:

(i) An interior of the VRLA battery does not connect continue with the surrounding atmosphere to exchange gases. This is the characteristic of the vented lead-acid battery.

(ii) The VRLA battery cannot be sealed completely but has to be equipped with a valve which opens even in normal operation conditions from time to time for gas escape. This basic is different from „sealed“ batteries [3].

The sealed lead-acid (SLA) cells are made in two designs; one with spirally wound plates (jelly-roll construction) in a cylindrical metal container and another with flat plates in a prismatic (usually plastic) container. The venting characteristics of the cylindrical and prismatic designs are usually different. The prismatic cell is designed to vent at low pressures ($0.04-1 \times 10^5$ Pa), and these designs are commonly referred to VRLA cells.

2.1.3 Type of VRLA batteries [1, 4]

The invention of VRLA battery utilizes two principals for immobilization the electrolyte within the cell. Two products with different concept of immobilizing are in commerce namely:

(i) AGM (absorptive glass mat) separators which are soaked in the acid so that liquid is not left within the cell.

(ii) Gel which is addition a type of thixotropic colloid in a soft solid state such as fumed silica, polysiloxane, colloid silica, etc.

After the first charging, both types are observed a certain amount of an electrolyte in the AGM separator or the gelled electrolyte that has been displaced by gas from larger pores in the felt or cracks of the gel. This liquid can be removed by suction to provide a void volume for fast oxygen transport in the separator. Otherwise, space is automatically formed by the gradual loss of water due to electrochemical decomposition. In the latter case, the rate of the internal oxygen cycle at the beginning is limited, and the battery initially operates partly like a flooded. A further advantage is that acid fumes do not escape from cells with immobilized electrolyte since they are hardly generated and there is no gas stream to carry them out of the cell.

2.1.4 Construction of VRLA battery

The construction of VRLA battery was shown in Fig.2.1. The different main component between flooded lead acid battery and VRLA battery is valves which allow some of gas in battery to escape and separator. The VRLA battery consists of:

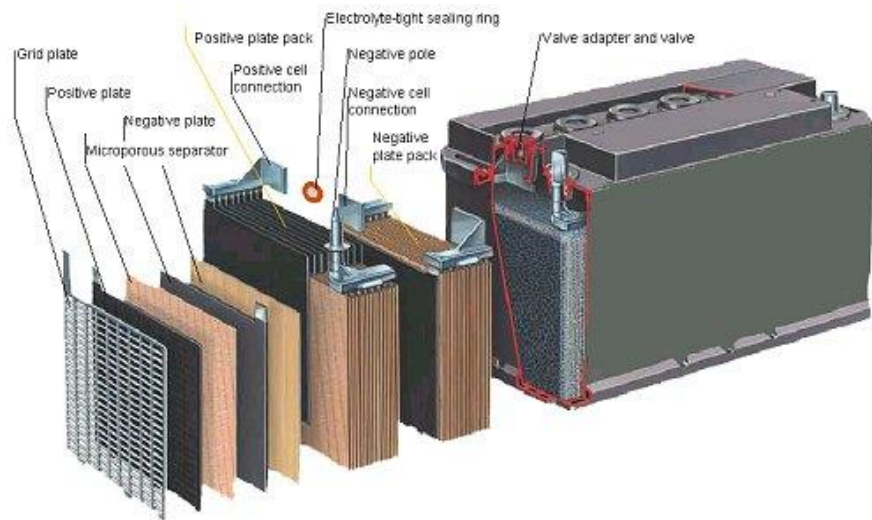


Figure 2.1 The construction of VRLA battery [5].

Active material in positive electrodes is occupied by lead dioxide about 50% of their volume. The other 50% is pores. The polymorphs of lead dioxide occur α -PbO₂ and β -PbO₂ in the active material. When the battery has been discharged and is charged again, only β -PbO₂ is formed on account of the acidic environment. For this reason, the content of α -PbO₂ decreases with the number of discharge/charge cycles, especially at an initially high α -PbO₂ content. Plates containing much α -PbO₂ show reduced initial capacity, which gradually increases on account of the conversion of α -PbO₂ into β -PbO₂.

Active material in negative electrodes is fairly fine crystals of metallic lead. As number of additives are required to preserve this fine structure and the performance of the active material as far as possible. Otherwise, decreasing of capacity is caused from charge to recharge mainly because of growth of metallic crystals and thereby active surface area is reduced. Additives required for the negative active material are called expanders because they expand the surface area of the lead electrode, or at least preserve its large true surface area. The general, expanders in total are added to less than 1%wt. Usual expander are BaSO₄, lignin, alizarine red, methyl orange, oil, etc.

Grid or plate support has to provide mechanical support for the active material and electronic conductivity for the collected current. Early grid materials for VRLA batteries consisted of pure lead or lead-calcium alloys for both the positive and negative plates. The selection of grid alloys must not only consider fabrication requirements, mechanical strength, but also corrosion resistance and creep strength, and must pay attention to the electrochemical problems. Many additives were added to the grid alloy such as tin (Sn), antimony (Sb), cadmium (Cd), aluminium (Al), etc.

Separator has not only to prevent electronic contact between positive and negative electrode, but it also has to provide space for the required volume of electrolyte. Furthermore, the separator must suppress the growth of lead dendrites from the negative to the positive electrodes when lead is precipitated during charging. The separator has been used such as polyvinylchloride (PVC), absorbent glass mat (AGM), polyethylene (PE) for VRLA battery.

Electrolyte is sulfuric acid solution which contain free ions to create the electrically conductive. Typical specific gravities of VRLA cells range from 1.250 to 1.340. By design, absorbed electrolyte VRLA cells have lower volumes of electrolyte than vented cells containing equivalent amounts of active materials. If AGM cells had the same electrolyte specific gravity as vented cells, they would exhibited the lower long-duration capacities. In gelled electrolyte cells, the gel interferes with electrolyte diffusion and convection, which results to reduce the high-rate capacities. A higher specific gravity results in higher capacity per unit volume. It also increases the chemical activity, thereby causing an increased positive plate corrosion rate. The increased corrosion reduces the service life of the battery.

Connecting elements are used to connect several electrodes of each polarity in parallel per cell to enlarge the surface area (except in cells with wound electrodes). Furthermore, a battery is mostly formed by a number of cells that have to be connected with one another. Depending on the layout of the battery, the outside plates can be positive or negative polarity. It is more customary to have negative plates at both outsides, that consists of n positive and $(n+1)$ negative plates.

Valve or battery cell plug is an essential element for VRLA batteries. It allows only the escape of gas at a certain overpressure but prevent any intake of air, which would cause discharge of the negative electrodes. It has to prevent a too high pressure within the cell that leads to deform the container (bulging of the cell) and may cause problems in regard to the contact pressure within the plate block. One design of valve is based on a rubber (or an elastomer) ring or cap that used to close the opening the cell in normal conditions, but is blown open when the internal pressure exceeds (a specific limit).

Battery case has first to keep the electrolyte within the cell, which requires proper sealing of the termination and connection between the container and its lid with VRLA batteries. In addition, air intake has to be prevented, since penetration of oxygen into the cell causes self-discharge. Furthermore, the container has to provide mechanical support for the plate group and in VRLA batteries a desired definite compression of the

separator, mentioned the mechanical stress on the container is increased, since then the internal pressure can vary and be different from the external pressure. There are various kinds of material for battery case such as ABS (acrylonitrile; butadiene, styrene), PC (polycarbonate), PP (polypropylene), PVC (polyvinyl chloride), SAN (styrene, acrylonitrile) [4].

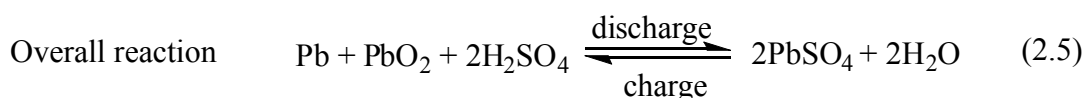
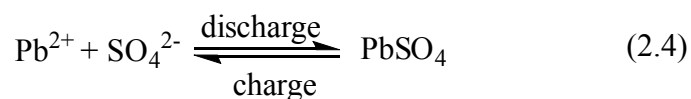
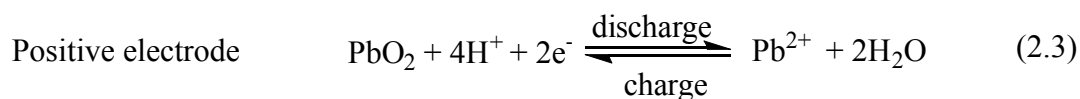
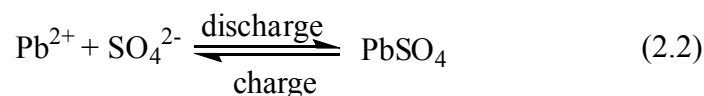
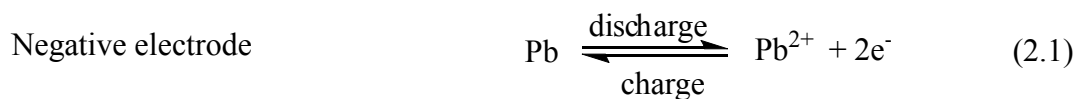
2.1.5 Applications of VRLA battery [1]

Mostly, the VRLA battery is one choice for small, medium and large scale energy storage system. There is increased demand in various applications for instance photovoltaic (solar), automotive, telecommunication and UPS system.

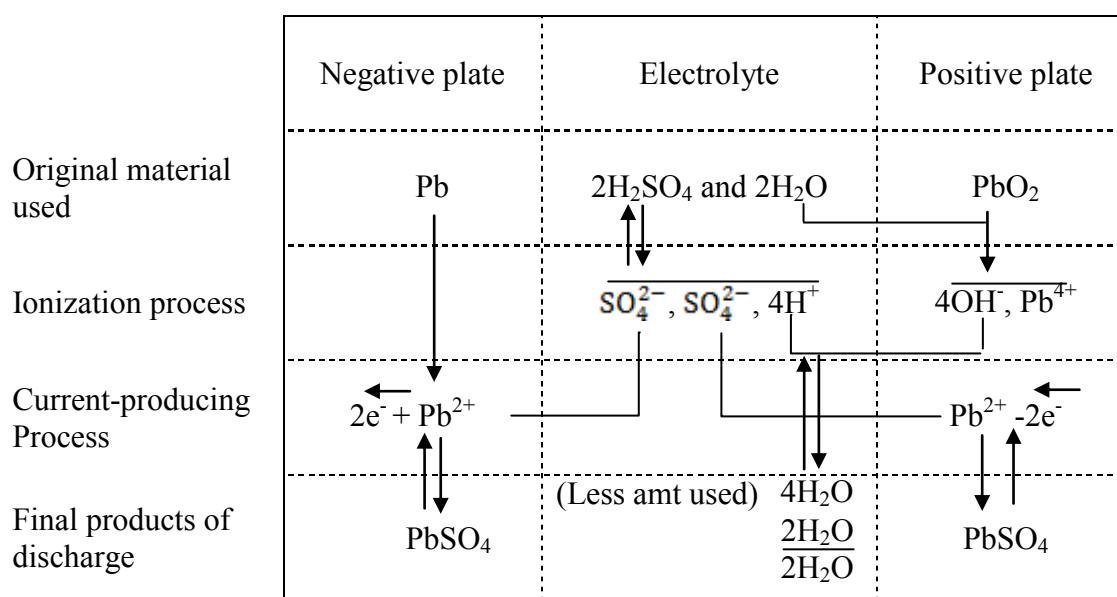
2.2 Performance characteristics of VRLA battery

2.2.1 Electrochemical reactions [2, 6-7]

The electrochemistry in VRLA battery reacts as same as the lead acid battery. Typically, a charged positive electrode contains both α -PbO₂ (orthorhombic) and β -PbO₂ (tetragonal) variations. The equilibrium potential of the α -PbO₂ is more positive than that of β -PbO₂ by 0.01 V. The α form is also larger and has a more compact crystal morphology, lead to have less active electrochemical reaction and slightly lower in capacity per unit weight, however, it promotes a longer cycle life. The preparation of the active material precursor consists of a series of mixing and curing operations using lead and lead oxide (PbO + Pb), sulfuric acid, and water. The ratios of the reactants and curing conditions (temperature, humidity, and time) affect to the development of crystallinity and pore structure. The plate curing consists of lead sulfate, lead oxide, and some residual lead (<5%). The electrolyte is a sulfuric acid solution, typically with a specific gravity of 1.28 or 37% acid by weight in a fully charged condition. As the cell discharges, both electrodes are converted to lead sulfate. The process reverses on charge:



The discharge-charge mechanism, known as the double-sulfate reaction, is shown graphically in Fig. 2.2. As the sulfuric acid in the electrolyte is consumed during discharge and produces water, the electrolyte in certain battery designs can be the capacity-limiting material.



(a)

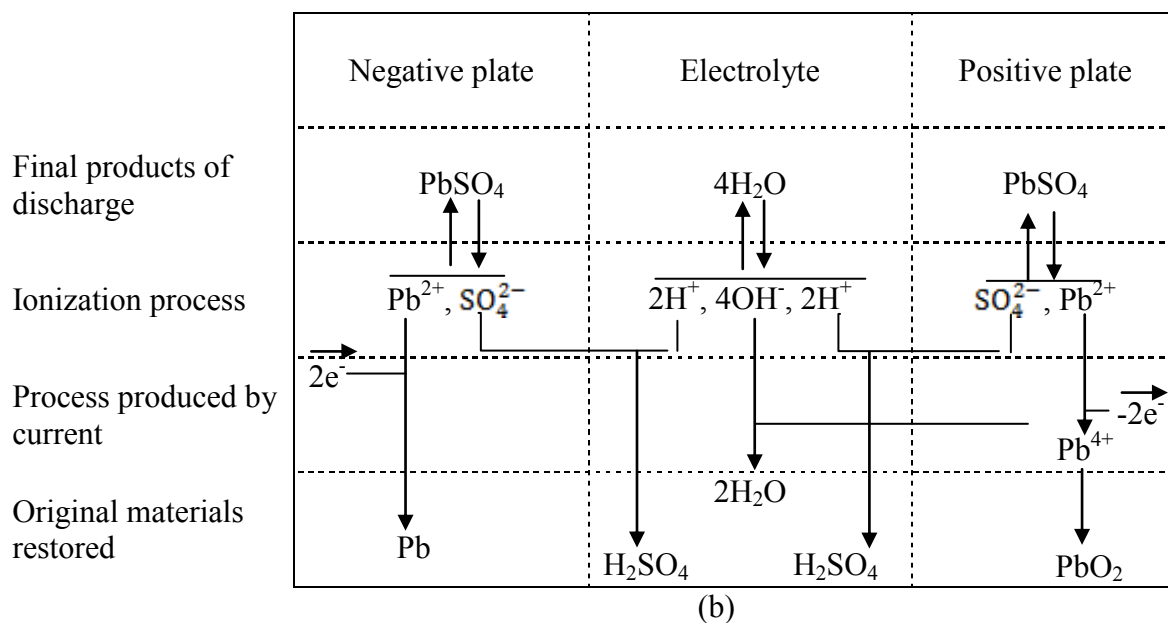
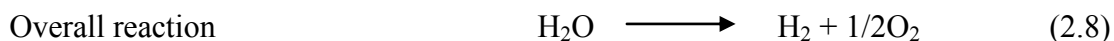
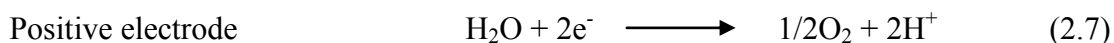
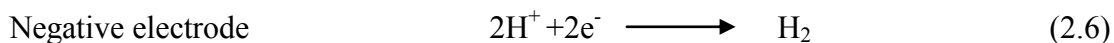


Figure 2.2 Discharge and charge reactions of the lead-acid cell. (a) Discharge reactions. (b) Charge reactions [2, 7].

When the cell approaches is full charge and the majority of the PbSO₄ has been converted to Pb or PbO₂, the cell voltage becomes greater than the gassing voltage (about 2.39V per cell) and the overcharge reaction begins, resulting in the production of hydrogen and oxygen (gassing) and the resultant loss of water. In VRLA cells this reactions is controlled to minimize hydrogen evolution and the loss of water by recombination of the evolved oxygen with the negative plate as shown below.



The general performance characteristics of the lead-acid cell, during charge and discharge, are shown in Fig. 2.3. As the cell is discharged, the voltage decreases due to depletion of the material, internal resistance losses, and polarization. If

the discharge current is constant, the voltage under load decreases smoothly to the cutoff voltage, and the specific gravity decreases in proportion to the discharge capacity (ampere-hours discharged).

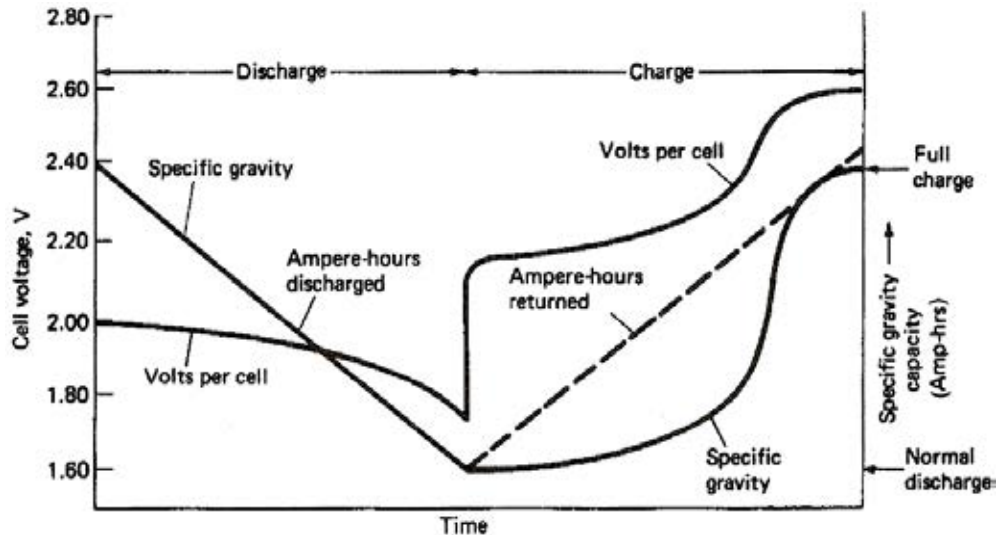


Figure 2.3 Typical voltage and specific gravity characteristics of lead-acid cell at constant rate discharge and charge [2].

2.2.2 Equilibrium voltage [4]

The dependence of the equilibrium voltage on concentration is given by the Nernst equation. The right hand side of the equation at temperature 298 K and the conversion $\ln = 2.303 \cdot \log$ can be expressed for a lead-acid battery as:

$$U^{\circ} = 1.923 - \frac{R \cdot T}{2 \cdot F} \cdot \ln \frac{(a_{H_2O})^2}{(a_{H^+})^2 \cdot (a_{HSO_4^-})^2} = 1.923 + 0.0592 \cdot \log \frac{a_{H^+} \cdot a_{HSO_4^-}}{a_{H_2O}} \quad (2.9)$$

where; U° is the equilibrium voltage of the cell (V)

R is the molar gas constant for an ideal gas ($8.3145 \text{ J} \cdot \text{K}^{-1} \cdot \text{mol}^{-1}$)

T is the temperature (K)

F is the Faraday constant (96,485 coulombs/equivalent.)

a_i is activity of the reacting component ($\text{mol} \cdot \text{cm}^{-3}$)

and the equilibrium voltage applies when the activities of the soluble components of the reaction, namely H^+ , HSO_4^- and H_2O amount to 1 mol/dm^3 , respectively.

According to this equation the equilibrium cell voltage depends only on the acid concentration and is independent of lead, lead dioxide and lead sulfate which present in the battery.

Results of equation (2.9) are plotted in Fig. 2.3 and also compiled in the column “Cell voltage” in Table 2.2 together with the single electrode potentials.

In battery practice, the approximation:

$$\text{Equilibrium cell voltage} = \text{acid density (in g/cm}^3 \text{ or kg/dm}^3) + 0.84 \quad (2.10)$$

Equation (2.10) is used instead of equation (2.9). Fig. 2.4 shows that the calculated curve and the approximate formula coincide quite well.

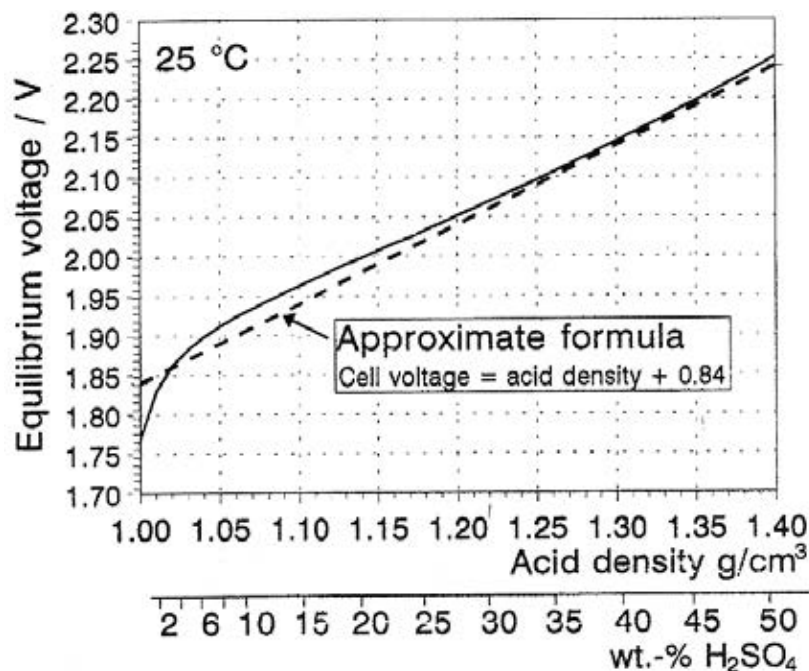


Figure 2.4 Equilibrium cell voltage of the lead-acid battery referred to acid density and acid concentration in weight% H_2SO_4 . The dashed line represents the approximation of equation (2.10) [4].

According to the equation (2.9), the equilibrium potential depends on the acid concentration. On the other hand H_2SO_4 participates in the electrode reaction, the electrolyte becomes more diluted during discharge and is re-concentrated during the charge. The participation of H_2SO_4 in the cell reaction has considerable consequences. This means that the cell voltage does not remain constant even at low discharge rates, and the conductivity of the acid varies when the battery is charged or discharged. If the discharge occurs in cold climates, the acid may be frozen. On the other hand, in flooded cells, acid dilution may be used as a tool to determine the state of charge.

Table 2.2 Acid-concentration parameters: acid density (kg/L), H_2SO_4 content and H_2SO_4 concentration in mol/L, and molality. Cell voltage and electrode potentials referred to the standard hydrogen electrode, $T=25^\circ\text{C}$.

Acid-concentration				Cell Voltage U° Volts	Electrode potentials	
Dens. kg/L	H_2SO_4 wt.%	Molarity mol/L	Molality mol/kg H_2O		V ref. to std. Positive	H_2 electrode Negative
1.02	3.48	0.362	0.367	1.860	1.595	-0.265
1.03	5.00	0.525	0.537	1.883	1.607	-0.276
1.04	6.49	0.688	0.708	1.899	1.616	-0.283
1.05	7.77	0.832	0.859	1.913	1.623	-0.290
1.06	9.42	1.018	1.060	1.924	1.630	-0.294
1.07	10.86	1.184	1.242	1.935	1.634	-0.301
1.08	12.28	1.352	1.428	1.945	1.641	-0.304
1.09	13.69	1.521	1.617	1.955	1.645	-0.310
1.10	15.08	1.691	1.811	1.964	1.650	-0.314
1.11	16.45	1.861	2.007	1.973	1.654	-0.319
1.12	17.80	2.032	2.207	1.982	1.659	-0.323
1.13	19.13	2.204	2.412	1.991	1.663	-0.328
1.14	20.46	2.378	2.623	2.000	1.668	-0.332
1.15	21.78	2.553	2.838	2.008	1.673	-0.335
1.16	23.08	2.729	3.059	2.017	1.667	-0.340
1.17	24.36	2.906	3.283	2.026	1.682	-0.344
1.18	25.63	3.084	3.514	2.034	1.687	-0.347
1.19	26.89	3.262	3.749	2.043	1.691	-0.352
1.20	28.14	3.443	3.992	2.052	1.696	-0.356
1.21	29.38	3.625	4.242	2.061	1.700	-0.361
1.22	30.61	3.807	4.498	2.070	1.705	-0.365

Table 2.2 Acid-concentration parameters: acid density (kg/L), H₂SO₄ content and H₂SO₄ concentration in mol/L, and molality. Cell voltage and electrode potentials referred to the standard hydrogen electrode, T=25°C (continued).

Acid-concentration				Cell Voltage U° Volts	Electrode potentials	
Dens. kg/L	H ₂ SO ₄ wt.%	Molarity mol/L	Molality mol/kg H ₂ O		V ref. to std. Positive	H ₂ electrode Negative
1.23	31.83	3.992	4.760	2.079	1.710	-0.369
1.24	33.05	4.178	5.033	2.088	1.715	-0.373
1.25	34.25	4.365	5.311	2.097	1.720	-0.376
1.26	35.44	4.553	5.597	2.107	1.725	-0.381
1.27	36.62	4.742	5.892	2.116	1.730	-0.386
1.28	37.79	4.932	6.194	2.126	1.735	-0.391
1.29	38.95	5.123	6.506	2.136	1.740	-0.396
1.30	40.10	5.315	6.826	2.145	1.745	-0.400
1.31	41.24	5.508	7.155	2.156	1.751	-0.405
1.32	42.37	5.702	7.496	2.166	1.757	-0.409
1.33	43.49	5.897	7.846	2.176	1.762	-0.414
1.34	44.59	6.092	8.206	2.187	1.768	-0.419
1.35	45.68	6.287	8.573	2.197	1.773	-0.424
1.37	47.80	6.677	9.336	2.219	1.783	-0.436
1.38	48.85	6.873	9.738	2.230	1.788	-0.442
1.39	49.89	7.070	10.149	2.241	1.794	-0.447
1.40	50.91	7.267	10.573	2.252	1.800	-0.452

2.2.3 Electrolyte stratification [3]

Electrolyte stratification is connected with the changes of the specific weight of the electrolyte associated with the concentration changes during charge and discharge. In flooded lead-acid batteries, an acid stratification may cause severe problems. The immobilization of the electrolyte in VRLA batteries, reduces stratification effects to a large extent, or practically eliminates them in a gelled electrolyte.

In Fig. 2.5 illustrates the origin of acid stratification. On the left, the battery has been floated for an extended period, or the electrolyte has been mixed by other means. The acid concentration is uniform all over the battery. This will always be

the final state when the battery is on float, because the diffusion process always equalizes the acid concentration. Stratification can only be caused by discharge/charge processes.

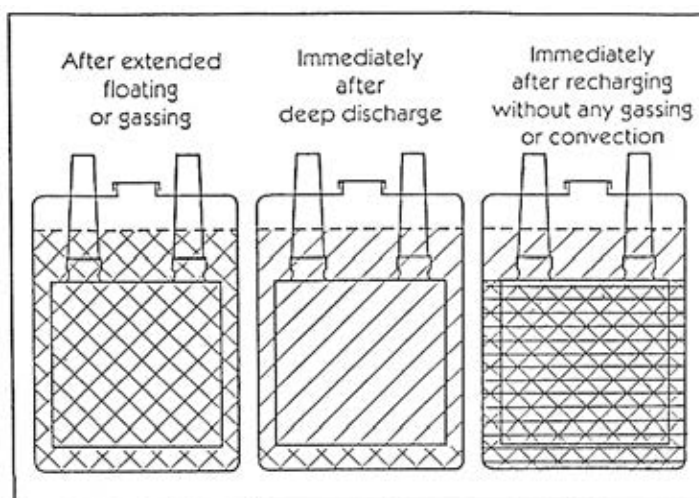


Figure 2.5 The origin of acid stratification, when the lead-acid battery is discharged and recharged without gassing or other means of mixing the electrolyte [3].

During charge, sulfuric acid is released from the active material in the plates and the concentration of the acid increases between the plates. Now the highest acid concentration is achieved between plates which initiate convection of this acid to the parts beside and underneath the plates. At the end of the charging process, the battery is filled with a slightly increased acid concentration to the upper edge of the plates. The acid above the plates remains diluted and there is no driving force for convection because of the low weight of this acid.

In the usual stationary application, acid stratification causes no problems, because the batteries are discharged only occasionally. There is enough time left for the diffusion to equalize the acid concentration. Furthermore, acid stratification may become dangerous because the concentration differences between the top and bottom parts of the cell are growing from cycle to cycle, especially in tall cells. The increasing acid concentration at the bottom may harm the negative plate, which is prone to sulfation when running in too high an acid concentration.

As a remedy against stratification, overcharging by 10 to 20% during each cycle is mostly applied for traction batteries. The gas evolution forms bubbles that mix the electrolyte. An immobilization of the electrolyte, as required for VRLA batteries, eliminates stratification effects almost completely.

2.2.4 Conductivity of sulfuric acid [4]

Due to the concentration changes during the charge or discharge reactions, the conductivity of the sulfuric acid also varies as shown in Fig. 2.5.

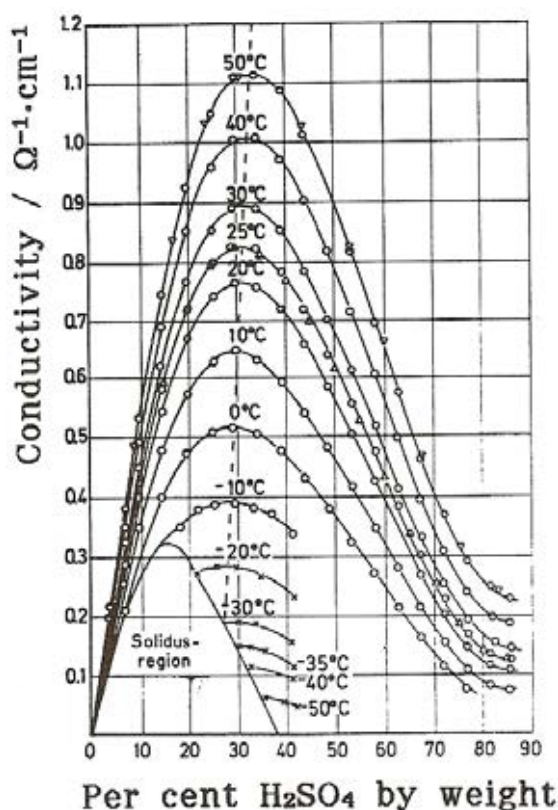


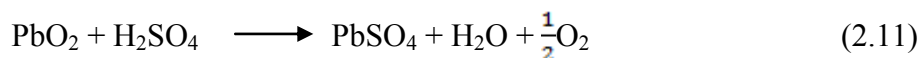
Figure 2.6 Specific electric conductance of aqueous solution of sulfuric acid and its dependence on temperature. The dotted line denotes the maximum [4].

This Figure shows that in charged batteries, the acid conductivity is close to its maximum. During deep discharge, the conductivity can reach fairly low values. Furthermore, the conductivity is considerably reduced at low temperatures.

2.2.5 Self-discharge [2]

The equilibria of the electrode reactions are normally with the discharged state being the most thermodynamically stable. The rate of self-discharge in lead-acid cell is fairly rapid but it can be reduced significantly by incorporating certain design features.

The rate of self-discharge depends on several factors. Lead and lead dioxide are thermodynamically unstable in an open circuit, they react with the electrolyte. Oxygen is evolved at the positive electrode and hydrogen at the negative, a rate of oxygen-hydrogen evolution depends on the overvoltage, temperature, and acid concentration (the gassing rate increases with increasing acid concentration) as shown follows:



For positives electrodes, the PbSO_4 formation by self-discharge is slow, typically much less than 0.5%/day at 25°C. The self-discharge on the negative electrode is generally more rapid, especially if the cell is contaminated with various metallic ions. For example, antimony lost from the positive grids by corrosion can diffuse to the negative, where it is deposited resulting in a local action discharge cell which converts some lead active material to PbSO_4 .

2.2.6 Aging and failure mechanisms [8]

The common failure mechanisms of positive plate corrosion and growth, active material failure, post seal leakage, and container seal leakage associated with vented cells also occur in VRLA cells. Some of these degradation mechanisms are more significant in the VRLA cell design. Also VRLA cells are susceptible to additional failure modes that are normally not associated with vented cells. The aging effects and failure modes are described in 2.2.6.1 through 2.2.6.7.

2.2.6.1 Dryout

A vented battery is expected to require periodic watering to restore lost water. While VRLA battery is usually irreversible in most designs because water cannot easily be added to the cell. As the VRLA cell loses water, it will eventually experience loss of capacity due to dryout.

The recombination process tends to be somewhat self-regulating in that recombination efficiency improves water loss. When first put into service, VRLA cell can lose water until it reaches optimal recombination efficiency, with little water loss thereafter. However, other effects which occur during normal and abnormal operation can also result in water loss and corresponding capacity loss. The effects are such grid corrosion, overcharging, high temperature, water vapor diffusion.

2.2.6.2 Thermal runaway

When a VRLA cell is operating overcharge in a fully recombinant mode, almost all of the overcharge energy results in heat generation. The additional current results in more recombination and heat generation that further raises battery temperature, and so on. The net effect can be accelerated dryout and/or melting of the battery. The potential problem is further aggravated by elevated ambient temperatures or by cell or charging system malfunctions. The possibility of thermal runaway can be minimized by using appropriate ventilation/cooling between around the cells and by limiting the charger output current and voltage such as by using temperature-compensated chargers. In the gelled electrolyte system provides better thermal conductivity than the absorbed electrolyte system but is still inferior to a vented system.

2.2.6.3 Negative plate self-discharge

Although the basic principle of the recombination process might be relatively easy to understand, the actual implementation in a VRLA cell is quite complicated. A delicate balance is maintained among oxygen recombination, positive grid corrosion and negative plate self-discharge (plate sulfation). If the balance is

incomplete, the negative plate may slowly self-discharge. Research has determined that premature loss of the capacity in VRLA cells is often due to a gradual discharge of the negative plates. Manufacturers may address this issue by using modified active materials to reduce the rate of negative self-discharge, or through the use of catalysts.

2.2.6.4 Seal or valve failures

Air ingress through a pressure relief valve or container crack can also lead to an eventual discharge of the negative plate. The cell will lose capacity while the negative plate discharges. Thus, air ingress is a failure mode for VRLA cells.

2.2.6.5 Temperature effects

The VRLA batteries tend to be more susceptible to degradation aging at higher temperatures than vented lead-acid batteries. The recombination process that allows these batteries to operate without the need for periodic water addition also generates heat. Some VRLA installations may have the cells tightly packed, limiting heat dissipation capability. All of these factors can combine to cause the VRLA battery to operate at a higher-than-ambient temperature, thereby decreasing battery life. Higher temperatures will also increase the possibility of dryout and susceptibility to thermal runaway.

2.2.6.6 Loss of absorbed glass mat compression

Loss of compression can be caused by relaxation of the container, due to container design and/or high-temperature environments. Small voids can develop between the mat and the plates, thereby decreasing the available capacity. Battery manufacturers have used various methods and materials to limit container expansion.

2.2.6.7 Ripple current

The direct current (DC) depends on the magnitude and frequency, this superimposed ripple can produce additional heating. VRLA cells appear to be more sensitive to the heating effect because of their lower heat transfer coefficient compared to

vented cells. A higher internal temperature in cells contributes to a decrease in expected service life.

2.2.7 Electrolyte specific gravity

By design, absorbed electrolyte VRLA cells have lower volumes of electrolyte than vented cells containing. If AGM cells had the same specific gravity of electrolyte as vented cells, they would exhibit lower long-duration capacities. In gelled electrolyte cells, gel interferes with electrolyte diffusion and convection, which results in reduced high-rate capacities. In both cases, the expected reductions in capacity may be partially compensated by increasing the specific gravity of electrolyte.

A higher specific gravity results in higher capacity per unit volume. It also increases chemical activity and causing an increased positive plate corrosion rate. An increased corrosion reduces the service life of the cell.

2.2.8 Charging voltage

2.2.8.1. Float voltage

The actual float voltage depends upon the specific gravity of the electrolyte being used. The recommended float voltage is provided by the battery manufacturer. This voltage is sufficient to keep the battery fully charged without causing excessive positive grid corrosion or forcing the battery to draw more current than is required to maintain a charge.

2.2.8.2 Temperature compensation of charging voltage

Temperature-compensated charging is any method of adjusting the output voltage of the battery charger to compensate for deviations in the battery operating temperature above or below a standard value, typically 25°C (77 °F). Owing to VRLA batteries are much more susceptible to thermal runaway than vented cells, temperature-compensated charging is strongly recommended when they are used in a constant voltage float charge regime.

2.2.9 Historical service life

The designed life of the cell is related to the intrinsic mechanical, electrochemical characteristics, and electrical of the cell. The designed life of the cell is rarely attained as a service life at the system level due to a variety of factors, including the mentioned in 2.3.3.

The industry experience shows that the actual VRLA battery system service life is often considerably less than its designed life. Also, the service life may be further reduced by environmental operating conditions in which the battery is placed. Although manufacturing practices continue to improve, and the new techniques have been developed to address particular failure modes, the user should not plan for the batteries to last the entire designed life for a single cell or multicell unit. In summary, VRLA cells will not last as long as vented cells.

2.3. Battery parameters and definition [4]

2.3.1 Current

When the battery is discharged, the active material in the positive electrode is reduced. A reducing current flow is called cathodic. In the negative electrode, the active material is oxidized by an anodic current. Both terms are strictly connected to the direction of current flow through the concerned electrode. During charging, the situation is reversed.

2.3.2 Voltage

The cell voltage was used to characterizes the battery system. The equilibrium voltage cannot exactly be measured even at open circuit, since secondary reactions cause a slight deviation. The open circuit voltage (OCV) or open cell voltage actually is measured. The cell voltage often is a function of the state of charge (SOC). Especially immediately after charging a slightly increased voltage may be measured due to oxides of higher valence that had been formed. Because of the instability of such

higher oxides, this excess voltage fades away within hours or days. The cell voltage under load, the closed circuit voltage (CCV), depends on the current, the state of charge, and on the cell's history which might influence its internal resistance. A further term is the nominal voltage of approximates the voltage of the concerned battery system for its characterization.

2.3.3 Capacity [9]

The battery delivers energy and the amount of this energy is described as a capacity (C). The nominal or rated capacity of a battery (C_r) is often referred to different durations. The current is expressed as a multiple of the capacity:

$$C = I\Delta t \quad (2.13)$$

with

I	=	current in ampere (A)
C	=	capacity in ampere-hour (Ah)
Δt	=	charge or discharge period

2.3.4 Cycling, Depth of discharge (DOD) [4, 9]

Batteries based on chemical reactions and the involved components undergo substantial changes during discharging or charging. The number of discharging/charging cycles and the depth of discharge (DOD) influence service life significantly. The relation between depth of discharge and the achieved cycle numbers for VRLA battery was shown in Fig. 2.7.

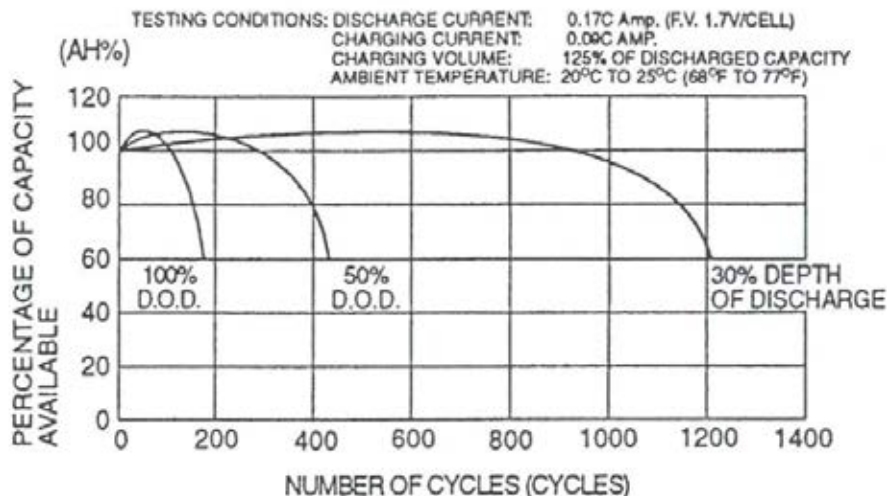


Figure 2.7 Cycle service life in relation to depth of discharge for VRLA battery [4].

2.3.5 Deep discharge

A special situation is caused by deep discharging which means that the battery is discharged beyond the end of discharge voltage specified by the manufacturer. Then an excessive capacity is drawn from the battery, the conversion of the active material is extended beyond the normal limit, and even reversal of the positive or negative electrode to its opposite sign may be included. Thus, the deep discharging means increased stress to the active material. It may diminish the possibility to re-establish the original structure by recharge, and can shorten the service life markedly. The deep discharge effects indicate that the high-rate discharge to low end voltages does not harm batteries unless heat evolution is too high. Complete discharges at low current densities, with excessive utilization of the active material, are more harmful.

2.3.6 Internal resistance

The internal resistance of a battery is an important parameter since a battery that is suitable for high-rate discharges must have a low internal resistance, otherwise the voltage drop, caused by the current, would limit the discharge too early.

$$R = V/I \quad (2.14)$$

Where: V = voltage (volts), I = current (amperes) and R = resistance of the solution (ohms). The internal resistance depends on the state of charge of the battery. At reduced temperature, the internal resistance is increased owing to reduced conductivity and retarded kinetic parameter.

2.3.7 Service life

The service life of the battery is necessarily limited and life expectancy of batteries an important question. Service life is judged differently, depending on the application of the battery. For standby batteries, which are only rarely discharged, service life expressed in calendar time is important parameter. For other applications, service life is characterized by the possible number of discharge/charge cycles.

2.3.8 Specific gravity

The specific gravity is used instead of sulfuric acid density in battery practice. The specific gravity is a dimensionless quality, namely the ratio

$$\text{Specific gravity} = \frac{\text{density of the acid}}{\text{density of water}} \quad (2.15)$$

The specific gravity includes the temperature dependence of the density of water. The differences between specific gravity and density are rather small and can usually be neglected.

2.4 Advantages for VRLA battery

Some of the advantages and disadvantages include the followings:

(i) *No watering*: Because VRLA cells do not need watering, many users operate them on an install and forget basis. This does not excuse the user from

maintenance. Those who do not perform maintenance open themselves up to an increased risk of battery failure.

(ii) *Easier installation:* VRLA batteries are typically less costly to install than vented batteries, and can be installed in less time than equivalently sized vented batteries.

(iii) *Non-spillage:* VRLA batteries that have passed the appropriate qualification tests set forth in the Code of Federal Regulation (CFR 49) can be classified by the U.S. Department of Transportation (DOT) as UN2800 – Batteries, Non-Spillage for road shipments (CFR 49). This classification allows these batteries to be transported with fewer restrictions than vented batteries. VRLA batteries can also be air-shipped as non-spillage, non-dangerous, as long as they meet the non-spillage requirements mentioned above, in addition to a separate International Air Transport Association (IATA) requirement (A67) for a puncture test. Because they are essentially non-spillage, most VRLA cells can be placed in more convenient space-saving configurations, such as front terminal, or horizontal.

(iv) *Thermal issue:* VRLA batteries are more inclined to potentially destructive and dangerous thermal runaway. They also have short lifetime in high temperature environments.

(v) *Long life:* VRLA batteries (even when kept in similar environments) have much longer average lifetimes than vented lead-acid batteries.

In this research, the gelled electrolyte was chosen. Fumed silica was used as a gelling agent, mixed to sulfuric acid and added to batteries forms a solid gel. It becomes a thixotropic gel that can be kept highly liquid by intensive agitation, which is taken advantage of when filling the battery.

2.5 Gelled electrolyte immobilization with fumed silica (pyrogenic silica) [10]

Fumed silica, also known as Pyrogenic silica is a very fine dispersed SiO_2 powder with Primary particle size 5–50 nm. Fumed silica particle can be seen with Transmission Electron Microscopy (TEM), as shown in Fig. 2.7 (a) and (b). Due to the small size of primary particles, the internal surface is very high, with measured as BET-surfaces of 50-600 m^2 per gram.

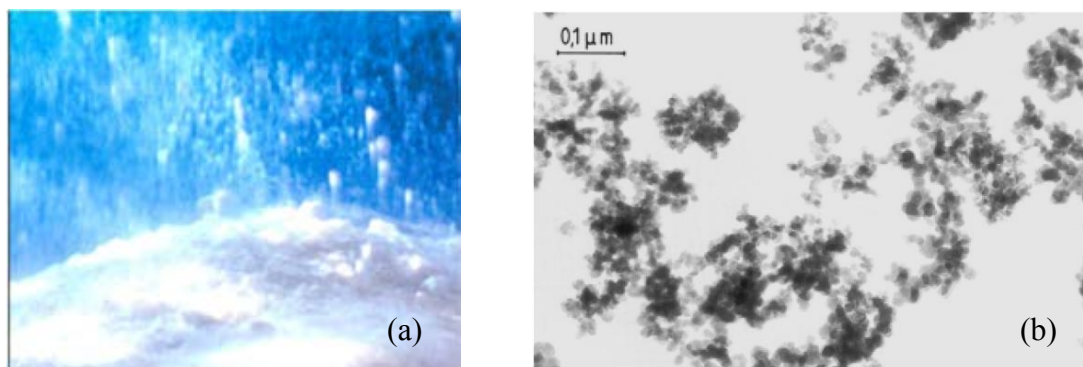


Figure 2.8 (a) Powder of pyrogenic silica and (b) TEM of pyrogenic silica [10].

The manufacturing process of pyrogenic silica:

Evaporation of silicon chloride is blown in an oxygen-hydrogen flame. At temperatures above 1500°C , SiO_2 molecules are formed. The SiO_2 molecules strongly bound in siloxane groups (Si-O-Si) bind together to spherical primary particles of 10 nm particles. As the particles move to colder areas, they bind together to form a chain-like aggregates with lengths up to approximately $1\mu\text{m}$. After further cooling, they form the agglomerates with a diameter of 10 to $250\mu\text{m}$. The binding force between primary particles is the hydrogen bridge linkage. The silanol groups (Si-O-H) of two particles come in contact and create the bridge linkage by exchanging their hydrogen atoms (Fig. 2.8).

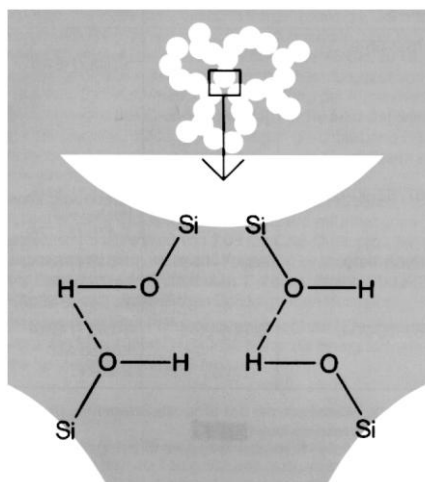


Figure 2.9 Hydrogen bridge linkages between particles [10].

These agglomerated aggregates of SiO_2 particles are mixed with acid and water, forming a liquid GEL (SOL). A silica gel or a sol will be formed in sulfuric acid solution as a colloidal silica gel after dispersed (Figure 2.9). The sulfuric acid solution is a weak hydrogen-bonding, aqueous media because the SO_4^{2-} ion plays a steric hindrance role. The silica particles are envisioned to interact directly with each other through hydrogen-bonding interactions between the surface silanol (Si-OH) groups. It is believed that hydrogen bonds interactions are responsible for the gel formation, not Van der Waals interactions. Therefore, a uniform distribution of silica particles in sulfuric acid would help to optimize the interaction of surface silanol (Si-OH) groups on the silica particles, resulting in the formation of the uniform, microscopic, three-dimensional gel structure, which provides the gel with high capacity and low inner resistance.

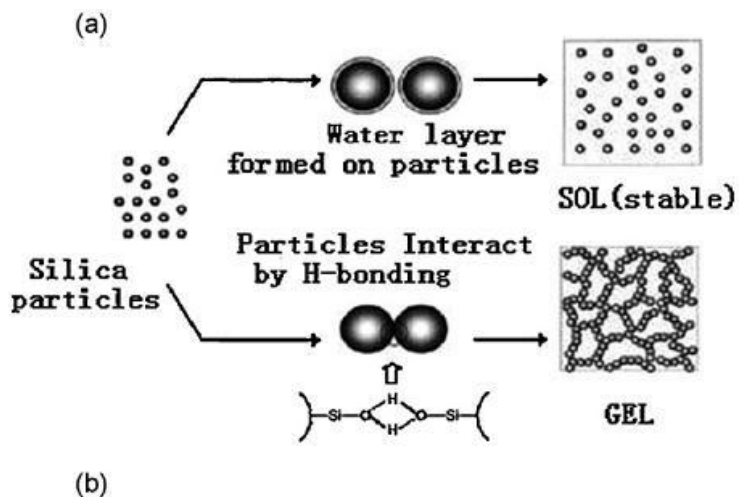


Figure 2.10 Interaction effect of solvent between fumed silica particle: (a) a strongly hydrogen-bonding liquid (water layer/hydration force is formed on the particles by hydrogen-bonding, resulting in a stable sol); (b) a weakly hydrogen-bonding liquid (the particles interact directly by hydrogen-bonding to form a gel) [11]

After several hours of setting, the hydrogen bridge linkages form a three-dimensional structure. This is the GEL, seen in the right hand side of Fig. 2.10.

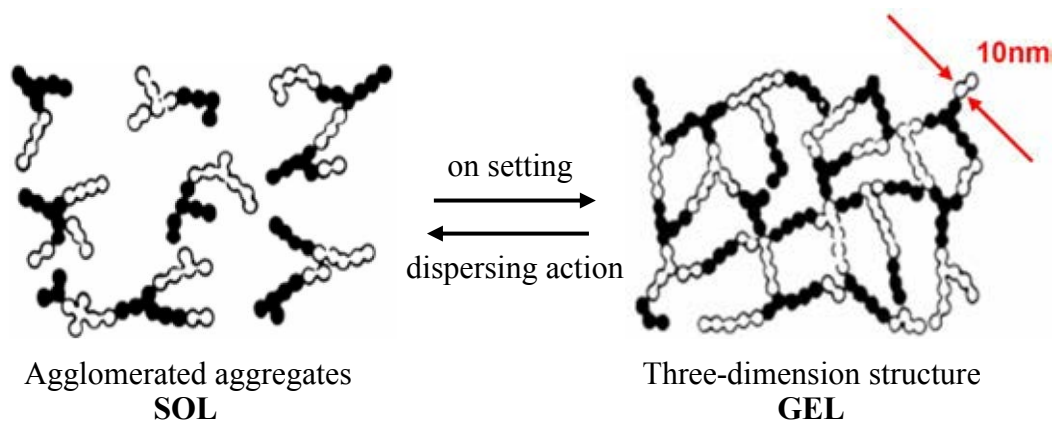


Figure 2.11 The formation of the GEL structure is reversible at the beginning, by dispersing SOL and by setting GEL [10].

The most important information is that sulfuric acid solution are trapped in this structure, which is formed by chains with a diameter of only 10 nm or 0.01 μ m.

2.6 Additives

2.6.1 Polypyrrole (PPy) [12]

Beginning in July 1988, conducting polymers were applied in various applications such as batteries, photovoltaic cells, chemical sensors, semiconductor devices and optical switches.

Among the conducting polymers, PPy has attracted great attention because of its high electrical conductivity and good environmental stability. PPy has been considered as the key material to many potential applications such as electronic devices, electrodes for rechargeable batteries and supercapacitors, solid electrolytes for capacitors, electromagnetic shielding materials, sensors, corrosion-protecting materials, actuators, electrochromic devices, or membranes [13-22]. The hetero-aromatic and extended π -conjugated backbone structure of PPy provides chemical stability and electrical conductivity, respectively. The π -conjugated backbone structure is not sufficient to produce appreciable conductivity on its own. Partial charge extraction from PPy chain is also required, which is achieved by a chemical or an electrochemical process referred to the doping. The conductivity of the neutral PPy is remarkably changed from an insulating regime to a metallic by doping. This is a very worthwhile feature for applications in which the electrical conductivity of the material must be controlled.

There was a report that the electronic and band structures of PPy were changed with the doping level of PPy chain. Neutral PPy, with the benzenoid structure shown in Fig. 2.11a, is categorized as an insulator and its proposed electronic energy diagram is shown in Fig. 2.12a. The band gap of neutral PPy is reported as 3.16 eV, which is too wide for electrons to transfer from the valence to the conduction band at room temperature. PPy chain is simultaneously doped during polymerization. Counteranions in the reaction medium are incorporated into the growing of PPy chain that can maintain electrical neutrality of the polymer system. Upon extraction of a negative charge from a neutral segment of PPy chain by doping process, a local deformation to the energetically favored quinoid structure occurs (Fig. 2.11b). In combination with the quinoid structure, the positive charge and the unpaired spin are

referred to as a polaron (Fig. 2.11b). Referring to Fig. 2.12b, the formation of a polaron induces two new intermediate states (bonding and antibonding) within the band gap while the unpaired electron occupies the bonding (low energy) state, thus giving the polaron a spin of 1/2.

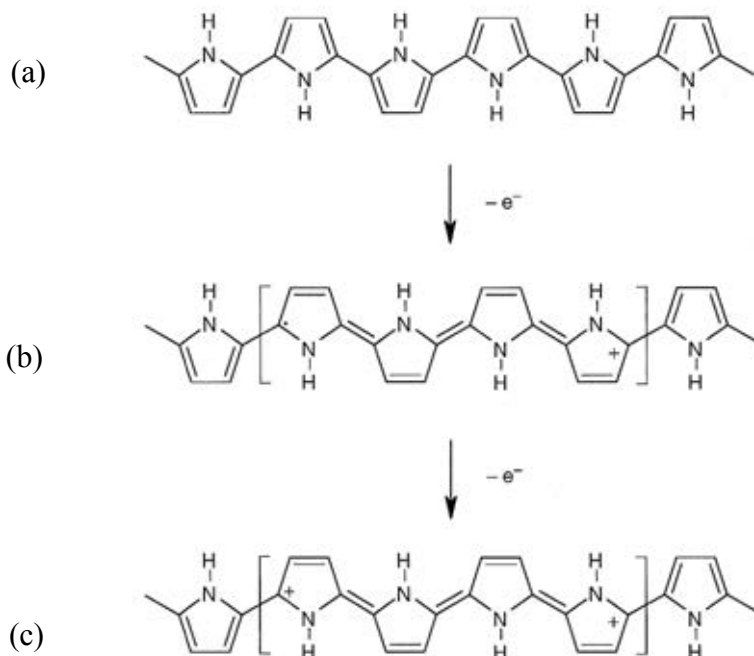


Figure 2.12 Electronic structures of (a) neutral PPy, (b) polaron in partially doped PPy and (c) bipolaron in fully doped PPy [22].

As oxidation continues further, another electron has to be removed from PPy chain that already contains a polaron, resulting in the formation of a bipolaron which is energetically preferred to the formation of two polarons. A bipolaron is known to extend over about four pyrrole rings (Fig. 2.11c). The bipolaron states lie further from the band edges. (Fig. 2.12c). The lower energy state of the bipolaron is empty, thereby leading to a species with zero spin. As the degree of oxidation increases, the bipolaronic energy state overlaps, resulting in the formation of narrow intermediate band structures (Fig. 2.12d). The energy diagram shown in Fig. 2.12d corresponds to a doped state of about 33 mol%, which is close to the maximum value found in electrochemically oxidized PPy. The typical doping level of PPy is in the range of 20 to 40 mol%. At this

doping level, bipolarons are predominant in PPy with few polarons, and thus the charge carriers in the conducting PPy have zero-spin number.

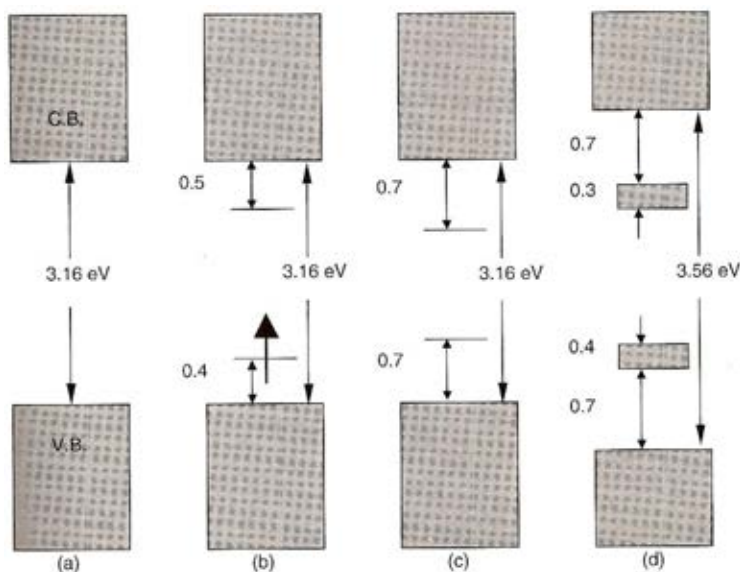


Figure 2.13 Electronic energy diagrams for (a) neutral PPy, (b) polaron, (c) bipolaron and (d) fully doped PPy [22].

2.6.2 Poly(3,4-ethylenedioxythiophene) : poly(styrenesulfonate) [23]

Poly(3,4-ethylenedioxythiophene) : poly(styrenesulfonate) or PEDOT:PSS (see Fig. 2.13) is a polymer mixture of two ionomers. One component in this mixture is made up of sodium polystyrene sulfonate which is a sulfonated polystyrene or PSS. The sulfonyl groups are deprotonated and carry a negative charge. The other component is poly(3,4-ethylenedioxythiophene) or PEDOT which is a conjugated polymer and carries positive charges and is based on polythiophene. Together the charged macromolecules form a macromolecular salt.

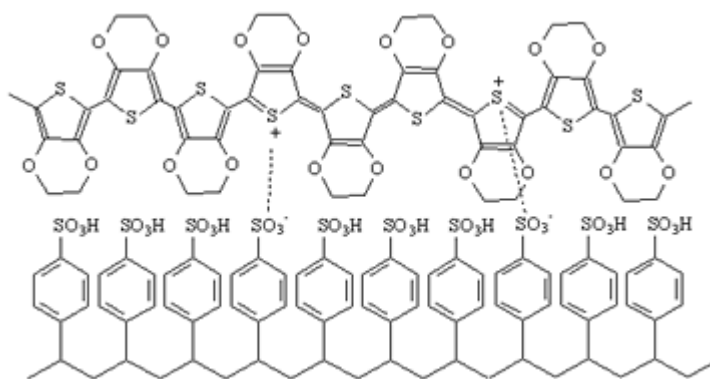


Figure 2.14 Structures of Poly(3,4-ethylenedioxythiophene) : poly(styrenesulfonate) [24].

It is used as a conductive polymer, transparent with high ductility in different applications. For example, AGFA coats 200 million photographic films per year with a thin, extensively-stretched layer of virtually transparent and colorless PEDOT:PSS as an antistatic agent to prevent electrostatic discharge during production and normal film use, independent of humidity conditions.

If high boiling solvents such methylpyrrolidone, dimethyl sulfoxide, sorbitol are added conductivity increases many orders of magnitude which makes it also suitable as a transparent electrode, for example in touchscreens, organic light-emitting diodes and electronic paper to replace the traditionally used indium tin oxide. Due to the high conductivity up to 1000 S/cm are possible, it can be used as a cathode material in capacitors replacing manganese dioxide or liquid electrolytes.

In general, this compound is applied as a dispersion of gelled particles in water. A conductive layer on glass is obtained by spreading a layer of the dispersion on the surface usually by spin coating and driving out the water or by heat. The special PEDOT:PSS inks and formulations were developed for different coating and printing processes. Water based PEDOT:PSS inks are mostly used in slot die coating, flexography, rotogravure and inkjet printing. If a high viscous paste and slow drying is required like in screen-printing processes PEDOT:PSS can also be supplied in high boiling solvents. Dry PEDOT:PSS pellets can be produced with a freeze drying method

which are redispersable in water and different solvents. Finally, to overcome degradation to ultraviolet light and high temperature / humidity conditions PEDOT:PSS UV-stabilizers are available.

2.6.3 Ponceau SS

Ponceau SS or acid red 150 is a sulfonic azo dye. Also, is an organic semiconductor due to a conjugated organics. Ponceau SS (Pss) molecules exhibit multilevel memory-switching property in the thin film transistors, light emitting devices, sensors and photovoltaic solar cells. Several classes of organic materials exhibited such applications, which occurred due to electrical bistability. A suitable voltage generally changes the conformer of a molecule [5,15]. The molecule of Pss was shown in Fig.2.14. When the both conformers are stable with a large difference in their conductivities, the molecules exhibit electrical bistability. A monolayer of Pss on doped Si (111) wafers deposited via electrostatic assembly the molecules exhibit one low- and two high-conducting states. The three states arise due to different conformers of the molecules.

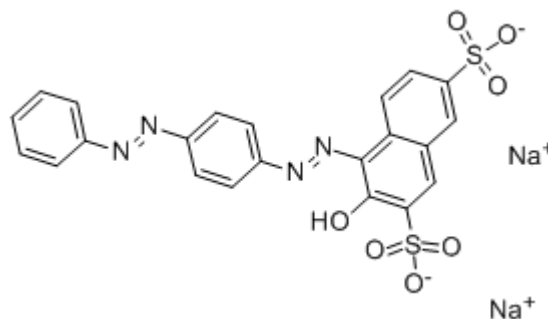


Figure 2.15 Structures of Ponceau SS molecule [25].

2.6.4 Ionic liquid [26]

Ionic liquids are organic salts that generally have melting points below 100 °C, unlike conventional salts; and the melts are liquid over a wide temperature range. Ionic liquids with melting points below or near room temperature (RTILs) are especially interesting. For example, reactions and extractions may be performed under mild

conditions, promoting lower likelihood of product thermal degradation and reducing energy costs. The types of organic cations used in ionic liquids include:

1. mono-, di-, and trisubstituted imidazoliums, and substituted pyridiniums and pyrrolidiniums [the free electron pairs of one of the two nitrogen atoms in the five-membered imidazoline ring and of the sole nitrogen atom in the five-membered pyrrolidine or six-membered pyridine ring have been donated to univalent alkyl groups to produce an N^+ cation]
2. tetraalkylammoniums (R_4N^+)
3. guanidiniums [$(NH_2)_3C^+$ and derivatives]
4. isouroniums and thioisouroniums [urea and thiourea derivatives of general formula $(NH_2)_2(RX)C^+$ where $X = O$ or S and $R = \text{alkyl}$]
5. tetraalkylphosphoniums (R_4P^+)

The nitrogen cation with four organic substituents in types 1 and 2 is called a quaternary ammonium ion. In types 3 and 4, the positively charged carbon atoms are electron-deficient. The anions used in ionic liquids include alkyl sulfates and sulfonates, halides, amides, imides, tosylates [toluenesulfonates], borates (e.g., tetrafluoroborate, BF_4^-), phosphates (e.g., hexafluorophosphate, PF_6^-), antimonates, and carboxylates. Ionic liquids are nonvolatile and nonflammable, have high thermal stability, and show remarkable dissolution capabilities for both organic and inorganic compounds. They are being increasingly examined as replacements for volatile organic solvents in a wide range of industrial and laboratory chemical processes such as synthesis, catalysis and enzymatic biocatalysis, electrolysis, and extraction. Ionic liquids can improve industrial processes by minimizing wastes and allowing efficient product extraction. Because of their negligible vapor pressure, products may often be readily separated from the reaction media simply by distillation. Solubility and other physical-chemical properties suitable for a particular application can be designed by appropriate combinations of the cations and anions. For example, in general, chlorides are water-soluble while hexafluorophosphates are water-insoluble. As reaction solvents, ionic liquids have been shown to increase reaction rates, selectivities, and yields. By changing

substitution patterns on the organic cation and changing anions, researchers can fine-tune reaction rates and selectivities for a particular catalyzed synthetic reaction. Because of their resistance to oxidation and reduction, they are suitable for electrochemical applications such as batteries, capacitors, electrochemical sensors, and photovoltaic devices. Ionic liquids are suitable for replacing organic solvents in two-phase system separation processes because partitioning of organic molecules in ionic liquid/water systems follow traditional octanol/water distributions. Ionic liquid mixtures with secondary solvents are not simple combinations. An appropriate co-solvent can solubilize hydrophobic ionic liquids. Another unique feature of ionic liquids is that they generally form liquid clathrates (inclusion compounds) in combinations with aromatic compounds.

2.7 Cyclic voltammetry [27]

Cyclic voltammetry is the most widely used technique for acquiring qualitative information about electrochemical reactions. The power of cyclic voltammetry results from its ability rapidly to provide considerable information on the thermodynamics of redox processes, the kinetics of heterogeneous electron transfer reactions and coupled chemical reactions or adsorption processes. Cyclic voltammetry technique is often the first experiment performed in an electroanalytical study. In particular, it offers a rapid location of redox potentials on the electroactive species, and convenient evaluation of the effect of media on the redox process.

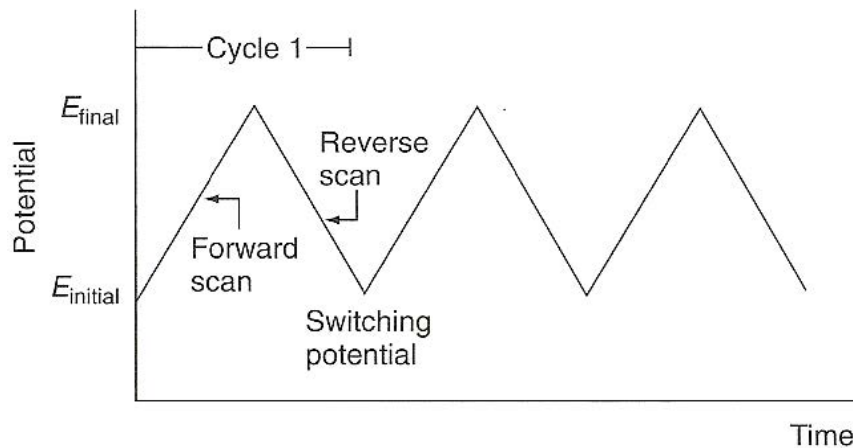


Figure 2.16 The potential-time excitation signal in a cyclic voltammetric experiment [27].

Cyclic voltammetry consists of linearly scanning the potential of a stationary working electrode (in an unstirred solution), using a triangular potential waveform (Fig. 2.15). Depending on the information sought, single or multiple cycles can be used. During the potential sweep, the potentiostat measures the current resulting from the applied potential. The resulting current-potential plot is termed a cyclic voltammogram. The cyclic voltammogram is a complicated, time-dependent function of a large number of physical and chemical parameters.

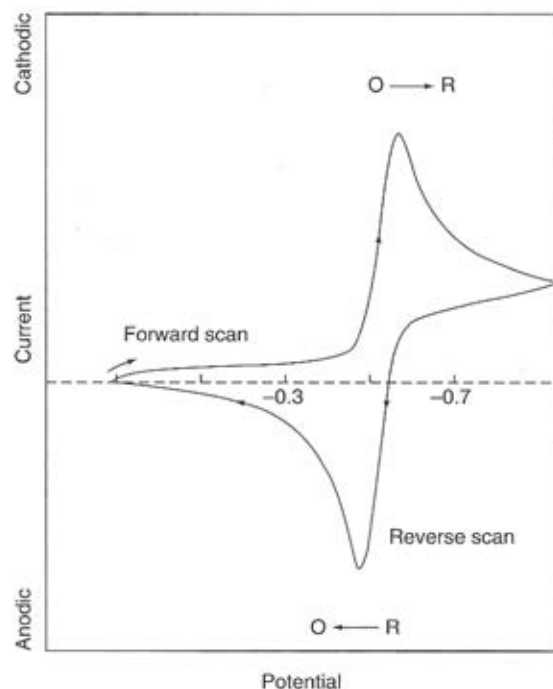


Figure 2.17 Typical cyclic voltammogram for a reversible $O + ne^- \rightleftharpoons R$ redox process [27].

Fig. 2.16 illustrates the expected response of a reversible redox couple during a single potential cycle. It is assumed that only the oxidized form of O is present initially. Thus, a negative potential scan is chosen for the first half-cycle, starting from a value where no reduction occurs. As the applied potential approaches the characteristic E^0 for the redox process, a cathodic current begins to increase, until a peak is reached. After traversing the potential region in which the reduction process takes place (at least $90/n$ mV beyond the peak), the direction of the potential sweep is reversed. During the reverse scan, R molecules (generated in the forward half-cycle, and accumulated near the surface) are reoxidized back to O, resulting in an anodic peak.

2.8 Electrochemical cells [27]

Three-electrode cells (see Fig. 2.17) are commonly used in controlled-potential experiments. The cell contains three electrodes (working, reference, and auxiliary), which are immersed in the sample solution. While the working electrode is the electrode at which the reaction of interest occurs, the reference electrode provides a stable and

reproducible potential, against which the potential of the working electrode is compared. Such buffering against potential changes is achieved by a constant composition of both forms of its redox couple, such as Ag/AgCl or $\text{Hg}/\text{Hg}_2\text{Cl}_2$ as common with the silver-silver chloride and the saturated calomel reference electrodes, respectively. To minimize contamination of the sample solution, the reference electrode may be insulated from the sample through an intermediate bridge. An inert conducting material, such as a platinum wire or graphite rod, is generally used as the current-carrying auxiliary electrode. The relative position of these electrodes and their proper connection to the electrochemical analyzer should be noted. The three electrodes, as well as the tube used for bubbling deoxygenating gas, are supported in five holes in the cell cover.

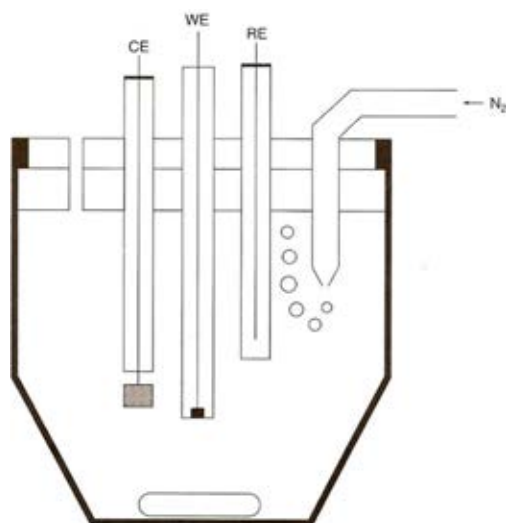


Figure 2.18 Schematic diagram of a cell for voltammetric measurements: WE-working electrodes; RE-reference electrode; CE-counter electrode. The electrodes are inserted through holes in the cell cover [27].

2.9 Electrical Conductivity [28-29]

2.9.1 Definition of conductivity

Conductivity is the ability of a material to conduct electric current. The principle by which instruments measure conductivity is simple. Two plates are placed in the sample, a potential is applied across the plates (normally a sine wave voltage), and the

resultant current is measured. Conductivity (C), the inverse of resistivity (R), is determined from the voltage and current values according to Ohm's law.

$$C = 1/R = I \text{ (amps)} / E \text{ (volts)} \quad (2.16)$$

Since the charge on ions in solution facilitates the conductance of electrical current, the conductivity of a solution is proportional to its ion concentration. In some situations, however, conductivity may not correlate directly to concentration. Fig. 2.18 illustrates the relationship between conductivity and ion concentration for two common solutions. Notice that the graph is linear for the sodium chloride solution, but is not linear for highly concentrated sulfuric acid. Ionic interactions can alter the linear relationship between conductivity and concentration in some highly concentrated solutions.

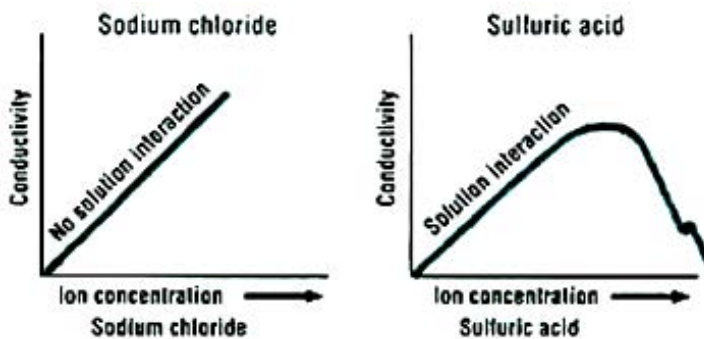


Figure 2.19 The relationship between conductivity and ion concentration for two common solutions [28].

2.9.2 The measurement of conductivity

Conductivity may be measured by applying an alternating electrical current (I) to two electrodes immersed in a solution and measuring the resulting voltage (V). During this process, the cations migrate to the negative electrode, the anions to the positive electrode and the solution acts as an electrical conductor as shown in Fig. 2.19.

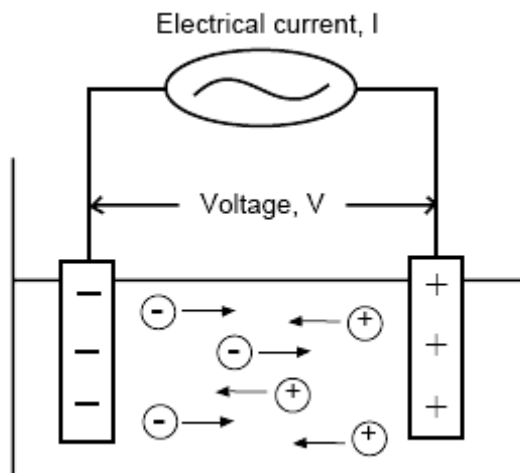


Figure 2.20 Migration of ions in solution [29].

2.9.3 Units of Measurement

The basic unit of conductivity is the siemens (S), formerly called the mho. Since cell geometry affects conductivity values, standardized measurements are expressed in specific conductivity units (S/cm) to compensate for variations in electrode dimensions. Specific conductivity (σ) is simply the product of measured conductivity (C) and the electrode cell constant (L/A), where L is the length of the column of liquid between the electrode and A is the area of the electrodes.

$$\sigma = C \times (L/A) \quad (2.17)$$

If the cell constant is 1 cm^{-1} then the specific conductivity is the same as the measured conductivity of the solution. Although electrode shape varies, an electrode can always be represented by an equivalent theoretical cell.

2.9.4 Conductive solution

Conductivity is typically measured in aqueous solutions of electrolytes. Electrolytes are substances containing ions, i.e., solutions of ionic salts or of compounds that ionize in solution. The ions formed in solution are responsible for carrying the electric current. Electrolytes include acids, bases and salts can be either strong or weak.

Most conductive solutions measured are aqueous solutions, as water has the capability of stabilizing the ions formed by a process called solvation.

2.9.4.1 Strong electrolytes

Strong electrolytes are substances that are fully ionized in solution. As a result, the concentration of ions in solution is proportional to the concentration of the electrolyte added. They include ionic solids and strong acids, for example HCl. Solutions of strong electrolytes conduct electricity because the positive and negative ions can independently migrate under the influence of an electric field.

2.9.4.2 Weak electrolytes

Weak electrolytes are substances that are not fully ionized in solution. For example, acetic acid partially dissociates into acetate ions and hydrogen ions, so that an acetic acid solution contains both molecules and ions. A solution with a weak electrolyte can conduct electricity, but usually not as well as a strong electrolyte because there are fewer ions to carry the charge from one electrode to the other.

2.9.5 Definition of terms

2.9.5.1 Resistance

The resistance of the solution (R) can be calculated using Ohm's law ($V = R \times I$).

$$R = V/I \quad (2.18)$$

Where: V = voltage (volts) , I = current (amperes) and R = resistance of the solution (ohms).

2.9.5.2 Conductance

Conductance (G) is defined as the reciprocal of the electrical resistance (R) of a solution between two electrodes.

$$G = 1/R \text{ (S)} \quad (2.19)$$

The conductivity meter in fact measures the conductance, and displays the reading converted into conductivity.

2.9.5.3 Cell constant

This is the ratio of the distance (d) between the electrodes to the area (a) of the electrodes.

$$K = d/a \quad (2.20)$$

Where: K = cell constant (cm^{-1}), a = effective area of the electrodes (cm^2) and d = distance between the electrodes (cm).

2.9.5.4 Conductivity

Electricity is the flow of electrons. This indicates that ions in solution will conduct electricity. Conductivity is the ability of a solution to pass current. The conductivity reading of a sample will change with temperature.

$$C = G \cdot K \quad (2.21)$$

Where: C = conductivity (S/cm), G = conductance (S), where $G = 1/R$ and K = cell constant (cm^{-1}).

2.10 Scanning electron microscopy [30]

The scanning electron microscope (SEM) uses a focused beam of high-energy electrons to generate a variety of signals on the surface of solid specimens. The signals were derived from electron-sample interactions reveal information about the sample including external morphology (texture), chemical composition, and crystalline structure and orientation of materials making up the sample. In most applications, data are collected over a selected area surface of the sample, and a 2-dimensional image is generated displays spatial variations in these properties. Areas ranging from

approximately 1 cm to 5 microns in width can be imaged in a scanning mode using the conventional SEM techniques (magnification ranging from 20X to approximately 30,000X, spatial resolution of 50 to 100 nm). The SEM is also capable of performing analyses of selected point locations on the sample; this approach is especially useful in qualitative or semi-quantitative determining chemical compositions by using EDS, crystalline structure, and crystal orientations by using EBSD.

Accelerated electrons in a SEM carry significant amounts of kinetic energy, and this energy is dissipated as a variety of signals produced by electron-sample interactions when the incident electrons are decelerated in the solid sample. These signals include secondary electrons which produce SEM images, backscattered electrons (BSE), diffracted backscattered electrons (EBSD) that are used to determine crystal structures and orientations of minerals, photons (characteristic X-rays that are used for elemental analysis and continuum X-rays), visible light using cathodoluminescence (CL), and heat. Secondary electrons and backscattered electrons are commonly used for imaging samples. Secondary electrons are most valuable for showing morphology and topography on samples and backscattered electrons are most valuable for illustrating contrasts in composition in multiphase samples. X-ray generation is produced by inelastic collisions of the incident electrons with electrons in discrete shells of atoms in the sample. As the excited electrons return to lower energy states, they yield X-rays that are of a fixed wavelength. Thus, the characteristic X-rays are produced for each element in a mineral that is excited by the electron beam. SEM analysis is considered to be non-destructive that is the x-rays generated by electron interactions do not lead to volume loss of the sample, so it is possible to analyze the same materials repeatedly.

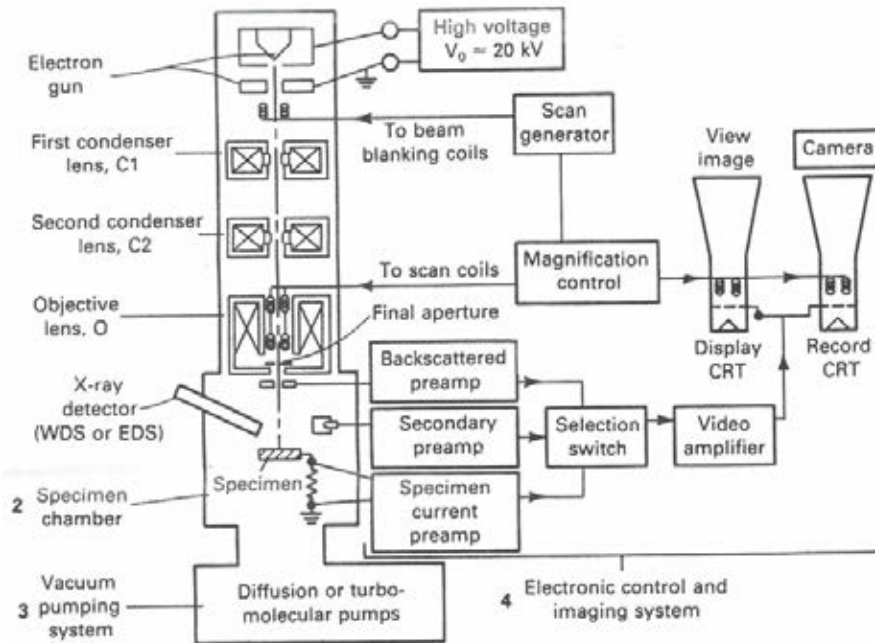


Figure 2.21 Fundamental of Scanning Electron Microscopy (SEM) [31].

2.11 X-ray diffractometry [32-34]

In 1912 Max von Laue, the German physicist, placed a crystal of copper (II) sulphate between a white X-ray source and a photographic plate. The resulting photograph contained a central bright spot due to that part of the beam which passed straight through the crystal. Surrounding the central spot was a number of fuzzy spots arranged in a regular pattern. The fuzzy spot had been produced by diffracted beams.

Laue's discovery of X-ray diffraction captured the interest of W.H. Bragg and his son W.L. Bragg who successfully applied X-ray diffraction to the determination in terms of a three dimensional grating, W.L. Bragg devised a sampler approach based on the reflection of X-rays by planes of atoms. The Bragg's equation is

$$2d \sin \theta = n\lambda \quad (2.22)$$

where :**d** is the spacing between adjacent Bragg planes in the crystal

θ is the wavelength of the x-rays.

λ is the angle between the x-ray beam and the plane of atoms

n is the order of the image.

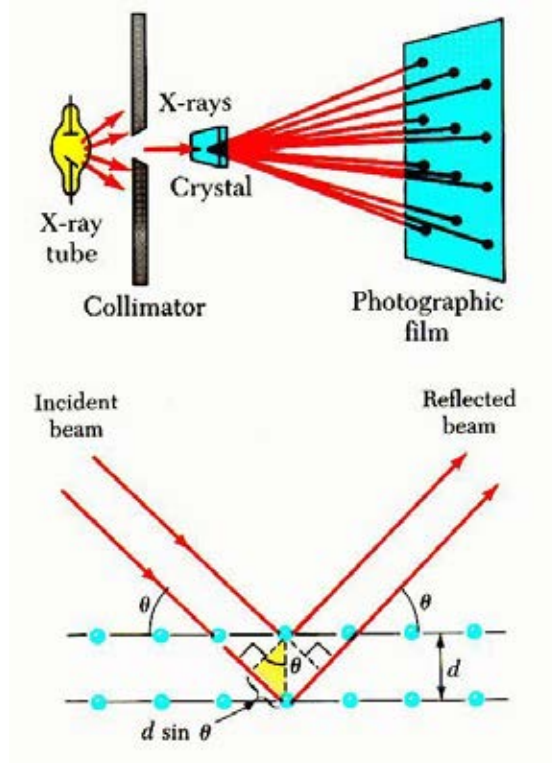


Figure 2.22 Fundamental of X-ray diffractometer [34].

Diffraction effects are observed when electromagnetic radiation impinges on periodic structures with geometrical variations on the length scale of the radiation's wavelength. The interatomic distances in crystals and molecules which correspond in the electromagnetic spectrum with the wavelength of x-rays having photon energies between 3 and 8 keV. Accordingly, phenomena like constructive and destructive interference should become observable when crystalline and molecular structures are exposed to x-rays. In the following sections, firstly, the geometrical constraints that have to be obeyed for x-ray interference to be observed are introduced. Secondly, the results are exemplified by introducing the $\theta/2\theta$ scan, which is a major x-ray scattering technique in thin-film analysis. Thirdly, the $\theta/2\theta$ diffraction pattern is used to outline the factors that determine the intensity of x-ray reflections. Thereby rely on numerous analogies to classical optics and frequently use will be made of the fact that the scattering of radiation has to proceed coherently.

2.12 Literature reviews of lead-acid batteries

In 2001, Torcheux and Lailier [35] developed a new electrolyte formulation for the cycling applications, especially for renewable energy markets. The new formulation developed was a mixture of H_2SO_4 , low concentration of liquid colloidal silica and other additives such as H_3PO_4 . The results showed that battery life is significantly increased using this formulation, the acid stratification decreased by using the colloidal silica with low concentration and the delay of positive active mass softening by using H_3PO_4 as an additive.

In 2002, Wu et al. [36] studied the influence of the content of SiO_2 (in the form of soot) on the capacity and the self-discharge of lead-acid batteries. Moreover, the structure of the gelled electrolyte was investigated in detail by means of CV, electrochemical impedance spectroscopy and scanning electron microscopy. They found that the content of SiO_2 and the viscosity of the gelled electrolyte are important factors which affected the capacity of batteries. The colloidal particles become smaller with increasing the SiO_2 content because the three-dimensional web structure of the gelled electrolyte is more compact. Therefore, the SiO_2 contents of gelled electrolyte have to be carefully controlled.

In 2002, Lambert et al. [37] improved the gelled electrolyte and increased the demand for an alternative gelling agent for VRLA batteries. The most commonly used gelling agent as fumed silica but it can contaminate from the local working environment, particular paste mixing and occupational hygiene and handling problems. To develop and maintain a stable gel structure, the particle size exerts a major influence on the pore volume and diameter, also be noted. Thus, an optimum particle size of silica sol is the important utilization. Silica sols can improve these problems and provide a lower cost to battery producer.

In 2003, Martha et al. [38] reported the performance characteristics of gelled electrolyte VRLA batteries built in-house. The gelled electrolyte was constructed by mixing 4.5 M aqueous H_2SO_4 and M-5 CAB-O-SIL[®] fumed silica to form thixotropic gel

was filled into all the six cell of 12V/25AH VRLA battery case. The performance of gelled electrolyte VRLA battery built in-house was compared with the AGM VRLA and flooded-lead-acid battery counterparts. While the performance of gelled electrolyte VRLA batteries was similar to both AGM VRLA and flooded-lead-acid batteries at temperature above 0°C, it was found that the performance of gelled electrolyte VRLA batteries is better than both AGM VRLA and flooded-lead-acid batteries at temperature between 0°C and -40°C.

In 2005, Park et al. [39] investigated the rheological behavior of silica gel in H₂SO₄ by a small amplitude dynamic oscillation measurement method. In this method, the storage modulus was monitored with time. The gel strength and the gelation rate were measured from the time evolution of storage modulus during the gelation. The gelled electrolyte was prepared from 2-15 wt.% of fumed silica, 15 or 38 wt.% of H₂SO₄ and polyacrylamide. The use of this gelled electrolyte can suppress the formation of micro-crack during battery operation. In addition, the gel strength and gelation rate were changed by changing the silica content, sulfuric acid concentration, gelation temperature and the amount of added polyacrylamide. The gel strength can be increased by decreasing the gelation temperature from 25 to 20°C and by adding polyacrylamide.

In 2006, Guo and co-workers [40] studied the performance of self-discharged gel VRLA battery. In this work, the VRLA battery consisted of eight positive and nine negative plates and had 10 AH capacity (2h rate). The H₂SO₄ solution (1.30 g/cm³) and 5% fumed silica were mixed to prepare the gelled electrolyte. The gel VRLA batteries were shelved for nearly 3 years. After shelved gel VRLA batteries, they found that there was not only stratification of the electrolyte, but also no sulfation on the positive plate. The positive grid also had a good corrosion layer structure meaning that the active mass structure of the positive plate and its polarization resistance were not substantially affected during the long shelving. On the negative plate, the potential of hydrogen evolution of the gel VRLA batteries was slightly more negative than that of AGM VRLA batteries. Its self-discharge rate was also slower.

In 2007, Tang et al. [41] prepared and investigated a polysiloxane-based gelled electrolyte (PBGE) as a new gelling agent for VRLA batteries. In addition, the initial cyclic properties of the absorptive glass mat (AGM)-PBGE and AGM-colloid silica gelled electrolyte (CSGE) hybrid batteries were investigated. They found that the comparison of AGM-PBGE batteries and AGM-CSGE, AGM-PBGE batteries display a superior initial electrochemical performance, improved low- and high-temperature properties and better recharge and discharge performance under overcharging conditions. On the other hand, the AGM-CSGE batteries gave a poorer cycle performance at 10-h rate under the condition 100% of deep of discharge. In the same year, they compared the AGM-PBGE batteries with PVC-fumed silica gelled electrolyte (PVC-FSGE) tubular batteries [45]. The comparison showed that AGM-PBGE ones not only presented superior initial performance such as a high discharge rate, high-low temperature properties and oxygen-recombination rate, but also had a shorter manufacturing time and lower cost.

In 2008, Chen et al. [42] studied the effects of preparation conditions and particle size distribution on fumed silica gel VRLA battery performance. In this work, the fumed silicas were Aerosil 200, Aerosil 150 (produced by Degussa Co., Germany denoted as A200 and A150) and HL200 (produced by GBS Co., China). Mechanical dispersion of fumed silica nanoparticles was investigated in the preparation of high performance gelled electrolytes as an important factor. The optimal dispersion time related to the operating temperature during preparation of gel, also the silica particle size and its distribution which effect on electrochemical properties. Also, a high stirring rate improves the electrode capacity and decreases the viscosity of the gelled electrolyte. For the fumed silica from different producers, fumed silica with a diameter of 10 nm tended to aggregate easily and aggregation of 20 nm diameter silica was more difficult.

In 2008, Siridetpan [43] developed the gelled electrolyte in valve-regulated lead-acid (VRLA) battery using various additives. The gelled electrolytes were investigated in term of the conductance, gel strength and gelling time. It was found that gelled electrolyte with polyacrylamide provided higher conductance, gel strength and gelling time. On the other hand, gelled electrolytes with sulfate salt caused lower conductance,

gel strength and gelling time. For the performance of gel VRLA battery, Na_2SO_4 effected on the longest battery discharging period, the highest improvement in the battery capacity and the greatest presenting battery efficiency.

In 2008, Chaiyasit [44] studied the effects of additives on the performance of gelled-electrolyte by measuring the conductivity values and discharge capacities of valve-regulated lead-acid (VRLA) batteries. The results showed that the high discharge capacities and conductivity were obtained from gelled electrolytes containing conducting polymer. The highest conductivity of gelled electrolyte and the highest discharge capacity of battery were exhibited in gel with 0.08 % (w/v) of PPy.

In 2009, Karami et al. [45] studied the recovery of discarded sulfated lead-acid batteries by inverse charge. The effect of inverse charge on the reactivation of sulfated active materials had been investigated after the deeply discharged. The electrolyte of battery was replaced 1.28 g/cm^3 of sulfuric acid solution. Then, the battery was inversely charged with the constant current method for 24 h and directly recharge was applied 48 h by constant voltage. Through these processes, a discarded battery can recover its capacity more than 80% of non-sulfated battery. Inverse oxidation and reduction of active material in battery can transform inactive sulfates.

In 2009, Rezaei et al. [46] studied the effects of ionic liquids (ILs) as an electrolyte additive in lead acid battery. This investigation of their electrochemical properties was performed by cyclic voltammetry and scanning electron microscopy. The results indicated the behaviors of electrode depend on ILs concentration in the electrolyte solution. Increasing overpotential with ILs as electrolyte additives, hydrogen and oxygen evolution will be decreased.

CHAPTER III

EXPERIMENTAL

3.1 Gelled electrolyte preparations

This chapter has given the information of instruments and equipments, apparatus, chemical and methodology used in this work.

3.1.1 Instrument

The instrument for gelled electrolyte preparations is rotating rod machine with speed of 3,000 rpm (supplied by Metrohm) as shown in Fig. 3.1. This rotating rod machine was used to prepare a small amount of gelled electrolytes for cyclic voltammetry and conductivity detection (lab scale). Gelled electrolytes for VRLA battery (industrial scale) were prepared by using electronic overhead stirrer with speed of 3,000-6,000 rpm (supplied IKA, Germany) as shown in Fig.3.2.



Figure 3.1 The setting of instruments for the gelled electrolyte preparation for lab scale.



Figure 3.2 The setting of instruments for the gelled electrolyte preparation for industrial scale.

3.1.2 Chemicals

The chemicals for gelled electrolyte preparations are listed in Table 3.1.

Table 3.1 List of chemicals for gelled electrolyte preparations

Chemicals	Suppliers
Fumed silica (Aerosil 200) particle size 12 nm BET surface area 200 ± 25 [m ² /g]	Degussa
Fumed silica (Aerosil 300) particle size 7 nm BET surface area 300 ± 25 [m ² /g]	Degussa
Sulfuric acid 95-97%	Merck
Polypyrrole, doped composite with carbon black, loading 20 wt.% carbon black, 30 S cm ⁻¹	Aldrich
Poly(3,4-Ethylenedioxythiophene)/poly (stylenesulfonate)	Aldrich
Ionic liquid, $\geq 95\%$	Aldrich
Ponceau SS	Aldrich
Conductivity standard solution (100,000 $\mu\text{S cm}^{-1}$)	Metter Toledo

3.1.3 Methodology

The gelled electrolyte was prepared by mixing 2-5% (w/v) of fumed silica A200 or A300 with 35-43% (w/v) of H₂SO₄ (1.210-1.325 sp.gr.), deionized water and 0.005% (w/v), 0.01% (w/v) and 0.02% (w/v) of additive, respectively. The suspension was stirred at room temperature (25±1°C) by rotating rod machine for lab scale and electronic overhead stirrer for industrial scale with speed of 3,000 rpm for 10 min.

Finally, a slurry of gelled electrolyte was generated as shown in Fig. 3.3 (a), (b), (c) and (d).

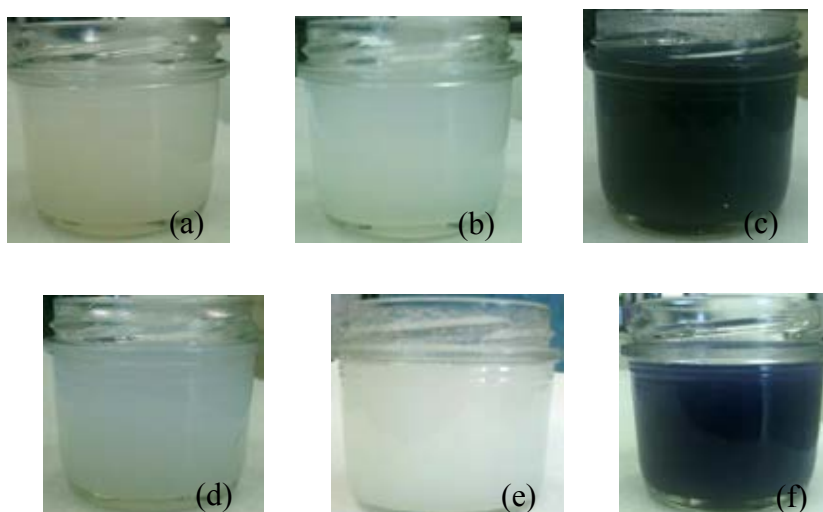


Figure 3.3 The gelled electrolyte consisting of fumed silica, H_2SO_4 and (a) fumed silica A200 without adding additives, (b) fumed silica A300 without adding additives, (c) adding PPy, (d) adding PEDOT:PSS, (e) adding IL, (f) adding Pss.

3.2 Battery testing

3.2.1 Instruments

The instruments for battery testing are listed in Table 3.2.

Table 3.2 List of instruments for battery testing

Instruments	Details
Digital Multi Meter	Sunwa version CD770
Clamp Meter	Ininipa version ET-3374
Halogen lamp 35 W	Philips
Battery charger	Tiger star
Stop watch	Timer-5

3.2.2 Gelled electrolytes for battery testing

Gelled electrolytes were filled into the 12V/4AH VRLA battery's case using battery filling machine (supplied by N.V. Battery Ltd,.). All of the gel batteries were investigated the performance by measuring the battery's charge-discharge capacity. The gel batteries were classified into five types; (i) without adding any additive, (ii) adding PPy, (iii) adding PEDOT:PSS, (iv) adding Pss, (v) adding IL as shown in Table 3.3.

Table 3.3 List of VRLA batteries with different formulation of gelled electrolytes for testing the performance

Type of additive	Fumed silica particle size (nm)	Fumed silica content % (w/v)	Density of H ₂ SO ₄ (sp.gr.)	Code name of battery
No additive	7	2	1.280	S7-1
		3	1.280	S7-2
		4	1.280	S7-3
	12	2	1.210	S12-1
		2	1.280	S12-2
		2	1.325	S12-3
		3	1.280	S12-4
		4	1.280	S12-5

Type of additive	Fumed silica particle size (nm)	Fumed silica content % (w/v)	Density of H ₂ SO ₄ (sp.gr.)	Code name of battery
0.01% (w/v) PPy	7	2	1.280	SP7-1
		3	1.280	SP7-2
		4	1.280	SP7-3
	12	2	1.280	SP12-1
		3	1.280	SP12-2
		4	1.280	SP12-3
0.005% (w/v) PPy	12	4	1.280	SP12-5
0.02% (w/v) PPy	12	4	1.280	SP12-6
0.01% (w/v) PEDOT:PSS	7	2	1.280	SPD7-1
		3	1.280	SPD7-2
		4	1.280	SPD7-3
	12	2	1.280	SPD12-1
		3	1.280	SPD12-2
		4	1.280	SPD12-3
0.005% (w/v) PEDOT:PSS	12	4	1.280	SPD12-4
0.02% (w/v) PEDOT:PSS	12	4	1.280	SPD12-5

Type of additive	Fumed silica particle size (nm)	Fumed silica content % (w/v)	Concentration of H ₂ SO ₄ (sp.gr.)	Code name of battery
0.01% (w/v) Pss	7	2	1.280	SPS7-1
		3	1.280	SPS7-2
		4	1.280	SPS7-3
	12	2	1.280	SPS12-1
		3	1.280	SPS12-2
		4	1.280	SPS12-3
0.005% (w/v) Pss	7	3	1.280	SPS7-4
0.02% (w/v) Pss	7	3	1.280	SPS7-5
0.01% (w/v) IL	7	2	1.280	SI7-1
		3	1.280	SI7-2
		4	1.280	SI7-3
	12	2	1.280	SI12-1
		3	1.280	SI12-2
		4	1.280	SI12-3
0.005% (w/v) IL	7	3	1.280	SI7-4
0.02% (w/v) IL	7	3	1.280	SI7-5

3.3.3 Methodology

The different formulations of gelled electrolytes were filled into VRLA batteries using a vacuum system in order to investigate the performance of 12V/4AH batteries. Charge and discharge capacities were tested 15 cycles for 1-hour rate (C_1) at room temperature ($25\pm 1^\circ\text{C}$). The experimental set up for charge and discharge were shown in Fig. 3.4 (a) and (b), respectively. The voltage and current were measured, throughout the experimental. For charge tests, the voltage and current were measured at every 15 minutes and cut-off point was 5 hours. On the other hand, discharge tests, the voltage and current were measured at every 5 min and discharge cutoff point was 9.0 V. The performance of VRLA batteries was totally tested for 15 cycles.

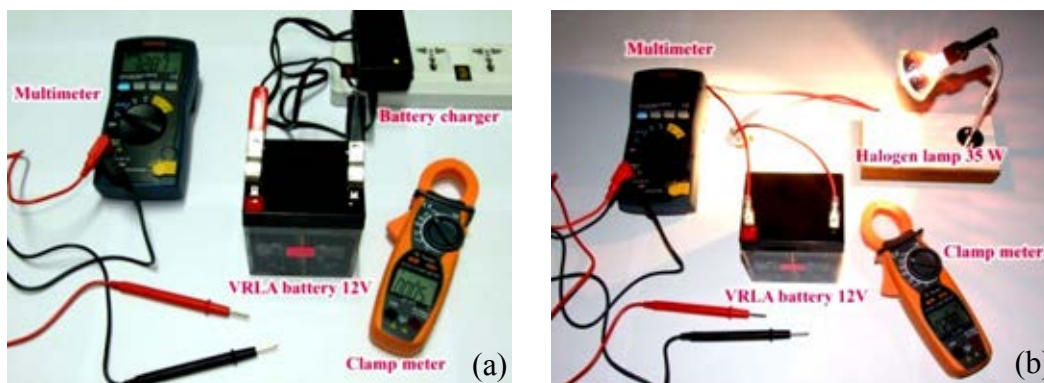


Figure 3.4 The setting of experimental for (a) battery charging and (b) battery discharging.

3.3 Electrical conductivity test

3.3.1 Instruments

The instrument for electrical conductivity test is S70-K SevenMulti conductivity meter with inlab 730 conductivity probe $1-1000 \text{ mS cm}^{-1}$ (supplied by Mettler Toledo) as shown in Fig. 3.5.



Figure 3.5 The conductivity meter and conductivity probe for electrical conductivity test.

3.3.2 Gelled electrolytes for conductivity test

The gelled electrolytes for conductivity test were prepared as same as the previous mentions (in section 3.1.3). The optimal concentration of H_2SO_4 was pretested by measuring conductivity in 40 and 43% (w/v) of H_2SO_4 solutions (1.280 and 1.325 sp.gr.). The experiment was classified into 2 types. The first type is gelled electrolytes without adding additives as shown in Table 3.4 and second types is gelled electrolytes with adding additives as displayed in Table 3.5, respectively. In the second type, the best gel characteristic and obtaining the highest conductivity obtained from fumed silica A200 and A300 were selected to next study. They were classified into two types; (i) 3 % (w/v) of fumed silica size 7 nm (A300) and H_2SO_4 with 1.280 sp.gr., (ii) 4 % (w/v) of fumed silica size 12 nm (A200) and H_2SO_4 with 1.280 sp.gr.. Both types were studied the effect of concentration on conductivity of gelled electrolytes as shown in Table 3.6.

Table 3.4 List of gelled electrolytes without adding additives for electrical conductivity test

Fumed silica content % (w/v)	Fumed silica particle size (nm)	H₂SO₄ (sp.gr.)
2	7, 12	1.280
3	7, 12	1.280
4	7, 12	1.280
5	7, 12	1.280

Table 3.5 List of gelled electrolytes with adding additives for electrical conductivity test

Fumed silica content % (w/v)	Fumed silica particle size (nm)	H₂SO₄ (sp.gr.)	Additive
2	7,12	1.280	0.01% (w/v) PPy, 0.01% (w/v) PEDOT:PSS, 0.01% (w/v) Pss, 0.01% (w/v) IL
3	7,12	1.280	0.01% (w/v) PPy, 0.01% (w/v) PEDOT:PSS, 0.01% (w/v) Pss, 0.01% (w/v) IL
4	7,12	1.280	0.01% (w/v) PPy, 0.01% (w/v) PEDOT:PSS, 0.01% (w/v) Pss, 0.01% (w/v) IL
5	7,12	1.280	0.01% (w/v) PPy, 0.01% (w/v) PEDOT:PSS, 0.01% (w/v) Pss, 0.01% (w/v) IL

Table 3.6 List of gelled electrolytes with adding additives for the effect of concentration on conductivity of gelled electrolytes

Fumed silica content % (w/v)	Fumed silica particle size (nm)	H ₂ SO ₄ (sp.gr.)	Additive
3	7,12	1.280	0.005% (w/v) PPy, 0.005% (w/v) PEDOT:PSS, 0.005% (w/v) Pss, 0.005% (w/v) IL
			0.02% (w/v) PPy, 0.02% (w/v) PEDOT:PSS, 0.02% (w/v) Pss, 0.02% (w/v) IL
4	7,12	1.280	0.005% (w/v) PPy, 0.005% (w/v) PEDOT:PSS, 0.005% (w/v) Pss, 0.005% (w/v) IL
			0.02% (w/v) PPy, 0.02% (w/v) PEDOT:PSS, 0.02% (w/v) Pss, 0.02% (w/v) IL

3.3.3 Methodology

The conductivity of gelled electrolyte was investigated to verify the relation of the battery capacity and the effect of additives on gelled electrolytes. The conductivity of gelled electrolyte was measured at 25±1°C by immersing the conductivity probe into the gelled electrolyte and press read after the gelled electrolyte covered the conductivity sensor. The conductivity sensor was calibrated with a conductivity standard solution (100,000 $\mu\text{S cm}^{-1}$) before use. In this work, the volume of gelled electrolytes was fixed at 80 mL.

3.4 Electrochemical test

3.4.1 Instruments

The instruments for electrochemical test are listed in Table 3.7.

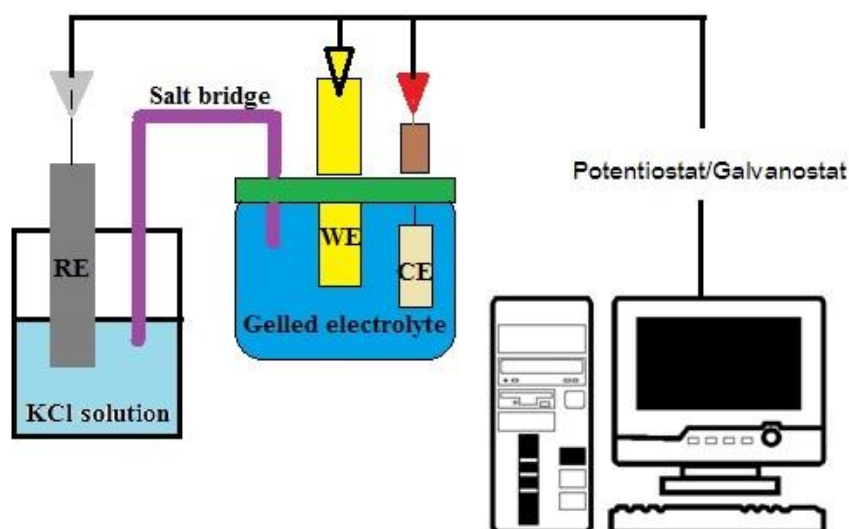
Table 3.7 List of instruments for electrochemical test

Instruments	Details
Potentiostat (PGSTAT30)	Auto lab
Planar Pb electrode (homemade)	Use for working electrode (WE)
Platinum gauze 80 mesh (BAS Inc.)	Use for counter electrode (CE)
Ag/AgCl electrode (Metrohm)	Use for reference electrode (RE)

3.4.2 Gelled electrolytes and acid solution for electrochemical test

In order to check the characteristic reaction of hydrogen-oxygen evolution of gelled electrolyte, the electrochemical test was used. All gelled electrolytes in Table 3.4, 3.5 and 3.6 were tested and compared. The relation among the battery capacity test, the conductivity and electrochemical test were analyzed.

3.4.3 Methodology

**Figure 3.6** The electrochemical cell for electrochemical technique.

The characteristic reaction of hydrogen-oxygen evolution of gelled electrolyte was tested by using the three-electrode system of cyclic voltammetry (CV). The experimental set up is demonstrated in Fig. 3.6. The geometric area of working electrode was fixed at 0.5 cm^2 as shown in Fig. 3.7. The experiments were carried out using gelled electrolyte and H_2SO_4 solution by Potentiostat method with a scan rate of 20 mV s^{-1} at $25 \pm 1^\circ\text{C}$. The CV curves were conducted over the potential range from -2.5 V to 2.9 V .

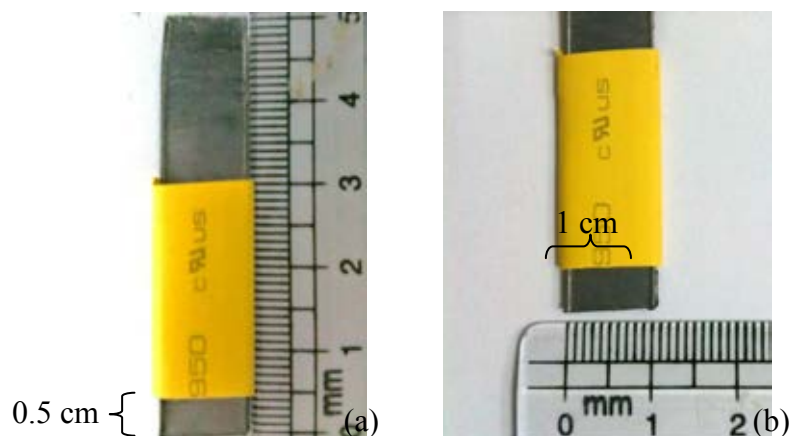


Figure 3.7 Planar lead (Pb) electrode used as working electrode (WE) with area of 0.5 cm^2 and (a) 0.5 cm of WE width, (b) 1 cm of WE length.

3.5 Scanning electron microscopic (SEM) analysis

3.5.1 Instruments

The instrument for scanning electron microscopic analysis is Joel scanning electron microscope JSM 6400

3.5.2 Methodology

The VRLA batteries were cleaved. The composition of gelled electrolytes from VRLA battery were shown in Table 3.8 and the morphology were analyzed using magnification $\times 1700$. The sample of gelled electrolyte was shown in Fig. 3.8.

Table 3.8 List of gelled electrolytes from VRLA battery for SEM

Code name of battery	Type of gelled electrolyte
S7-2	3% (w/v) of A300 fumed silica without additive
S12-5	4% (w/v) of A200 fumed silica without additive
SP12-3	4% (w/v) of A200 fumed silica with 0.01% (w/v) of PPy
SPD12-5	4% (w/v) of A200 fumed silica with 0.02% (w/v) of PEDOT:PSS
SPS7-2	3% (w/v) of A300 fumed silica with 0.01% (w/v) of Pss
SI7-2	3% (w/v) of A300 fumed silica with 0.01% (w/v) of IL

**Figure 3.8** The sample of gelled electrolyte for SEM.

3.6 X-ray diffraction (XRD) analysis

3.6.1 Instruments

The instrument for X-ray diffraction analysis is Bruker X-ray diffractometer D8-Discover.

3.6.2 Methodology

Negative plate electrodes (Pb) from S12-5, SP12-3, SPD12-5, SPS7-2 and SI7-2 VRLA batteries were trimmed a cubic pieces as shown in Fig.3.9. A piece of negative plate was analyzed by XRD techniques.

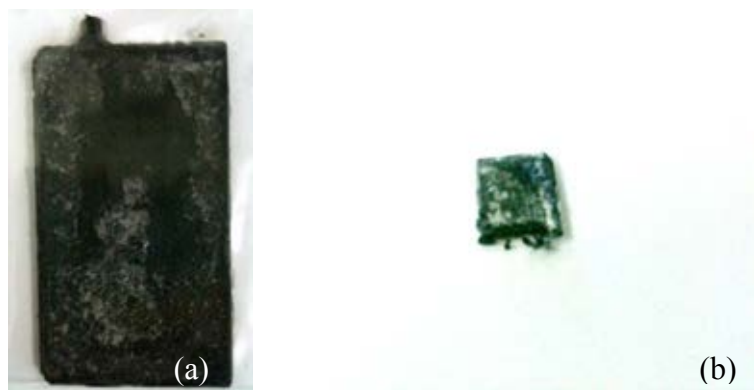


Figure 3.9 The negative plate electrode (a) negative plate electrode from VRLA battery (b) a sample cubic negative plate for XRD.

CHAPTER IV

RESULTS AND DISCUSSION

4.1 Characterization of gelled electrolytes

Gelled electrolyte suspensions are monitored by visualization before filling into the battery cases. Table 4.1 shows the characteristics of gelled electrolytes with different content of fumed silica, fumed silica particle sizes and H₂SO₄ after stirring 3000 rpm at room temperature (25±1°C). The results showed that 2% (w/v) of both fumed silica particle sizes and 35-43% (w/v) of H₂SO₄ or 1.210-1.325 sp.gr. H₂SO₄ provided a characteristic of sedimentation after setting in 1 week. The first characteristic of a gel were observed at the electrolyte with 5% (w/v) of fumed silica particle size 12 nm (A200) in 1.280 sp.gr. H₂SO₄. The electrolytes with 3-4% (w/v) of fumed silica content in 1.280-1.325 sp.gr. H₂SO₄ characterized like slurry. Between Fumed silica particle size 7 nm and 12 nm, there was no difference because this characteristic cannot be indicated by visualization.

Table 4.1 The characterization of gelled electrolytes with various components.

Concentration of H ₂ SO ₄ (sp.gr.)	Type of additive	Fumed silica particle size (nm)	Fumed silica content %(w/v)			
			2	3	4	5
1.210	No additive	7	S	S	Sl	Sl
		12	S	S	Sl	Sl
1.280	No additive	7	S	Sl	Sl	G
		12	S	Sl	Sl	G
1.325	No additive	7	S	Sl	Sl	G
		12	S	Sl	Sl	G

Table 4.1 The characteristics of gelled electrolytes with various components.

Concentration of H ₂ SO ₄ (sp.gr.)	Type of additive	Fumed silica particle size (nm)	Fumed silica content %(w/v)			
			2	3	4	5
1.280	Ppy	7	S	Sl	Sl	G
		12	S	Sl	Sl	G
	PEDOT:PSS	7	S	Sl	Sl	Sl
		12	S	Sl	Sl	Sl
	Pss	7	S	Sl	Sl	G
		12	S	Sl	Sl	G
	IL	7	S	Sl	G	G
		12	S	Sl	G	G

* S = Sedimentation, Sl = Slurry, G = Gel

From Table 4.1, it can be implied that increasing the fumed silica content and the H₂SO₄ concentration lead to gels. However, some additive also affect to characteristic of gel such as the PEDOT:PSS decreased the gel strength because of their large molecule and its polystyrene sulfonate group, which can possibly react to form the hydrogen bond on the silanol particles. Therefore, the gelation is destroyed. For Pss, there is no difference from no additive. Whereas IL influenced the short gelling time may be concern to their sulfonate group. Moreover, the gel characterization also depended on the concentration of H₂SO₄ owing to interaction effect of a weakly hydrogen-bonding solvent [42].

Practically, the gelled electrolyte inside battery was set as a gel more quickly than the outside due to heat and vacuum state. For 2% (w/v) and 3% (w/v) of fumed silica content, gelled electrolyte was also being sedimentation in battery. On the other hand, the gelled electrolytes with 4% (w/v) of fumed silica content and specific gravity of H_2SO_4 over 1.280 were being as a gel. Hence, 4% (w/v) of A200 fumed silica for gel formulation.

4.2 Battery testing

4.2.1 The discharge capacity of VRLA batteries

The discharge capacity of S12-1 to 12-3 batteries was measured at C_1 during 4 cycles because the measuring time was reduced. The results are shown in Fig. 4.1. The discharge capacity was increased when the concentration of H_2SO_4 increased. However, increasing the concentration of H_2SO_4 is caused the corrosion of positive plates and reduced the service life.

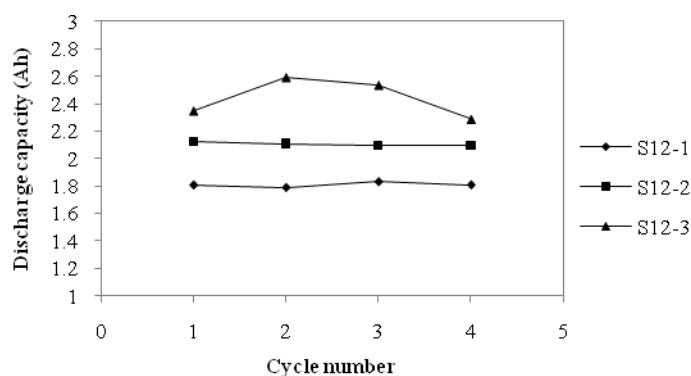


Figure 4.1 The discharge capacity of S12-1 to S12-3 batteries at C_1 during 4 cycles.

The initial voltage of S12-1 battery was only 12.41 Volt because the S12-1 battery contained the lowest of H_2SO_4 concentration. Therefore, it provided the lowest initial voltage, discharge period and capacity. Meanwhile, the highest discharge capacity was S12-3 battery which was contained the highest density of H_2SO_4 . According to the Nerst's equation and the reaction in battery cells affect to cell voltage, plates and related capacity. Thus, the increasing of H_2SO_4 in battery provided the higher capacity.

Nevertheless, the higher H₂SO₄ concentration was risk to higher grid and increased the corrosion of both active materials which related to short service life of the battery.

In this work, the optimal H₂SO₄ concentration was 1.280 sp.gr.. The effect of fumed silica content, fumed silica particle sizes and additives on the performance of VRLA batteries was investigated by measuring the discharge capacity during 15 cycles. The battery groups were divided following the types of additive.

4.2.1.1 No additive

The S12-2, S12-4, S12-5 batteries were contained the gelled electrolyte of 2-4% (w/v) of fumed silica particle size 12 nm (A200) without additive. They were measured the discharge capacity during 15 cycles and were compared the discharge capacity among the 2-4% (w/v) of fumed silica content as shown in Fig. 4.2 a). Also, in Fig. 4.2 b) was shown the discharge capacity of the S7-1 to S7-3 batteries which were contained the gelled of fumed silica particle size 7 nm (A300) without additive. For the gelled electrolyte at 5% (w/v) of both fumed silica particle size (A200 and A300) without additive was hardly filled into the battery case owing to short gelling time [44-45]. In addition, the time of filling process and cost of battery were decreased.

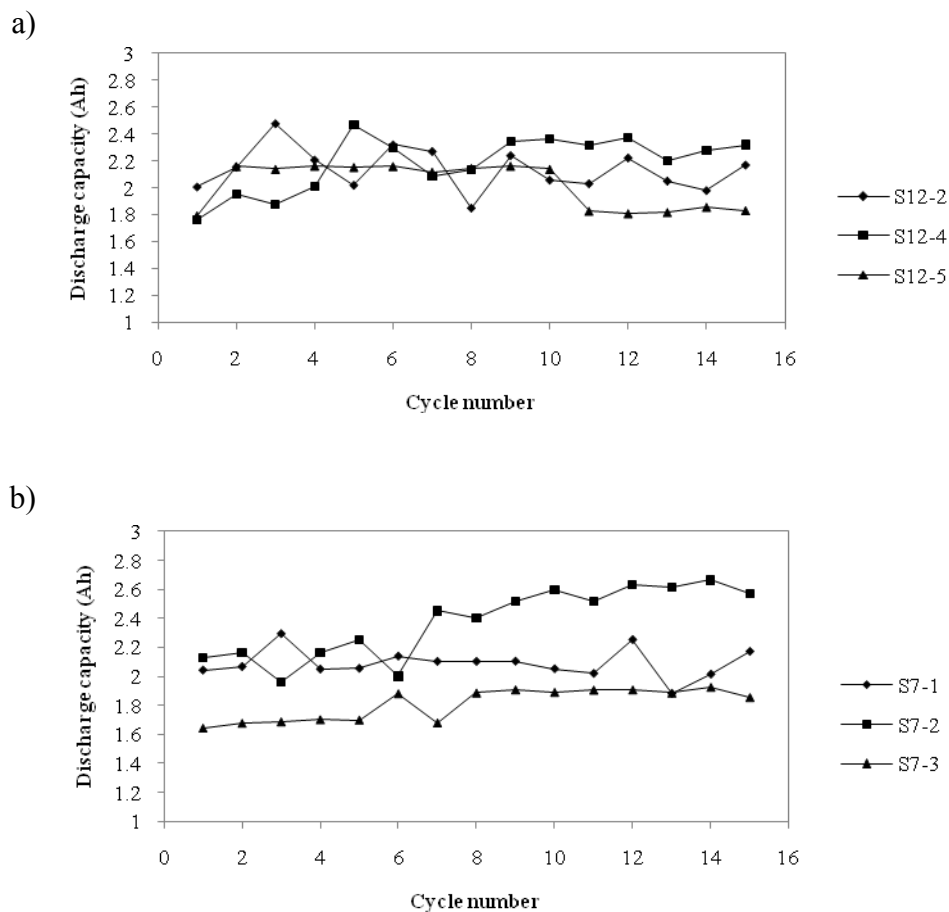


Figure 4.2 The discharge capacity of gel batteries without additive at C_1 during 15 cycles: a) batteries with fumed silica particle size 12 nm (A200) at 2-4% (w/v) of fumed silica content, b) batteries with fumed silica particle size 7 nm (A300) at 2-4% (w/v) of fumed silica content.

The results showed that the highest discharge capacity was S7-2 battery which provided the average discharge capacity 2.38 Ah. This battery remained some liquid which can leak or spill out from the container as same as the S12-4 battery. For the S12-2 and S7-1 battery, their gelled electrolytes characterized as sedimentation that was unsuitable for gel VRLA batteries. The gelled electrolyte in S12-5 battery characterized as a gel, there is no leakage or spillage of electrolyte from this battery. However, it provided the lowest discharge capacity. From these results, it can be suggested the 4% (w/v) of fumed silica content and 3% (w/v) of fumed silica should be the suitable for comparative study.

4.2.1.2 Polypyrrole (PPy)

In the previous work, Chaiyasit [45] studied the conductivity of gelled electrolyte with conducting polymer as additive. The result was shown that 0.08% (w/v) of PPy content in gelled electrolyte present the highest conductivity nearby 0.01% (w/v) of PPy. The concentration of 0.01% (w/v) of PPy was chosen because it can save amount of additive and cost for VRLA batteries. The discharge capacity during 15 cycles of gel VRLA batteries with PPy as additive was compared between employed various fumed silica content of A300 and A200. The results were shown in Fig 4.3 a) and b), respectively.

The highest discharge capacity was SP12-3 battery. This battery contained 4% (w/v) of fumed silica A200, 1.280 sp.gr. of H₂SO₄ and 0.01% (w/v) of PPy that was no leakage and spillage. The average discharge capacity of SP12-3 battery was 2.50 Ah that is higher than S12-5 battery about 0.5 Ah. Almost of the gel VRLA batteries with PPy provided the average discharge capacity higher than the gel VRLA batteries without additive. Therefore, PPy can increase the discharge capacity of the battery due to its conductive property.

Moreover, the discharge capacity of gel VRLA batteries with PPy was compared to those obtained from various concentration of PPy at 4% (w/v) of fumed silica content and 1.280 sp.gr. of H₂SO₄. In Fig.4.4 shows the discharge capacity of gel VRLA batteries with various PPy containing. The highest discharge capacity was SP12-5 battery. Thus, the optimal concentration of PPy was 0.01% (w/v) that corresponded to the conductivity of gelled electrolytes in the previous work.

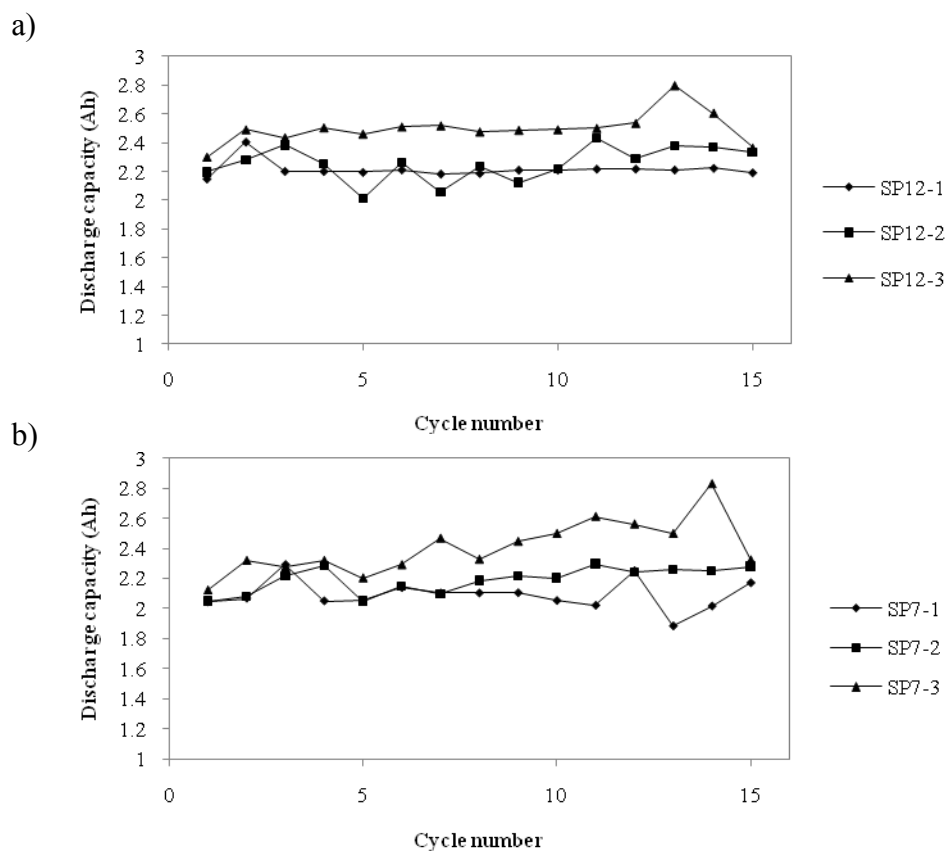


Figure 4.3 The discharge capacity of gel batteries containing PPy as an additive at C_1 during 15 cycles: a) batteries with fumed silica particle size 12 nm (A200) at 2-4% (w/v) of fumed silica content, b) batteries with fumed silica particle size 7 nm (A300) at 2-4% (w/v) of fumed silica content.

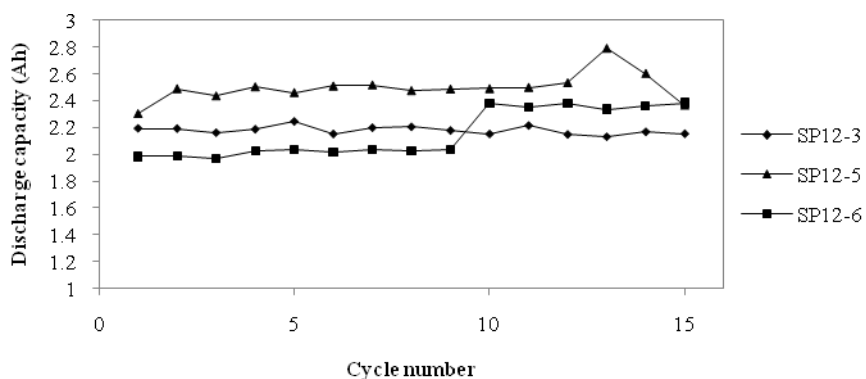


Figure 4.4 The discharge capacity of gel VRLA batteries with 0.005 (SP12-3), 0.01 (SP12-5) and 0.02% (w/v) of PPy containing (SP12-6) at C_1 during 15 cycles.

4.2.1.2 PEDOT:PSS

The discharge capacity during 15 cycles of gel VRLA batteries with PEDOT:PSS (SPD12-1 to SPD12-3 and SPD7-1 to SPD7-3) was investigated. The results were shown in Fig 4.5 a) and b), respectively. The highest discharge capacity was SPD12-1 battery which provided the average discharge capacity at 2.33 Ah during 15 cycles. This battery contained 2% (w/v) of fumed silica A200, 1.280 sp.gr. of H_2SO_4 and 0.01% (w/v) of PEDOT:PSS. This gelled electrolyte inside the battery was sedimentation.

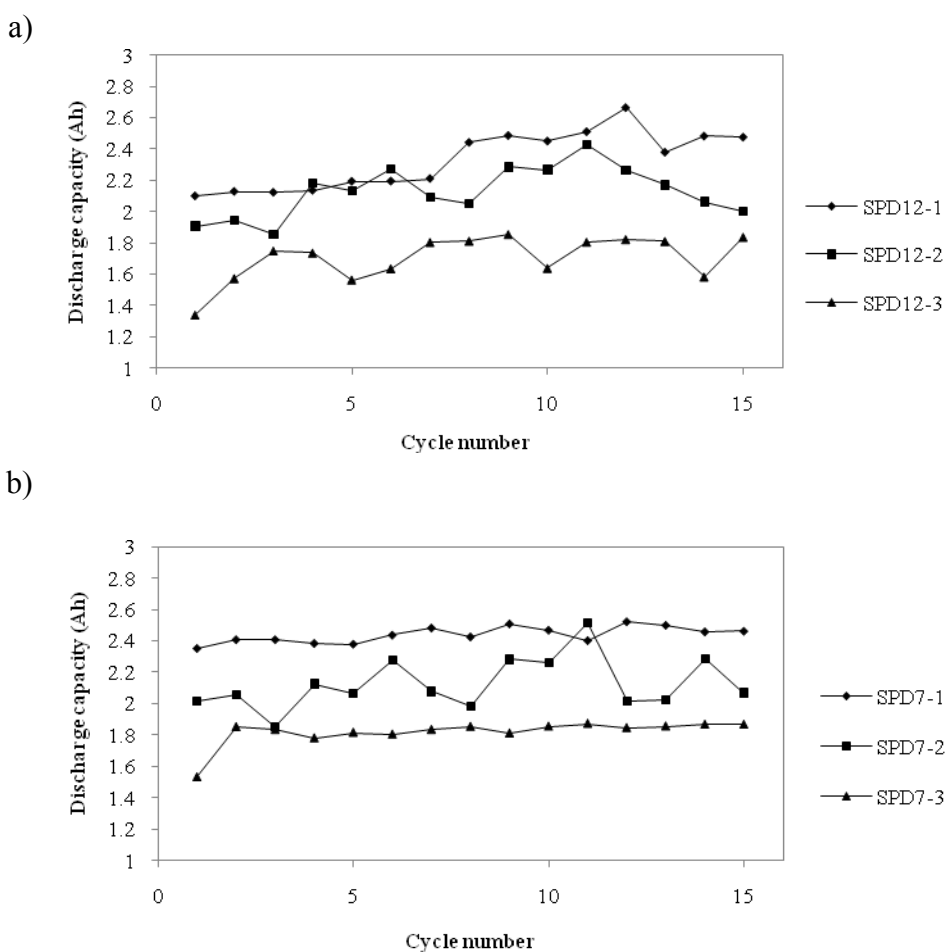


Figure 4.5 The discharge capacity of gel batteries containing PEDOT:PSS as an additive at C_1 during 15 cycles: a) batteries with fumed silica particle size 12 nm (A200) at 2-4% (w/v) of fumed silica content, b) batteries with fumed silica particle size 7 nm (A300) at 2-4% (w/v) of fumed silica content.

Although the adding content of fumed silica to assist more gelation, the aqueous solution still appeared inside the battery with PEDOT:PSS as additive. This additive made the poor gel strength due to the PSS molecule. Increasing fumed silica content reduced the discharge capacity and decreased internal resistance because silica is non-conductive [42]. Hence, the fumed silica content at 4% (w/v) of A200 was chosen as the optimal content for working with PEDOT:PSS.

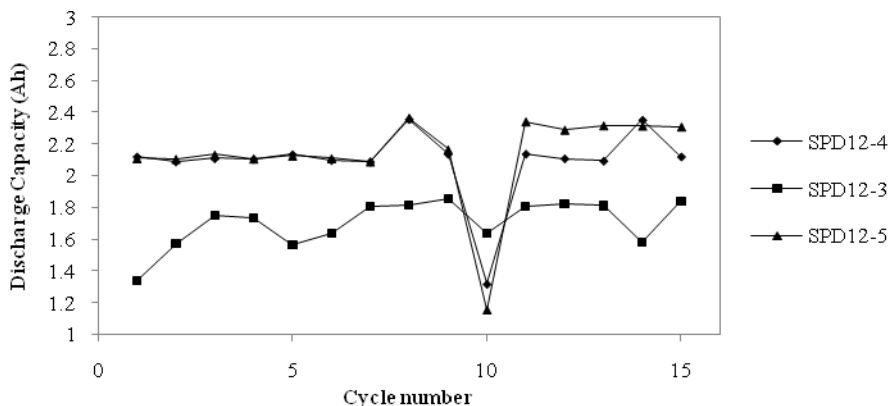


Figure 4.6 The discharge capacity of gel batteries with 0.005, 0.01 and 0.02%(w/v) of PEDOT:PSS containing at C_1 during 15 cycles.

Fig.4.6 showed the discharge capacity of gel VRLA batteries with various concentration of PEDOT:PSS. The highest discharge capacity was SPD12-5 battery which obtained from using 0.02% (w/v) of PEDOT:PSS concentration.

4.2.1.3 Ponceau SS (Pss)

Fig 4.7 a) showed the discharge capacity of the batteries obtained from using A300 with 0.01% (w/v) of Pss, 1.280 sp.gr. of H_2SO_4 and b) obtained from using A200 with 0.01% (w/v) of Pss, 1.280 sp.gr. of H_2SO_4 , respectively.

The SPS7-1 to SPS7-3 VRLA batteries showed higher discharge capacity than SPS12-1 to SPS12-3 VRLA batteries. The highest average discharge capacity was SPS7-2 with 2.43 Ah. For this additive, the content of both fumed silica was distinctly ineffective on the performance of VRLA batteries, however,

their performance depended on the concentration of Pss (see in Fig.4.8). From the results, it was found that fumed silica particle size for this additive was A300 fumed silica.

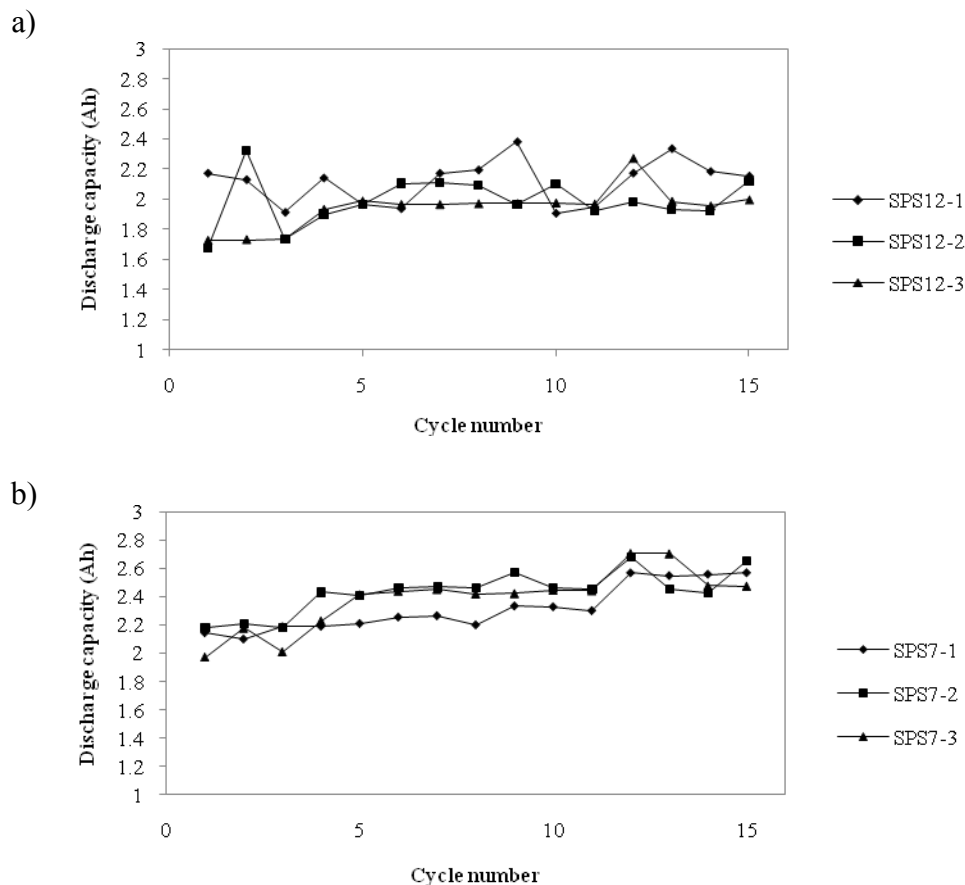


Figure 4.7 The discharge capacity of gel batteries containing Pss as an additive at C_1 during 15 cycles: a) batteries with fumed silica particle size 12 nm (A200) at 2-4% (w/v) of fumed silica content, b) batteries with fumed silica particle size 7 nm (A300) at 2-4% (w/v) of fumed silica content.

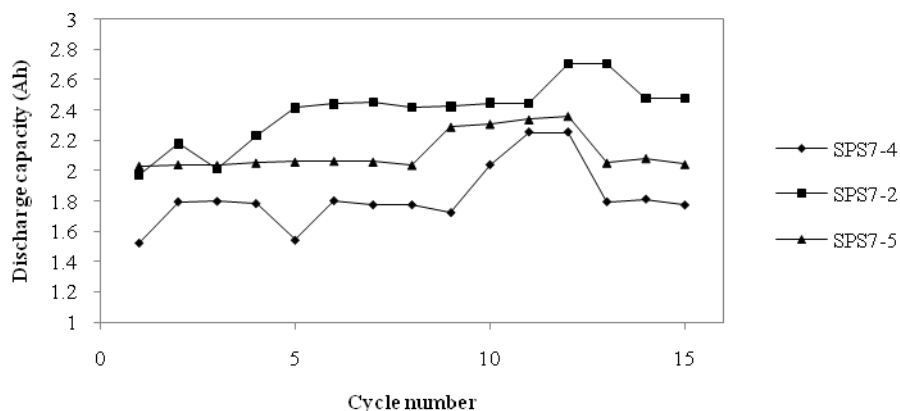


Figure 4.8 The discharge capacity of gel batteries with 0.005, 0.01 and 0.02%(w/v) of Pss containing at C_1 during 15 cycles.

4.2.1.4 Ionic liquid (IL)

The results of the discharge capacity during 15 cycles of gel VRLA batteries with IL at various fumed silica content and particle sizes were shown in Fig 4.9 a) SI12-1to SI12-3 batteries and b) SI7-1 to SI7-3 batteries, respectively. It was remarkable notice that the IL affected to the performance by decreasing discharge capacity and dropping the initial voltage. At 2% (w/v) of fumed silica content exhibited the stable discharge capacity in both of fumed silica particle sizes during 15 cycles. The highest discharge capacity was SI7-1 battery with 2.26 Ah. Among three selected additives, the use of IL displayed the lowest capacity. As a result, IL did not improved the discharge capacity but it might cause the high stable capacity on the flooded lead-acid battery.

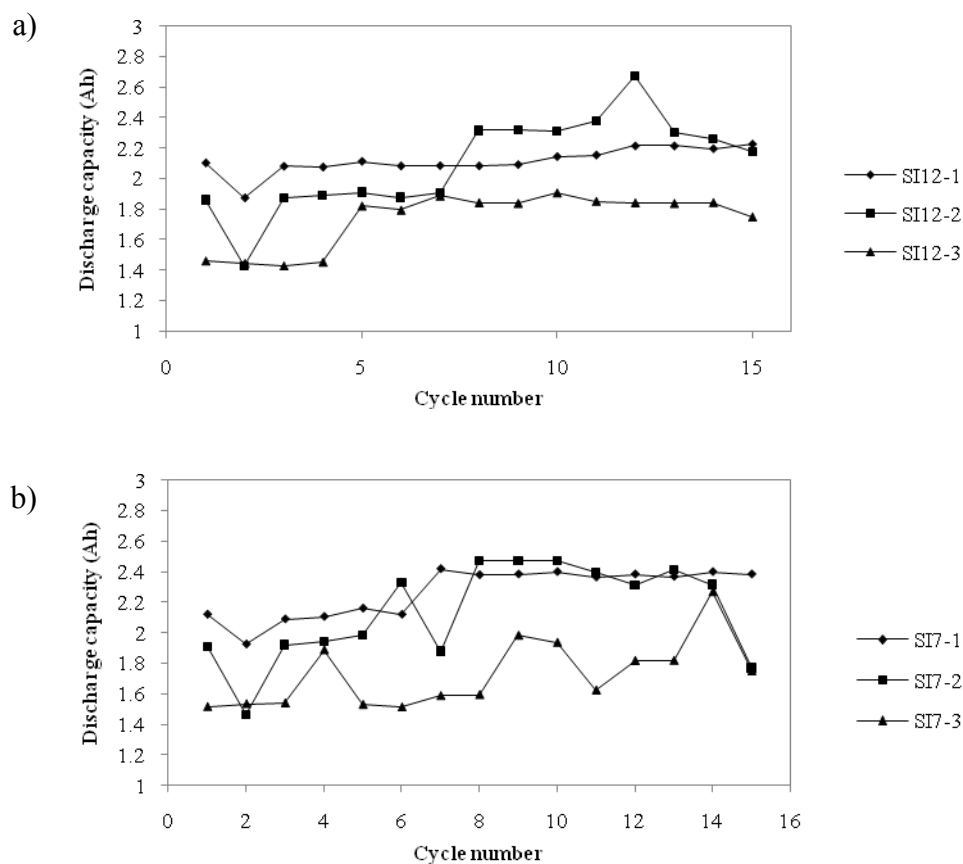


Figure 4.9 The discharge capacity of gel batteries containing IL as an additive at C₁ during 15 cycles: a) batteries with fumed silica particle size 12 nm (A200) at 2-4% (w/v) of fumed silica content, b) batteries with fumed silica particle size 7 nm (A300) at 2-4% (w/v) of fumed silica content.

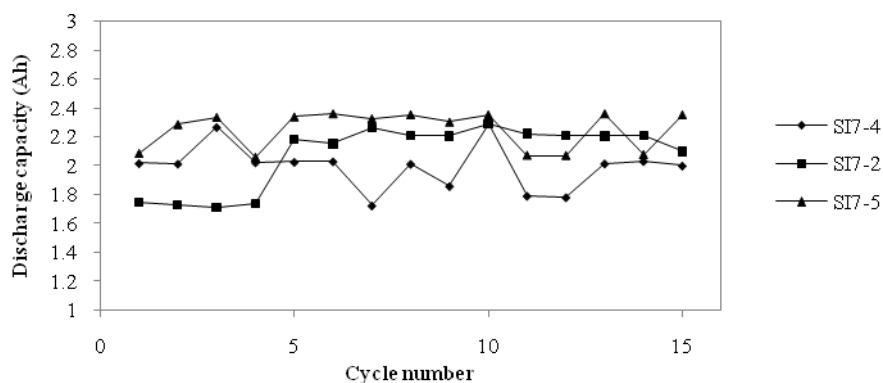


Figure 4.10 The discharge capacity of gel batteries with 0.005, 0.01 and 0.02% (w/v) of IL containing at C₁ during 15 cycles.

Fig.4.10 showed the discharge capacity in different concentration of IL. SI7-5 battery presented higher discharge capacity than SI7-2 battery, however, SI7-2 battery exhibited more stable than SI 7-5 battery.

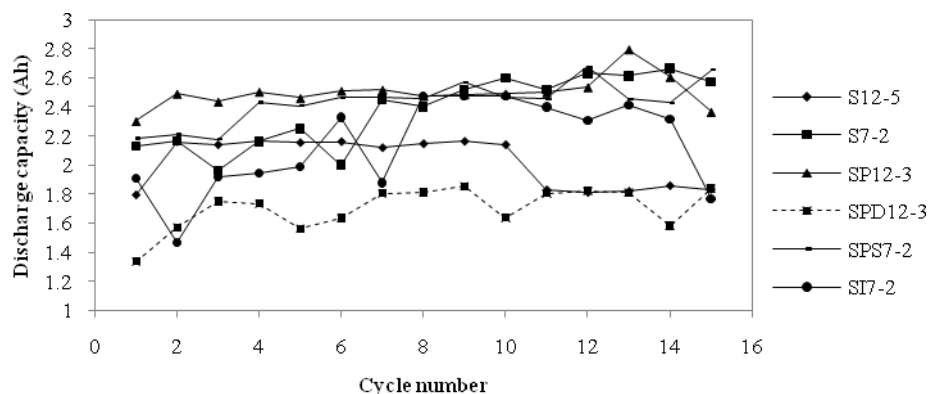


Figure 4.11 The discharge capacity of various gel batteries.

Fig.4.11 illustrated the discharge capacity of various gel batteries. The highest discharge capacity was SP12-3 and the secondary was SPS7-2.

Under the study of discharge capacity of VRLA batteries, it can be suggested that the high discharge capacity depended on the optimal concentration of additive, fumed silica content, fumed silica particle sizes and type of additive.

4.2.2 Initial discharge curves of VRLA batteries

Fig. 4.12 (a-d) showed the initial discharge curves of the gelled electrolytes in VRLA batteries. The data can be noticed that the battery performance was directly affected to the optimal concentration of additive, fumed silica content and fumed silica particle sizes. Similar to the discharge capacity results, the gel VRLA battery containing PPy showed the longest curves of usage time in a cycling and provided the high initial voltage. It means that tendency of discharge capacity is related to the initial discharge values. From both of criterias, it can be addressed that only PPy and Pss can be used to improve performance of gel VRLA battery.

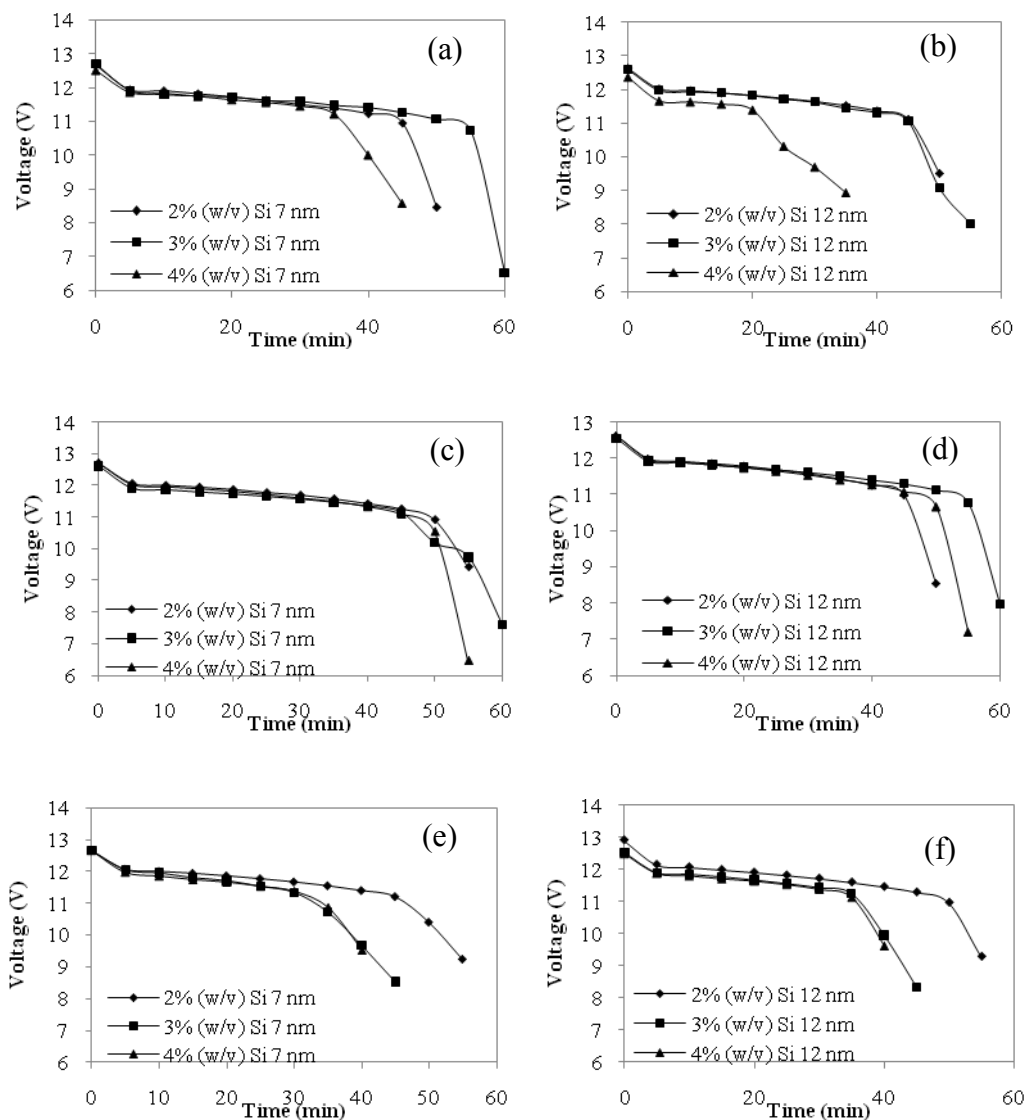


Figure 4.12 Initial discharge curves of battery with gelled electrolytes; (a) 2-4% (w/v) of fumed silica A300 without additive (S7-1 to S7-3), (b) 2-4% (w/v) of fumed silica A200 without additive (S12-2, S12-4, S12-5), (c) 2-4% (w/v) of fumed silica A300 with Pss (SPS7-1 to SPS7-3), (d) 2-4% (w/v) of fumed silica A200 with PPy (SP12-1 to SP12-3), (e) 2-4% (w/v) of fumed silica A300 with IL (SI7-1 to SI7-3) at 1-hour rate and $25^{\circ}\text{C}\pm 1$, and (f) 2-4% (w/v) of fumed silica A200 with PEDOT:PSS (SPD12-1 to SPD12-3).

4.3 Conductivity of gelled electrolytes

4.3.1 Different fumed silica contents and particle sizes

The various gelled electrolytes were investigated by measuring the conductivity at 25°C in order to verify with the performance of the battery. Fig.4.13 displayed the comparison of conductivity between gelled electrolytes with fumed silica A300 and A200 at various contents.

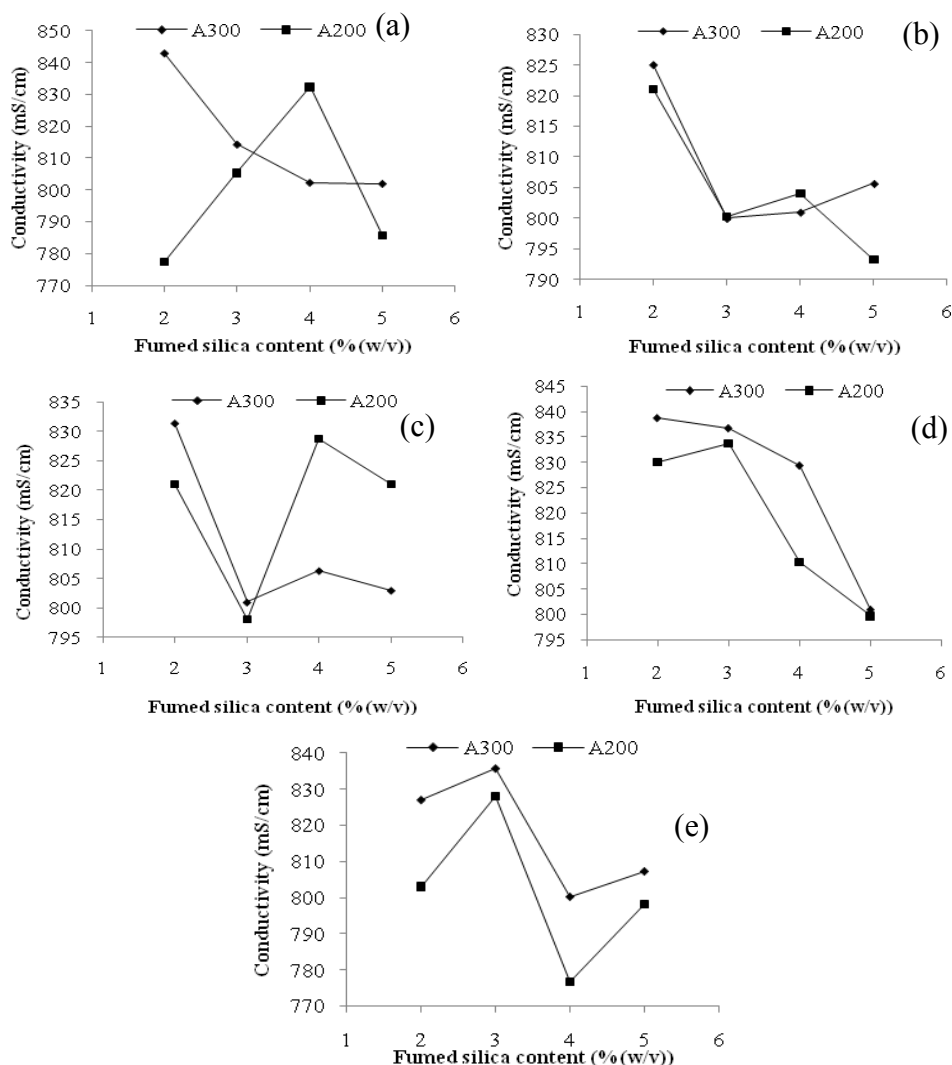


Figure 4.13 Comparison the conductivity of gelled electrolytes between various A300 and A200 fumed silica content; a) without additive, b) PPy, c) PPEDOT:PSS, d) Pss, e) IL.

The gelled electrolyte without additive containing 2% (w/v) of A200 fumed silica and 1.280 of H₂SO₄ showed the highest conductivity of 843 mS/cm with a standard deviation of 1.63 but gel characteristic was not being as a gel. The secondary high conductivity was gelled electrolyte without additive containing 4% (w/v) of A200 fumed silica and 1.280 of H₂SO₄ at 832.33 mS/cm with a standard deviation of 1.25 which gel characteristic was being as a gel (see Fig.4.13 a)). All of the gelled electrolytes containing 2% (w/v) of both fumed silica particle sizes characterized the sedimentation which was inapplicable for gel VRLA battery. Therefore, the gelled electrolytes over 3% (w/v) of fumed silica content were considered. Fig. 4.3 b), the gelled electrolyte containing 4% (w/v) of A200 fumed silica, 1.280 sp.gr. of H₂SO₄ and 0.01% (w/v) of PPy provided the conductivity of 804 mS/cm with standard deviation of 2.62. Fig. 4.3 c), the gelled electrolyte containing 4% (w/v) of A200 fumed silica, 1.280 sp.gr. of H₂SO₄ and 0.01% (w/v) of PEDOT:PSS provided the conductivity of 828.67 mS/cm with standard deviation of 1.25. Fig. 4.3 d), the gelled electrolyte containing 3% (w/v) of A300 fumed silica, 1.280 sp.gr. of H₂SO₄ and 0.01%(w/v) of Pss provided the conductivity of 836.67 mS/cm with standard deviation of 3.87. In Fig. 4.3 e), the gelled electrolyte containing 3% (w/v) of A300 fumed silica, 1.280 sp.gr. of H₂SO₄ and 0.01% (w/v) of Pss provided higher conductivity of 835.67 mS/cm with standard deviation of 3.77. The highest conductivity was the gelled electrolyte containing 3% (w/v) of A300 fumed silica, 1.280 sp.gr. of H₂SO₄ and 0.01% (w/v) of Pss. The conductivity decreased when the ionic conductivity is excess, which can make the exchanges of ionic conductivity are difficult [4]. Anyway, the results showed that the tendency of conductivity resembled as the performance of the batteries, except gelled electrolyte with PEDOT:PSS as additive.

4.3.2 Different concentration of additives

In order to investigated the effect of the concentration of additives on the conductivity, the concentrations of additives at 0.005% (w/v), 0.01% (w/v), 0.02% (w/v) were investigated and shown in Table. 4.2-4.5.

Table 4.2 The conductivity values of gelled electrolytes containing various concentration of PPy.

Type of fumed silica	Concentration of PPy		
	0.005% (w/v)	0.01% (w/v)	0.02% (w/v)
4% (w/v) Fumed silica A200	773	804	773

From Table 4.2, 4% (w/v) of A200 fumed silica, 1.280 sp.gr. of H₂SO₄ and 0.01% (w/v) of PPy provided the highest conductivity value. 4% (w/v) of A200 fumed silica and 3% (w/v) of A300 fumed silica were chosen to verify the optimal concentration because of above mention in 4.2.1..

Table 4.3 The conductivity values of gelled electrolytes containing various concentration of PEDOT:PSS.

Type of fumed silica	Concentration of PEDOT:PSS		
	0.005% (w/v)	0.01% (w/v)	0.02% (w/v)
4% (w/v) Fumed silica A200	796	829	782

From Table 4.3, 4% (w/v) of A200 fumed silica, 1.280 sp.gr. of H₂SO₄ and 0.01% (w/v) of PEDOT:PSS provided the highest conductivity value but the highest battery's performance was 4% (w/v) of A200 fumed silica, 1.280 sp.gr. of H₂SO₄ and 0.02% (w/v) of PEDOT:PSS. It can be seen that the results were not in agreement each other. This phenomena cannot be explained. Therefore, it still need time for study.

Table 4.4 The conductivity values of gelled electrolytes containing various concentration of Pss.

Type of fumed silica	Concentration of Pss		
	0.005% (w/v)	0.01% (w/v)	0.02% (w/v)
3% (w/v) Fumed silica A300	804	837	789

From Table 4.4, 3% (w/v) of A300 fumed silica, 1.280 sp.gr. of H₂SO₄ and 0.01% (w/v) of Pss provided the highest conductivity value.

Table 4.5 The conductivity values of gelled electrolytes containing various concentration of IL.

Type of fumed silica	Concentration of IL		
	0.005% (w/v)	0.01% (w/v)	0.02% (w/v)
3% (w/v) Fumed silica A300	780	836	779

From Table 4.5, 3% (w/v) of A300 fumed silica, 1.280 sp.gr. of H₂SO₄ and 0.01% (w/v) of IL provided the highest conductivity value but 3% (w/v) of A300 fumed silica, 1.280 sp.gr. of H₂SO₄ and 0.02% (w/v) of IL exhibited the highest discharge capacity.

From the investigation, some additive probably improved the conductivity due to an ionic strength. Hence, the exchanges of the ionic conductivities were simply occurred.

The gelled electrolytes with different additives showed the different conductivity behavior. The more significant increases were observed from the gelled electrolyte containing Pss as an additive. The highest conductivity of 837 mS/cm was obtained from the gelled electrolyte containing 0.01% (w/v) of Pss. The high conductivity of the gelled electrolyte was generally explained by increasing free ion concentration as well as structural characteristics. However, the mechanism was still not clearly understood. In addition, the measured conductivity method cannot definitely verify the preliminary result of the battery's performance.

4.4 Hydrogen and oxygen evolution of gelled electrolyte

The hydrogen and oxygen evolution was the effect of water loss in battery due to the overcharging process. The rate of hydrogen and oxygen evolution needed to be balance, otherwise led to negative plate degradation or softening of PAM that affect to its service life [47]. All gelled electrolytes were studied by using cyclic voltammetry. Fig. 4.14-4.23 showed the cyclic voltammograms of various gelled electrolytes. The cyclic voltammograms showed the similar redox peaks in the potential range -2.5 V–2.9

V, indicating that the hydrogen and oxygen evolution was depended on the additive type, concentration of additive, fumed silica content and fumed silica particle sizes. The oxidation of PbSO_4 to PbO_2 appeared at -0.5 V and the reduction of PbO_2 to PbSO_4 appeared at -0.4 V.

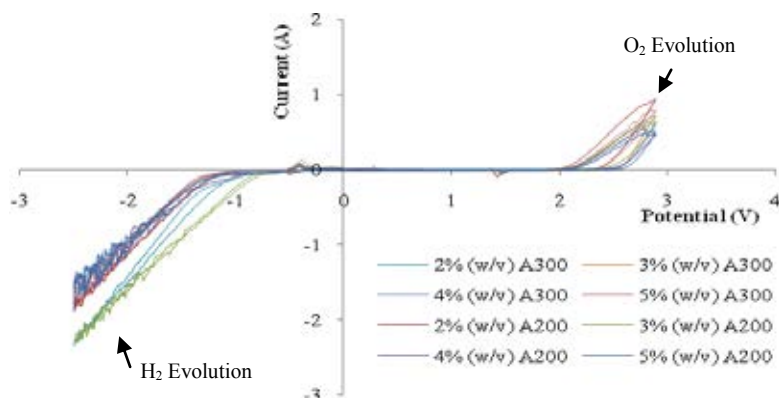


Figure 4.14 Cyclic voltammogram of gelled electrolytes without additive at 2-5%(w/v) of A300 and A200 fumed silica, scan rate of 20 mV s^{-1} .

From the redox peaks current, it can be seen that the lowest hydrogen and oxygen evolution was found to be at 5% (w/v) of A200 fumed silica which is very close to result obtained 4% (w/v) of A200 fumed silica as shown in Fig. 4.14. The highest hydrogen evolution was 2% (w/v) of A300 fumed silica and 3% (w/v) of A200 fumed silica.

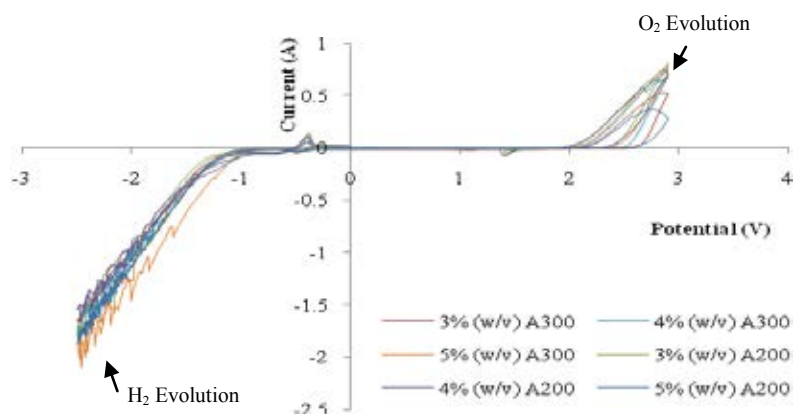


Figure 4.15 Cyclic voltammogram of gelled electrolytes with 0.01% (w/v) PPy at 2-5% (w/v) of A300 and A200 fumed silica, scan rate of 20 mV s^{-1} .

Fig. 4.15 presents the cyclic voltammogram of gelled electrolytes with 0.01% (w/v) of PPy. The lowest oxygen evolution was 5% (w/v) of A200 fumed silica but it exhibited the high hydrogen evolution. As the secondary lowest oxygen evolution was observed at 4% (w/v) of A200 fumed silica which was balanced with hydrogen evolution. Therefore, 4% (w/v) of A200 fumed silica was chosen as suitable fumed silica content to study the effect of PPy in term of hydrogen and oxygen evolution accompany with the performance of VRLA battery and conductivity as shown in Fig. 4.16.

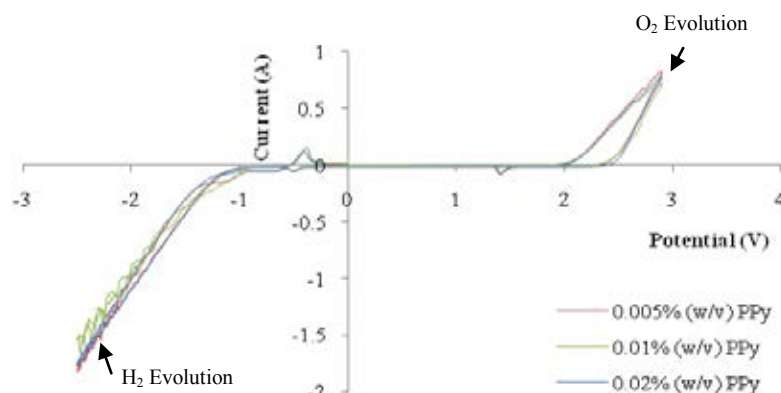


Figure 4.16 Cyclic voltammogram of gelled electrolytes with PPy at 4% (w/v) of A200 fumed silica, scan rate of 20 mV s^{-1} .

Fig. 4.16, It can be observed that the concentration of PPy was insignificantly influence on the hydrogen and oxygen evolution. However, the lowest hydrogen and oxygen evolution was 0.01% (w/v) of PPy.

In the same way, the other additives were studied to get the suitable amount for using in gelled electrolyte.

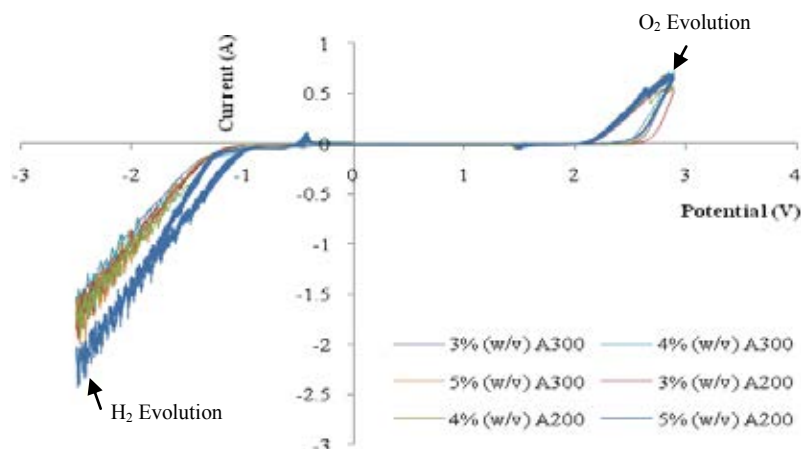


Figure 4.17 Cyclic voltammogram of gelled electrolytes with 0.01% (w/v) PEDOT:PSS at 2-5% (w/v) of fumed silica content, scan rate of 20 mV s^{-1} .

Fig. 4.17 is the result obtain from the gelled electrolyte with 0.01% (w/v) PEDOT:PSS. The lowest redox peak was 3% (w/v) and 4% (w/v) of A200 fumed silica. According to the results of battery's performance and the conductivity of gelled electrolyte was presented, 4% (w/v) of A200 fumed silica was considered to monitor in different concentration of PEDOT:PSS.

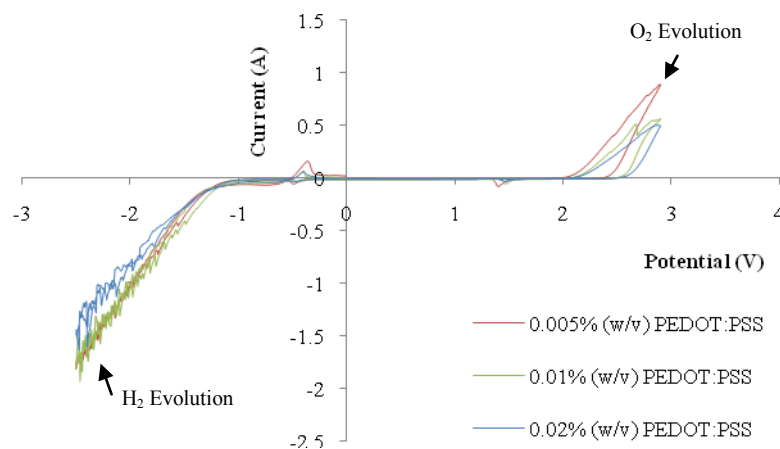


Figure 4.18 Cyclic voltammogram of gelled electrolytes with PEDOT:PSS at 4% (w/v) of A200 fumed silica, scan rate of 20 mV s^{-1} .

From Fig. 4.18, the concentration of PEDOT:PSS affected to the redox peak as well. The lowest hydrogen and oxygen evolution was 0.02% (w/v) of PEDOT:PSS.

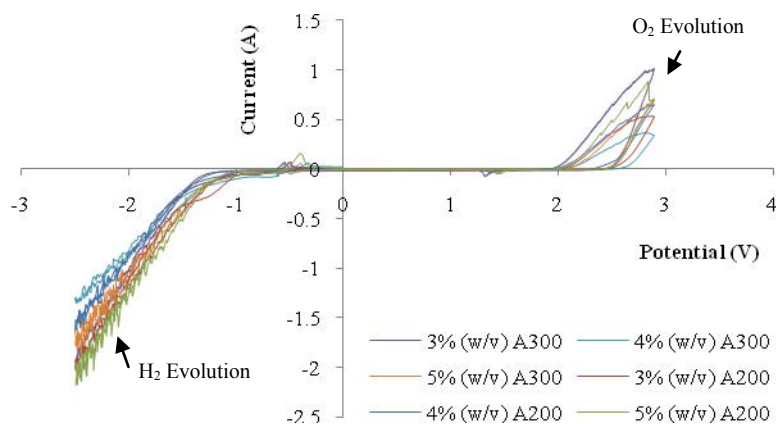


Figure 4.19 Cyclic voltammogram of gelled electrolytes with 0.01% (w/v) Pss at 2-5% (w/v) of fumed silica content, scan rate of 20 mV s^{-1} .

Fig. 4.19 present the cyclic voltammogram of gelled electrolytes with 0.01% (w/v) Pss. The lowest redox peak was 4% (w/v) of A300 fumed silica. On the other hand, the highest redox peak was 3% (w/v) of A300 fumed silica which provided high battery's performance and the conductivity of gelled electrolyte. Thus, the use of 3% (w/v) of A300 fumed silica with 0.01% (w/v) Pss was possibly suitable amount added into gelled electrolyte.

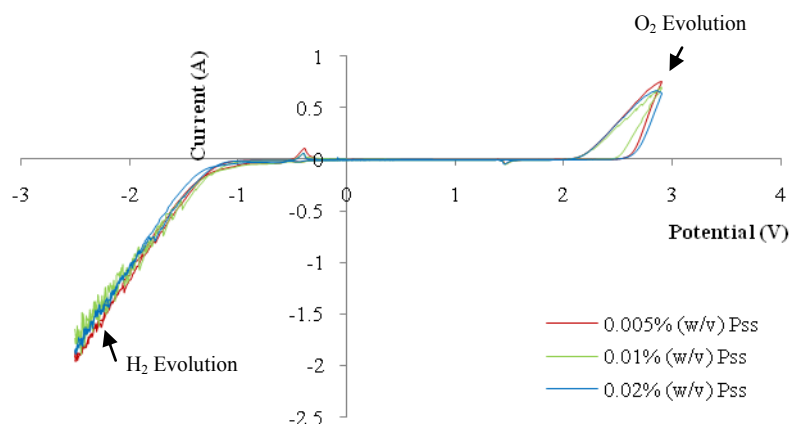


Figure 4.20 Cyclic voltammogram of gelled electrolytes with Pss at 4%(w/v) of A300 fumed silica, scan rate of 20 mV s^{-1} .

Fig. 4.20 displayed the effect of Pss concentration on the reduction peak. The lowest oxygen evolution was 0.02% (w/v) of Pss, which is nearby 0.01% (w/v) of Pss. Thus, 4% (w/v) of A300 fumed silica with 0.01% (w/v) of Pss was chosen in order to compromise the cost effective.

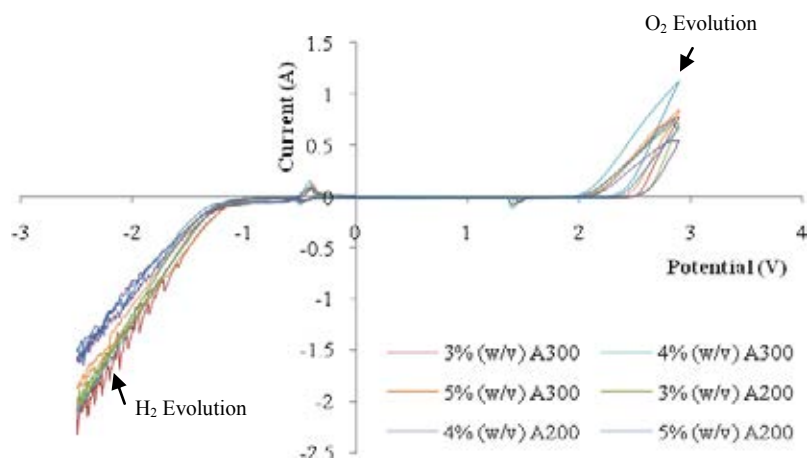


Figure 4.21 Cyclic voltammogram of gelled electrolytes with 0.01% (w/v) IL at 2-5% (w/v) of A300 and A200 fumed silica, scan rate of 20 mV s^{-1} .

Fig. 4.21 is the results of using ionic liquid as additive. The lowest redox peak was 4% (w/v) of A200 fumed silica but it provided the lowest battery's performance and the conductivity of gelled electrolyte. Inexplicable reason, the 3% (w/v) of A300 fumed

silica was selected as the model to study the effect of IL's concentrations owing to its higher performance and conductivity. From Fig 4.22, the lowest redox peak was 0.005% (w/v) of IL with 3% (w/v) of A300 fumed silica. The redox peak relied on the concentration of IL.

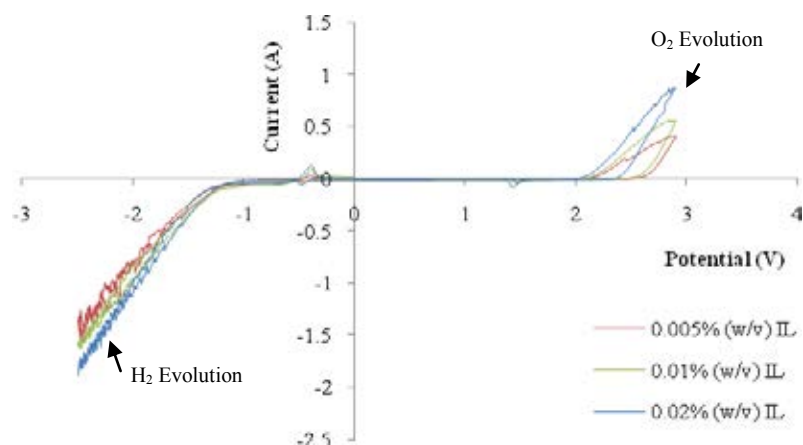


Figure 4.22 Cyclic voltammogram of gelled electrolytes with IL at 3% (w/v) of A300 fumed silica, scan rate of 20 mV s^{-1} .

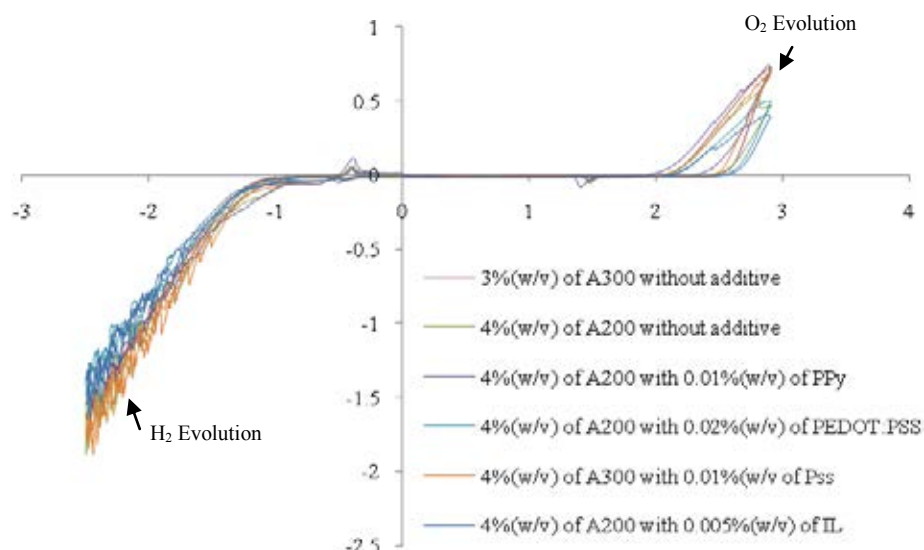


Figure 4.23 Cyclic voltammogram of various gelled electrolytes.

Fig. 4.23 summarized the results obtained from each optimal condition. For the various gelled electrolytes, in comparison, the oxygen evolution peaks were diminished when increased fumed silica content was used. Furthermore, optimal concentration of additive type led to a reduction in hydrogen and oxygen evolution. The cyclic voltammetry investigation resulted in the long-term cycle life in battery performance. The cyclic voltammogram of 4% (w/v) of A200 with 0.005% (w/v) of IL showed the lowest hydrogen and oxygen evolution, whereas 3% (w/v) of A300 with 0.01% (w/v) of Pss and 4% (w/v) of A200 with 0.01% (w/v) of PPy showed the highest peak. Thus, a gelled electrolyte with 0.005% (w/v) of IL, 1.280 sp.gr. of H_2SO_4 and 4% (w/v) of A200 may be probable for providing the long cycle life for VRLA battery.

4.5 Morphology of gelled electrolyte

Gelled electrolytes from VRLA batteries were next observed for their morphology. After the battery was tested, the 6 batteries were cleaved and the gels were taken to be investigated by using scanning electron microscope (SEM). The 6 morphologies of gelled electrolytes were shown in Fig. 4.24.

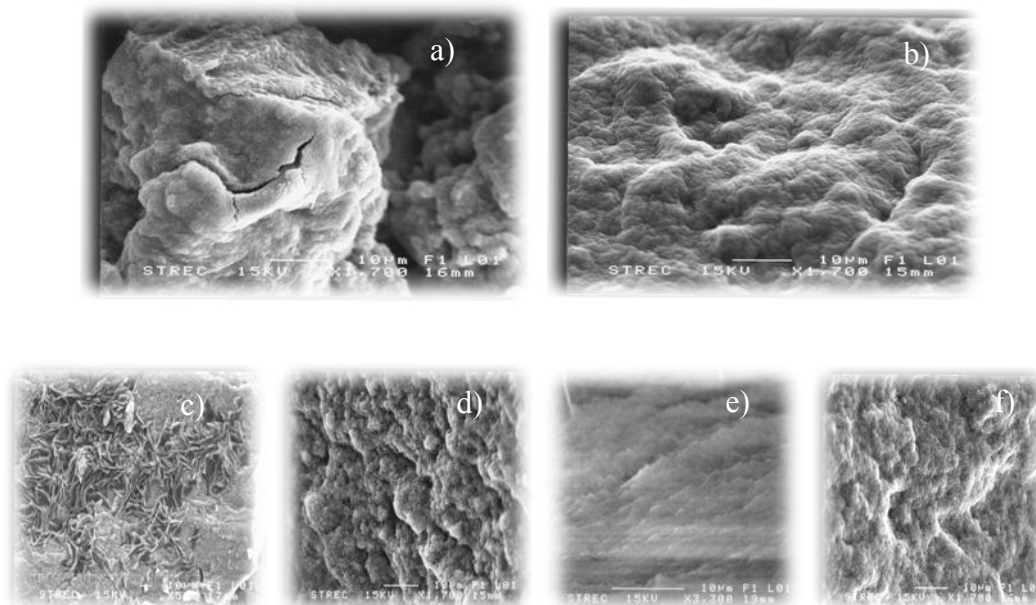


Figure 4.24 Morphology of gelled electrolytes from VRLA battery; a) 3% (w/v) of A300 fumed silica with additive, b) 4% (w/v) of A200 fumed silica without additive, c) 4%

(w/v) of A200 fumed silica with 0.01% (w/v) of PPy, d) 4% (w/v) of A200 fumed silica with 0.02% (w/v) of PEDOT:PSS, e) 3% (w/v) of A300 fumed silica with 0.01% (w/v) of Pss, f) 3% (w/v) of A300 fumed silica with 0.01% (w/v) of IL.

Comparison between Fig. 4.24 a) and b), the gel morphology of 3% (w/v) of A300 fumed silica without additive was denser and dryer than the gel morphology of 4% (w/v) of A200 fumed silica without additive. This dry gel might cause increased the hydrogen and oxygen evolution. In Fig. 4.2 c) to f), there was the difference of characteristic in SEM images. Obviously in Fig. 4.24 c), appearing PPy inside the gelled electrolyte means that PPy was insoluble in sulfuric acid solution. This might cause unsteadiness of each battery. On the other hand, gelled electrolyte with others additive showed the homogeneous. The morphology of gelled electrolyte with PEDOT:PSS showed more porosity than the others as shown in Fig. 4.24 d). This morphology possibly caused the decreasing of the performance of battery, however, there was no any basis to confirm the reason. The more gel strength was good for prevented leakage or spillage but is worse transference of electrolyte. However, the use of Pss as additive (see in Fig. 4.24 e)) can improve the electron transference by its ionic strength. The gel morphology in Fig.4.24 f) was similar in Fig. 4.24 b).

4.6 XRD analysis

A cubic negative plate from different VRLA batteries was analyzed by using X-ray diffractometer (XRD). All the cubic negative samples were shown the XRD pattern in Fig. 4.25 by mean of red straight line as lead sulfate (PbSO_4) and blue straight line as lead (Pb). Fig. 4.25 a) to f) indicated that there were only PbSO_4 (red) peak, Pb (blue) peak and some noise which possibly mean amorphous. From these results, it seems that the additives were no reaction with the negative plate electrode and mostly lead surface was used by lead sulfate.

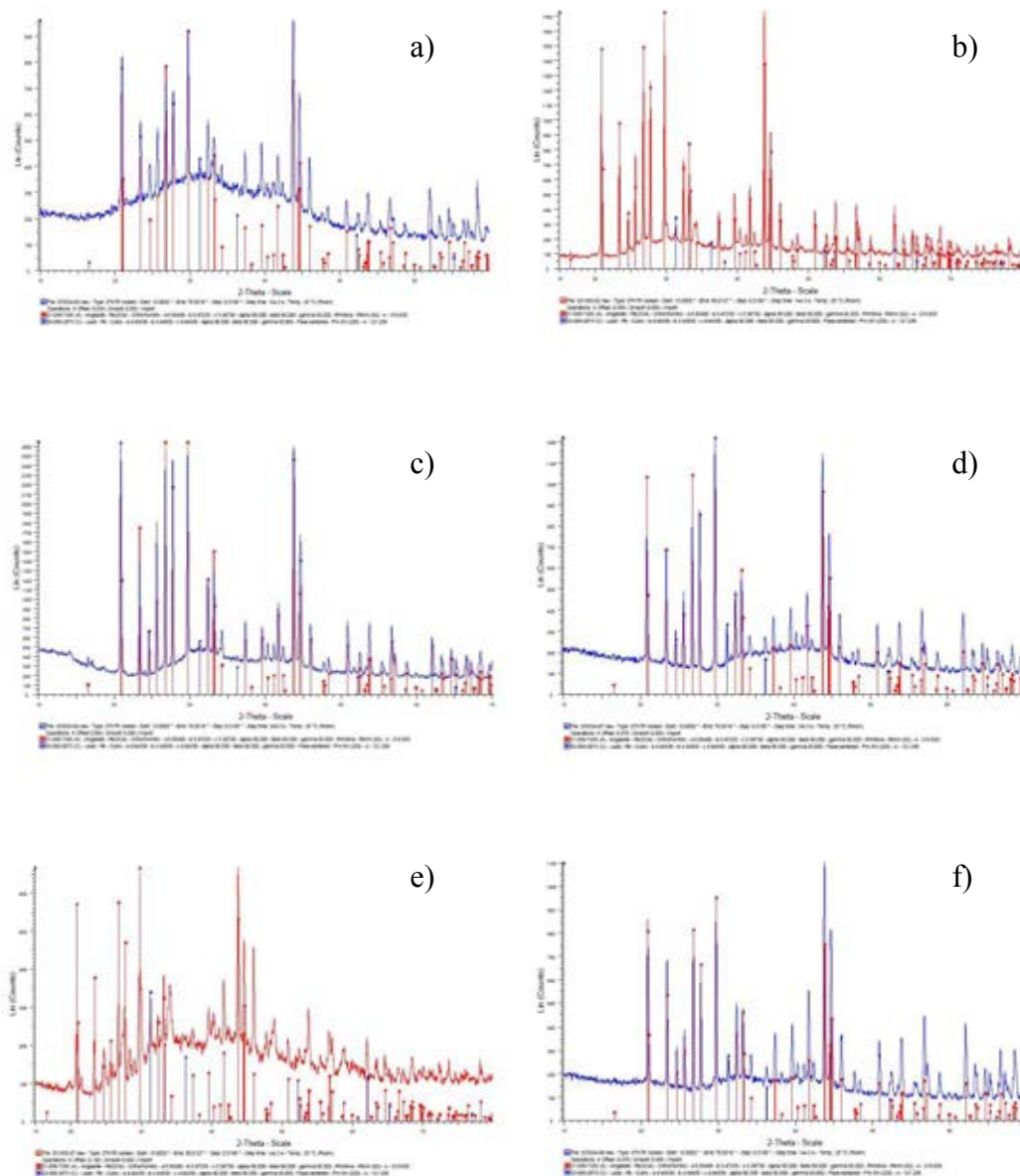


Figure 4.25 XRD pattern of PbSO_4 (blue) and Pb (red) on negative electrode from various VRLA battery; a) S7-2, b) S12-5, c) SP12-3, d) SPD12-5, e) SPS7-2, f) SI7-2.

CHAPTER V

CONCLUSIONS AND FUTURE PERSPECTIVE

5.1 Conclusions

In conclusion, the increasing fumed silica content not only influence on the decreasing of discharge capacity but also affect to hardly filling process, The fumed silica particle size also affect to the discharge capacity. Gel characteristic of fumed silica particle size 12 nm was better than fumed silica particle size 7 nm but provided the lower discharge capacity. The conducting polymer used as additive provided the higher battery's performance. However, the optimal concentration of additive, type of additive, fumed silica content and fumed silica particle sizes can improve gel characteristic and the battery's performance. For the electrical conductivity of the gelled electrolytes depended on concentration of additive, type of additive, fumed silica content and fumed silica particle sizes likewise the battery's performance. The measurement of conductivity and monitoring gel characteristic were another parameter to find out the optimization of gel. The cycle life of the battery was investigated the hydrogen-oxygen evolution by using cyclic voltammetry. The gelled electrolyte containing 4%(w/v) of A200 fumed silica, 1.280 sp.gr. of H₂SO₄ and 0.01%(w/v) of PPy provided the highest discharge capacity of 2.5 Ah. Moreover, it provided the high initial voltage, conductivity and good balance of hydrogen-oxygen evolution. On the other hand gelled electrolyte containing 3%(w/v) of A300 fumed silica, 1.280 sp.gr. of H₂SO₄ and 0.01%(w/v) of Pss provided the high discharge capacity of 2.43 Ah and high conductivity of 836 mS/cm. The lowest of hydrogen-oxygen evolution was obtained from the gelled electrolyte with 4%(w/v) of A200 fumed silica, 1.280 sp.gr. of H₂SO₄ and 0.005%(w/v) of IL. The morphology of gelled electrolyte was different when different additives were added. Finally, all additives were inefficient on the negative electrode.

In addition, the novel gelled electrolytes had surprising capacity results when compared to those of standard capacity of 2.3 Ah at 1-hour rate (at 25°C) (supplied by

N.V. Battery) [46]. Such the promising characteristic of proposed gelled electrolyte, this gel technology could be applied to various application in the future.

5.2 Future perspective

The novel gelled electrolytes consisting of PPy and Pss showed high performance in VRLA batteries. Hence, other additives may be similarly used to enhance the higher performance of VRLA batteries.

REFERENCES

- [1] Rand, D.A.J.; Moseley, P.T.; Garche, J. and Parker, C.D. Valve-regulated Lead-Acid Batteries. Amsterdam, The Netherlands : ELSEVIER B.V., 2004
- [2] Linden, D. Handbook of batteries. United States of America: McGraw-Hill, 1995.
- [3] Berndt, D. Maintenance-free batteries lead-acid, nickel/cadmium, nickel/hydride a handbook of battery technology. Great Britain: John Wiley & Sons, 1993.
- [4] Berndt, D. Maintenance-free batteries based on aqueous electrolyte lead-acid, nickel/cadmium, nickel/hydride a handbook of battery technology. Great Britain: John Wiley & Sons, 2003.
- [5] The Encyclopedia of Alternative Energy and Sustainable Living, Lead-acid battery, [online]. Available from: http://www.daviddarling.info/encyclopedia/L/AE_lead-acid_battery.html [2010, January 27].
- [6] Bullock, K. R. Lead/acid batteries. Journal of Power Sources 51 (1994): 1-17.
- [7] Hehner, N.E. Storage battery manufacturing manual. United States of America: Independent battery manufacturers association, 1986.
- [8] IEEE guide for selection of valve-regulated lead-acid (VRLA) batteries for stationary applications [online]. (n.d.). Available from: <http://ieeexplore.ieee.org/stamp/stamp.jsp?arnumber=00531501> [2008 , September 23].
- [9] Derek, P. Industrial electrochemistry. United States of America: Chapman and hall, 1982.
- [10] Rusch, W.; Vassallo, K. and Hart G. Understanding the real differences between gel and AGM batteries [Online]. (n.d.). Available from: <http://www.battcon.com/paperfinal2007/rushpaper2007.pdf> [2007, September 23].
- [11] Raghavan, S.R.; Walls, H.J. and Khan, S.A., Lithium/V₃O₅ cells using silica nanoparticle-based composite electrolyte. Langmuir 16 (2000): 7920–7930.

- [12] Skotheim, T.A.; and Reynolds, J.R. Conjugated polymers theory, synthesis, properties, and characterization. United States of America: CRC Press Taylor & Francis Group, 2007.
- [13] Soontornworajit, B.; et al. J. Induced interaction between polypyrrole and SO₂ via molecular sieve 13X. Materials Science and Engineering: B 136 (2007): 78-86.
- [14] Chew, S. Y.; et al. Novel nano-silicon/polypyrrole composites for lithium storage. Electrochemistry Communications 9 (2007): 941-946.
- [15] Wu, A.; Venancio, E. C.; and MacDiarmid, A. G. Polyaniline and polypyrrole oxygen reversible electrodes. Synthetic Metals 157 (2007): 303-310.
- [16] Al-Mashat, L.; Tran, H. D.; Wlodarski, W.; Kaner, R. B.; and Kalantar-zadeh, K. Polypyrrole nanofiber surface acoustic wave gas sensors. Sensors and Actuators B: Chemical 134 (2008): 826-831.
- [17] Lu, Q.; and Li, C. M. One-step co-electropolymerized conducting polymer-protein composite film for direct electrochemistry-based biosensors. Biosensors and Bioelectronics 24 (2008): 767-772.
- [18] Dutta, K.; and De, S. K. Transport and optical properties of SiO₂-polypyrrole nanocomposites. Solid State Communications 140 (2006): 167-171.
- [19] Cheng, Q.; Pavlinek, V.; Li, C.; Lengalova, A.; He, Y.; and Saha, P. Synthesis and characterization of new mesoporous material with conducting polypyrrole confined in mesoporous silica. Materials Chemistry and Physics 98 (2006): 504-508.
- [20] Sharma, R. K.; Rastogi, A. C.; and Desu, S. B. Nano crystalline porous silicon as large-area electrode for electrochemical synthesis of polypyrrole. Physica B: Condensed Matter 388 (2007): 344-349.
- [21] Spires, J. B.; Peng, H.; Williams, D. E.; Wright, B. E.; Soeller, C.; and Travas-Sejdic, J. The effect of the oxidation state of a terthiophene-conducting polymer

and of the presence of a redox probe on its gene-sensing properties. Biosensors and Bioelectronics 24 (2008): 928-933.

- [22] Wang, J.-Z.; et al. Paper-like free-standing polypyrrole and polypyrrole-LiFePO₄ composite films for flexible and bendable rechargeable battery. Electrochemistry Communications 10 (2008): 1781-1784.
- [23] PEDOT:PSS [Online]. (n.d). Available from: <http://en.wikipedia.org/wiki/PEDOT:PSS> [2010, December 27]
- [24] Sapp, S. Intrinsically conducting polymers [Online]. Boston (TDA). Available from: <http://www.tda.com/eMatls/icp.htm> [2009, October 2]
- [25] Acid red 150 [Online]. (n.d). Available from: http://www.chemicalbook.com/ChemicalProductProperty_EN_CB9317310.htm [2009, October 2]
- [26] Scott, A. Toxicological Summary for Ionic Liquids. North Carolina, United States of America: Integrated Laboratory Systems, Inc., 2004.
- [27] Wang, J. Analytical electrochemistry. United States of America: John Wiley & Sons, 2006.
- [28] Introduction to conductivity [Online]. (n.d.). Available from: <http://www.eutec.hinst.com/techtips/tech-tips25.htm> [2010, July 4].
- [29] Conductivity theory and practice [Online]. (n.d.). Available from: http://www.analytical_chemistry.uoc.gr/pdf/Agwgimometria_2.pdf [2010, July 4].
- [30] Swapp, S. Scanning Electron Microscopy (SEM) [Online]. (n.d.). Available from: http://serc.carleton.edu/research_education/geochemsheets/techniques/SEM.html [2011, January 22]

- [31] Scanning Electron Microscopy (SEM) [Online]. (NHML). Available from: <http://www.nhml.com/resources/1998/10/1/scanning-electron-microscopes-sem> [2011, January 22]
- [32] Whiston, C. Analytical chemistry by open learning X-ray method. London, UK: John Wiley & Sons, 1987.
- [33] X-RAY DIFFRACTION BASICS [Online]. (n.d.). Available from: <http://www.spec2000.net/09-xrd.htm> [2011, January 22]
- [34] Template X-ray [Online]. (n.d.). Available from: <http://www.teachnet.ie/dkeenahan/page21.html> [2011, January 22]
- [35] Torcheux, L.; and Lailier, P. A new electrolyte formulation for low cost cycling lead acid batteries. Journal of Power Sources 95 (2001): 248-254.
- [36] Wu, L.; Chen, H. Y.; and Jiang, X. Effect of silica soot on behavior of negative electrode in lead-acid batteries. Journal of Power Sources 107 (2002): 162-166.
- [37] Lambert, D. W. H.; Greenwood, P. H. J.; and Reed, M. C. Advances in gelled-electrolyte technology for valve-regulated lead-acid batteries. Journal of Power Sources 107 (2002): 173-179.
- [38] Martha, S.; Hariprakash, B.; Gaffoor, S.; and Shukla, A. Performance characteristics of a gelled-electrolyte valve-regulated lead-acid battery. Bulletin of Materials Science 26 (2003): 465-469.
- [39] Park, J.; et al. Rheological characterization and optimization of gelled electrolyte for sealed lead-acid batteries by small amplitude dynamic oscillation measurement. Journal of Non-Crystalline Solids 351 (2005): 2352-2357.
- [40] Guo, Y.; Hu, J.; and Huang, M. Investigations on self-discharge of gel valve-regulated lead-acid batteries. Journal of Power Sources 158 (2006): 991-996.

- [41] Tang, Z.; et al. Investigation and application of polysiloxane-based gel electrolyte in valve-regulated lead-acid battery. Journal of Power Sources 168 (2007): 49-57.
- [42] Chen, M. Q.; Chen, H. Y.; Shu, D.; Li, A. J.; and Finlow, D. E. Effects of preparation condition and particle size distribution on fumed silica gel valve-regulated lead-acid batteries performance. Journal of Power Sources 181 (2008): 161-171.
- [43] Siridetpan, Effects of preparation condition and particle size distribution on fumed silica gel valve-regulated lead-acid batteries performance. Journal of Power Sources 181 (2008): 161-171.
- [44] Chaiyasit, A. Effect of polymers on gel electrolyte properties in lead-acid battery. Degree of Master of Science Program in Petrochemistry and Polymer Science Faculty of Science Chulalongkorn University, 2008.
- [45] Karami, H. and Asadi, R. Recovery of discarded sulfated lead-acid batteries. Journal of Power Sources 191 (2009): 165-175.
- [46] Rezaei, B.; Mallakpour, S., and Taki, M. Application of ionic liquids as an electrolyte additive on the electrochemical behavior of lead acid battery. Journal of Power Sources 187 (2009): 605-612.
- [47] HGL4.0-12 Valve Regulated Sealed Lead-Acid Battery Lion [Online]. (n.d.). Available from: <http://www.nvbattery.com/products.asp?page=2&Parent ID=228> [2008, October 27].

APPENDICES

APPENDIX A

GELLED ELECTROLYTE



Figure B1 Characteristic of gelled electrolyte; a) the sedimentation of gelled electrolyte, b) gel characteristic of gelled electrolyte.



Figure B2 Characteristic of gelled electrolyte in VRLA battery; a) the sedimentation of gelled electrolyte, b) gel VRLA battery

APPENDIX B

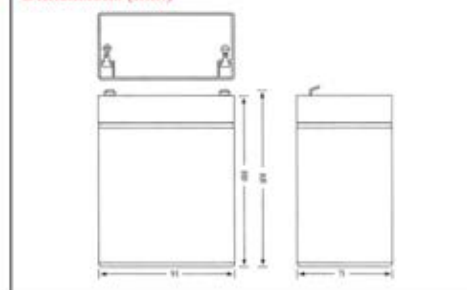
HGL4.0-12

HGL4.0 -12

Valve Regulated Sealed Lead-Acid Battery

LION[®]

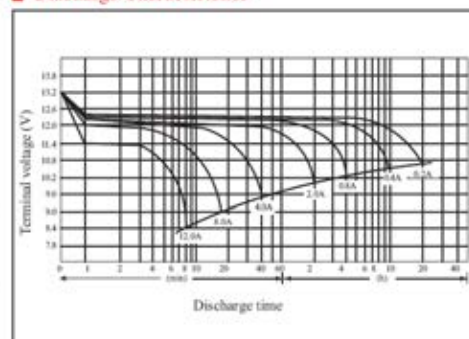
Dimensions (mm)



■ Specifications

Nominal Voltage		12V
Rated Capacity (20 hours rate)		4.0Ah
Dimensions (± 2mm)	Total Height (with terminals)	106mm
	Length	91mm
	Width	71mm
Height		100mm
Approx. Weight		1.64kg
Standard Terminal		F1

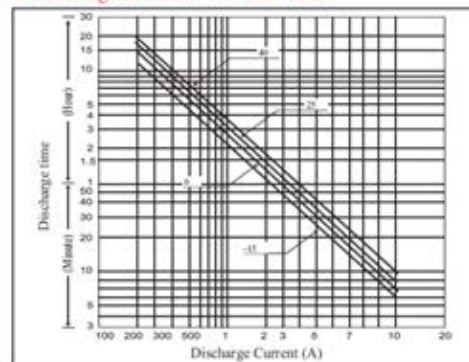
■ Discharge Characteristics



■ Characteristics

Capacity (25°C)	20 hour rate (200mA)	4.0AH	
	10 hour rate (372mA)	3.7AH	
	5 hour rate (680mA)	3.4AH	
	1 hour rate (2.3A)	2.3AH	
Internal Resistance	Fully charged Battery 25°C	Approx. 35m	
Capacity affected by temperature (20 hour rate)	40°C	102%	
	25°C	100%	
	0°C	85%	
Self Discharge (25°C)	Capacity after 3 months storage	92%	
	Capacity after 6 months storage	83%	
	Capacity after 12 months storage	65%	
Charge Method (Constant Voltage)	Cycle use	Initial Current	1.20A or smaller
		Control Voltage	14.4 to 15.0V (25°C)
	Standby use	Initial Current	1.20A or smaller
		Control Voltage	13.5 to 13.8V (25°C)

■ Discharge current & Duration Time



* The above data are average and obtained within three charge/discharge cycles. Cycles not the minimum values.

APPENDIX C

DISCHARGE CAPACITY

Table C1 The average discharge capacity of gel VRLA batteries in various fumed silica content.

Type of additive	Fumed silica content,%(w/v)					
	Size 12 nm			Size 7 nm		
	2	3	4	2	3	4
No additive	2.14	2.19	2.02	2.09	2.38	1.81
PPy	2.21	2.26	2.50	2.09	2.19	2.41
PEDOT:PSS	2.33	2.13	1.70	2.44	2.13	1.82
Pss	2.11	2.00	1.94	2.32	2.43	2.39
IL	2.16	2.10	1.73	2.27	2.14	1.73

Table C2 The average discharge capacity of gel VRLA batteries in various concentrations of additives.

Type of additive	Concentration,%(w/v)		
	0.005	0.01	0.02
Ppy	2.17778	2.49899	2.1534
PEDOT:PSS	2.091188	1.70365	2.136598
Pss	1.8291	2.43	2.12379
IL	1.99285	2.14	2.24828

VITA

Name : Miss Preeyaporn Sangarattanapiman

Date of birth : October 16, 1985

Gender : Female

Education : 2001-2004 M.6 at Mahapruttaram Girl's School,
Major of Science-Mathematic

2004-2008 Bachelor's Degree of Science at
Srinakharinwirot University,
Major of Chemistry

2008-20011 Master's Degree of Science at
Chulalongkorn University, Major of
Petrochemistry and Polymer Science

Home Address : 28/54, Ramkhamhang 1, Tambol Suanluang, Amphur
Phrapradang,
Suanluang 10250, Thailand

Proceedings :

Sangarattanapiman, P.; Siangproh, W. and Chailapakul, O. (16 November-19 November, 2010) Influence of additives on gel valve-regulated lead-acid battery performance. Proceeding of REMSEA2010, Bangkok, Thailand.